AWARD NUMBER: W81XWH-15-1-0083

TITLE: "The Function of NFAT3 in Ovarian Cancer Cell Quiescence and Chemotherapy Resistance"

PRINCIPAL INVESTIGATOR: Ronald J Buckanovich

RECIPIENT: Magee-Womens Research Institute and Foundation Pittsburgh, PA 15213

REPORT DATE: FEBRUARY 2020

TYPE OF REPORT: Final Technical Report

PREPARED FOR: U.S. Army Medical Research and Materiel Command
Fort Detrick, Maryland 21702-5012

REPORT DOCUMENTATION PAGE

Form Approved
OMB No. 0704-0188

1. REPORT DATE: FEB 2020	**2. REPORT TYPE:** Final	**3. DATES COVERED** 15 May 2015 - 15 October 2019

4. TITLE AND SUBTITLE

The Function of NFAT3 in Ovarian Cancer Cell Quiescence and Chemotherapy Resistance

5a. CONTRACT NUMBER W81XWH-15-1-0083

5b. GRANT NUMBER

5c. PROGRAM ELEMENT NUMBER

6. AUTHOR(S) Dr. Ronald Buckanovich

E-Mail: buckanovichrj@mwri.magee.edu

5d. PROJECT NUMBER

5e. TASK NUMBER

5f. WORK UNIT NUMBER

7. PERFORMING ORGANIZATION NAME(S) AND ADDRESS(ES)
Magee-Womens Research Institute & Foundation
3339 Ward Street
Pittsburgh, PA 15213-4430

8. PERFORMING ORGANIZATION REPORT NUMBER

9. SPONSORING / MONITORING AGENCY NAME(S) AND ADDRESS(ES)

U.S. Army Medical Research and Development Command
Fort Detrick, Maryland 21702-5012

10. SPONSOR/MONITOR'S ACRONYM(S)

11. SPONSOR/MONITOR'S REPORT NUMBER(S)

12. DISTRIBUTION / AVAILABILITY STATEMENT

Approved for Public Release; Distribution Unlimited

13. SUPPLEMENTARY NOTES

14. ABSTRACT

The majority of deaths from ovarian cancer are related to disease recurrence and the subsequent development of chemotherapy-resistant disease, which is inevitably fatal. Elucidating mechanisms of chemoresistance in ovarian cancer cells may identify critical therapeutic targets to prevent or treat relapsed ovarian cancer. One feature that might contribute to the chemotherapy resistance is quiescence. Quiescence promotes chemotherapy resistance of adult stem cells. Quiescence in the adult hair follicle stem cell is mediated by Nuclear Factor of Activated T cells-1 (NFAT1). NFAT proteins are master transcriptional regulators that function in conjunction with the AP1 transcription factors c-Fos and c-Jun to regulate cellular stress responses; NFAT:AP1 regulate the cell cycle via transcriptional down-regulation of the cyclin dependent kinases CDK4/CDK6. NFAT proteins also regulate protein synthesis via transcriptional control of ribosomal protein subunit expression. Interestingly, quiescent hematopoietic stem cells have reduced protein synthesis.

15. SUBJECT TERMS
Quiescence, Cancer Stem Cells, chemotherapy resistance, NFAT3, CDK4/6 inhibitors

16. SECURITY CLASSIFICATION OF:			**17. LIMITATION OF ABSTRACT**	**18. NUMBER OF PAGES**	**19a. NAME OF RESPONSIBLE PERSON** USAMRMC
a. REPORT	**b. ABSTRACT**	**c. THIS PAGE**			**19b. TELEPHONE NUMBER** *(include area code)*
Unclassified	Unclassified	Unclassified	Unclassified	**68**	

Table of Contents

Page

1. INTRODUCTION:

The majority of deaths from ovarian cancer are related to disease recurrence and the subsequent development of chemotherapy-resistant disease, which is inevitably fatal. Elucidating mechanisms of chemoresistance in ovarian cancer cells may identify critical therapeutic targets to prevent or treat relapsed ovarian cancer. One feature that contributes to the chemotherapy resistance is quiescence. Quiescence promotes chemotherapy resistance of adult stem cells. Our data indicate that the master transcription factor NFAT3 is highly expressed in a subset of ovarian cancer initiating cells with stem cell characteristics and drives a quiescence in response to therapy; treatment of ovarian cancer cells with chemotherapy is associated with translocation of NFAT3 from the cytoplasm (inactive) to the nucleus (active). Furthermore, we have found that expression of a constitutively active NFAT3 is associated with reductions in expression of CDK6 and numerous ribosomal proteins and significantly restricts cellular proliferation. We have now confirmed our overarching hypothesis is that NFAT3 regulates ovarian cancer cell quiescence and chemotherapy resistance. Based on our studies we have enrolled 32 (of a targeted 40) in a clinical trial targeting this pathway. Further we have now identified downstream targets of NFAT3 that drive chemotherapy resistance.

2. KEYWORDS:

Quiescence, Cancer Stem Cells, chemotherapy resistance, NFAT3, CDK4/6 inhibitors

3. ACCOMPLISHMENTS:

We have now completed all proposed tasks. A manuscript is under review at Cancer Research. A clinical trial derived from these studies has now enrolled 19 of 38 patients.

A. Major Task 1: Assess the effects of NFAT3 on ovarian cancer quiescence versus proliferation:

I. To evaluate NFAT3 expression in quiescent ovarian cancer cells. Using qRT-PCR we have found that NFAT3 is (i) enriched in ALDH+, CD133+ CSC, (ii) enriched in vital dye retaining cells, and expression correlates with slower proliferation rates (Fig 1a-d).

II. To evaluate cNFAT-GFP cell growth in competition with control cells in vivo using In vivo competition assays: Using the cNFAT cell lines we have performed in vitro and in vivo mixing studies. GFP labeled cNFAT cells were mixed with DsRED or wild type controls. Tumors were resected when tumors reached 500mm3. FACS evaluation of tumors with mixing demonstrated resultant tumors are 99% derived from wild type cells (data not shown).

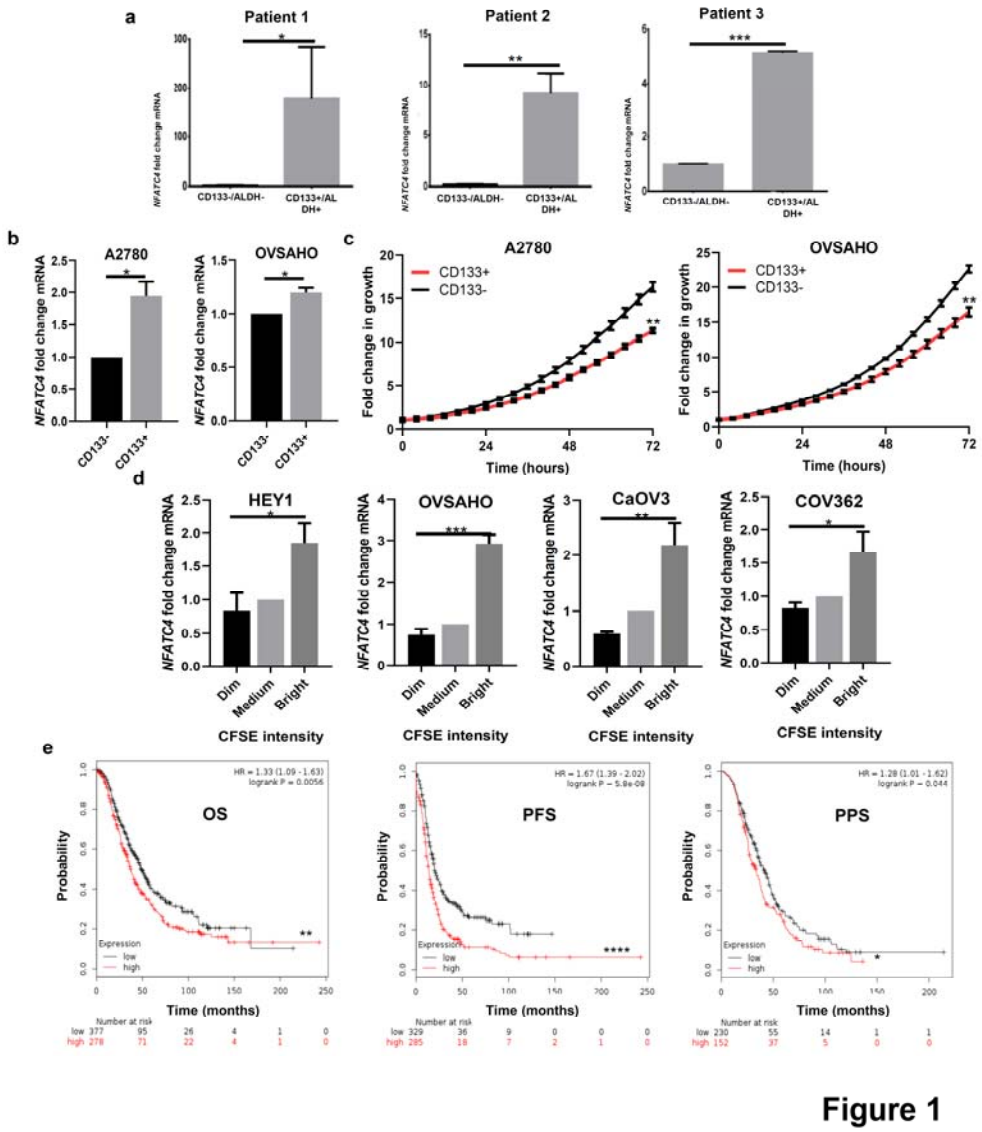

Figure 1

Figure 1. NFATC4 is enriched in ovarian stem like cancer cells and expression correlates with a decrease in cellular proliferation and patient survival. **a** *NFATC4* mRNA expression in ALDH$^+$/CD133$^+$ ovarian cancer stem-like cells and bulk ALDH$^-$/CD133$^-$ cancer cells from 3 patients. **b** *NFATC4* mRNA expression in CD133$^+$ and CD133$^-$ ovarian cancer cell lines. **c** Representative growth curves of CD133$^+$ and CD133$^-$ ovarian cancer cell lines. **d** *NFATC4* mRNA expression levels in 4 cell lines stained with CFSE. CFSE intensity; bright=slowly dividing, medium=bulk cells, dim=rapidly dividing. T-tests and one-way ANNOVARs were performed to determine significance. **e** Kaplan-meier survival plots displaying Overall Survival (OS), Progression Free Survival (PFS), Post Progression Survival (PPS) of ovarian cancer patients expressing high or low *NFATC4*.All experiments were repeated a minimum of 3 times with 3 technical replicates per experiment. *p<0.05, **p<0.01, ****p<0.0001.

III. Construct inducible cell lines. Inducible cNFAT3 (IcNFAT3) Hey1 and SKOV3cells were generated. Interestingly, IcNFAT vectors lost inducibility in our HGSC cell lines. We therefore generated cNFAT A2780, CaOV3, COV362, and OVSAHO lines. . We were unable to develop a shRNA that knocked down >50% of NFAT expression and thus results with this approach were all negative. Knockdown with a gap-mir proved toxic.

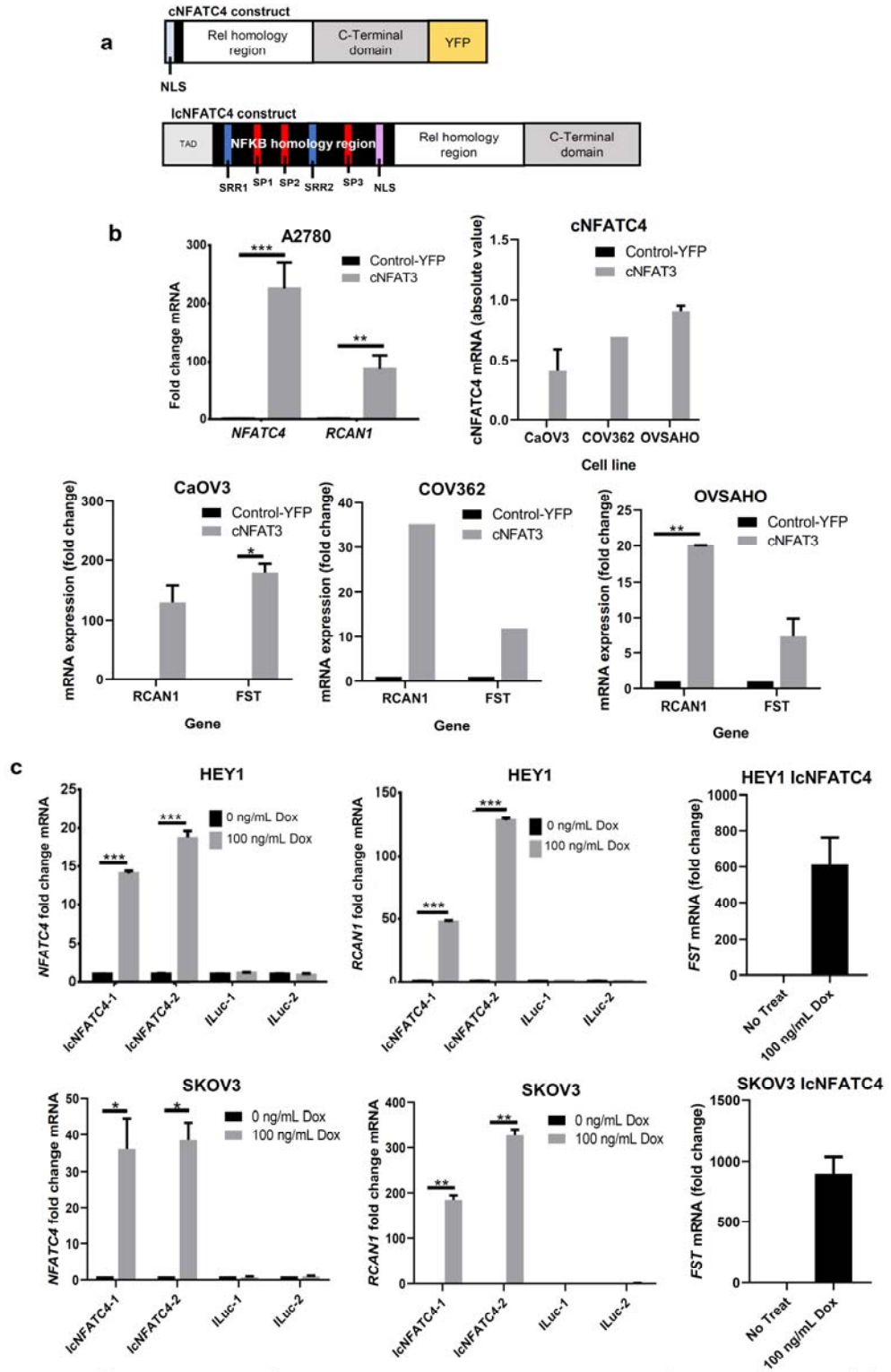

Figure 2. Characterization of NFATC4 overexpression constructs. **a** Schematic diagram of the two constitutive activation *NFTAC4* overexpression constructs; cNFATC4 (truncated regulatory domain and tagged with a yellow fluorescent protein (YFP)), and IcNFATC4 (NLS phosphorylation sites mutated). **b** cNFATC4, RCAN1 and FST mRNA expression in HGSC cells (CaOV3, OVSAHO and COV362) and A2780 cells expressing cNFATC4 or Control-YFP construct (n=2). **d** *NFATC4, RCAN1* and FST (n=3) mRNA expression in HEY1 and SKOV3 cells expressing IcNFATC4 or a ILuc control constructs treated with or without 100 ng/mL doxycycline for 72 h. T-tests and one-way ANNOVARs were performed to determine significance. All experiments were repeated a minimum of 3 times with at least 3 technical replicates per experiment. *p<0.05, **p<0.01, ***p<0.001.

IV. Evaluate impact of inducible cNFAT3 proliferation, cell cycle, and senescence vs. apoptosis.

a. Proliferation – We have now demonstrated that cNFAT3 and IcNFAT3 cell grow approximately 3-X slower than controls cells. This has been confirmed using cell counts and real time imaging (Fig 3a-d)

b. 1B), BRDU incorporation (Fig 3a-c), and single cell microfluidic analysis of single cell divisions (Fig 4a-b).

c. Cell Cycle – We have now completed extensive analysis of cell cycle. Surprisingly, despite the very strong impact of IcNFAT3 on cell proliferation we see only a modest (~10%) increasing in the number of cells in G0/G1 in the cell cycle (not-shown). We see a similar increase in the number of cells with low Hoechst/Pyronin labeling (which identifies cells with 2N DNA and low rRNA content consistent with quiescent/subG0 cells (not shown).

Finally, we have used cell cycle specific cellular reporters and demonstrated that induction of cNFAT3 results in cells entering a G0 state (Fig 3d-f).

d. Quiescent cells are typically smaller and have lower RNA content. We have now demonstrated that IcNFAT expression leads to a 10-30% reduction in cellular size and total RNA content (data not shown).

V. Impact of NFAT knockdown. See- above- shRNA constructs have been generated but are generally ineffective. Current studies have shown limited impact on proliferation or chemotherapy resistance. This may be due to the fact that knockdown is only ~50%. Alternatively other family members may compensate. We also attempted to use gap-miRs but these, while effective, were highly toxic. As an alternate approach we use the Pna-NFAT inhibitor VIVIT (see below).

e. Senescence and Apoptosis – Extensive evaluation of Annexin labeling and Tunnel stain demonstrate cNFAT3 and IcNFAT3 expression are not associated with an increase in apoptosis (not shown). Similarly evaluation of senescence associated-B-gal staining indicates no increase in senescence (not shown).

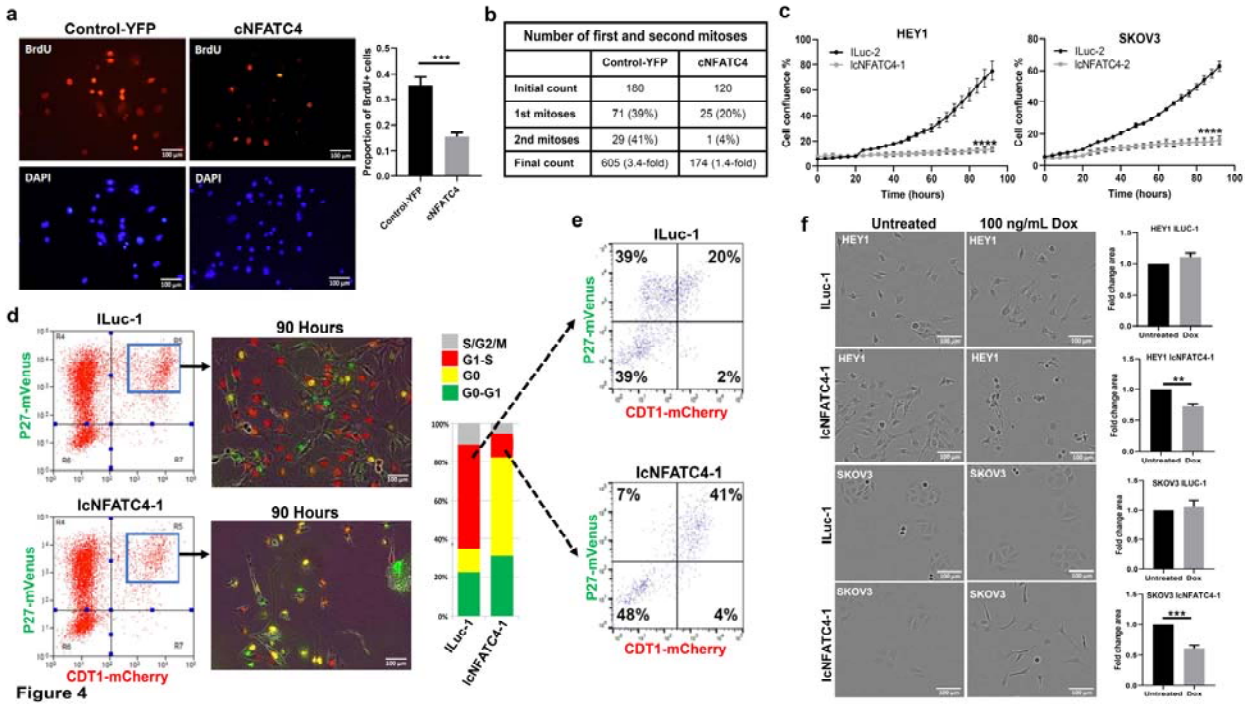

Figure 4

Figure 3. NFATC4 promotes a quiescent phenotype. **a** Representative images and quantitation of BrdU incorporation of ID8 cells expressing control-YFP or cNFATC4. **b** Table displaying the number of first

and second mitosis of ID8 cells expressing the cNFATC4 or control-YFP constructs, grown in single cell capture microfluidic chips. **c** IncuCyte growth curves of IcNFATC4 or ILuc cells treated with or without doxycycline. **d** FACS plots demonstrating the isolation and quantification of IcNFATC4 and ILuc HEY1 cells expressing the Fucci cell-cycle reporter vectors. Bar graph summarizing the cell cycle phase of cell expressing either construct. **e** Cell cycle analysis of G1-S phase enriched ILuc and IcNFATC4. **f** Representative images and quantification of cells size changes in ILuc and IcNFATC4 cells following doxycycline treatment for 106 h. T-tests and one-way ANNOVAs were performed to determine significance. Microfluidics experiment and Fucci cell cycle experiments were performed twice, all other experiments were repeated a minimum of 3 times with at least 3 technical replicates per experiment. **p<0.01, ***p<0.001.

B. Major Task 2: Determine the effects of NFAT3 on chemoresistance and tumor growth

I. Determine the impact of NFAT3 on tumorigenesis and chemoresistance in vitro using cell lines as above. We have now demonstrated that, despite slower growth rates, cNFAT3 and IcNFAT3 cells are resistant to chemotherapy. Furthermore, in wild-type cells, chemotherapy treatment is associated with a nuclear translocation wild-type NFAT3 and increased expression of the NFAT transcription target RCAN. Reciprocally, the NFAT inhibitor VIVIT increases chemotherapy response (Fig 5a-d).

II. Assess the effects of NFAT3 on tumorigenesis and chemoresistance in vivo.

a. To test the tumor initiation capacity following in vitro treatment with cisplatin. IcNFAT cells treated with doxycycline in vitro demonstrated significant chemotherapy resistance. Consistent with this, when injected based on starting tumor number we observed greater tumor initiation (not shown). However, to control for absolute cell numbers, doxycycline had to be discontinued and in this scenario we did not observe increate tumor initiation rates.

b. To assess the impact of NFAT3 on tumor growth *in vivo.* We have now completed in vivo growth studies with cNFAT and IcNFAT cells. Both cell lines demonstrate a significant reduction in tumor growth. IcNFAT3 cells are leaky at baseline, and grow slower than luciferase controls. Further induction of NFAT3 is associated with greater growth arrest (Fig 6a-c).

c. To evaluate the impact of NFAT3 expression on chemoresistance in vivo. We have completed these studies using the IcNFAT3 constructs. IcNFAT3 tumors demonstrate significant chemotherapy resistance with cNFAT3 induction and expansive growth with de-repression (Fig 6d).

d. To test the ability of VIVIT to act as a chemosensitizer. As noted above, we have completed in vitro analysis demonstrating VIVIT increases chemotherapy response in vitro (Fig 5g) and modestly in vivo (not shown).

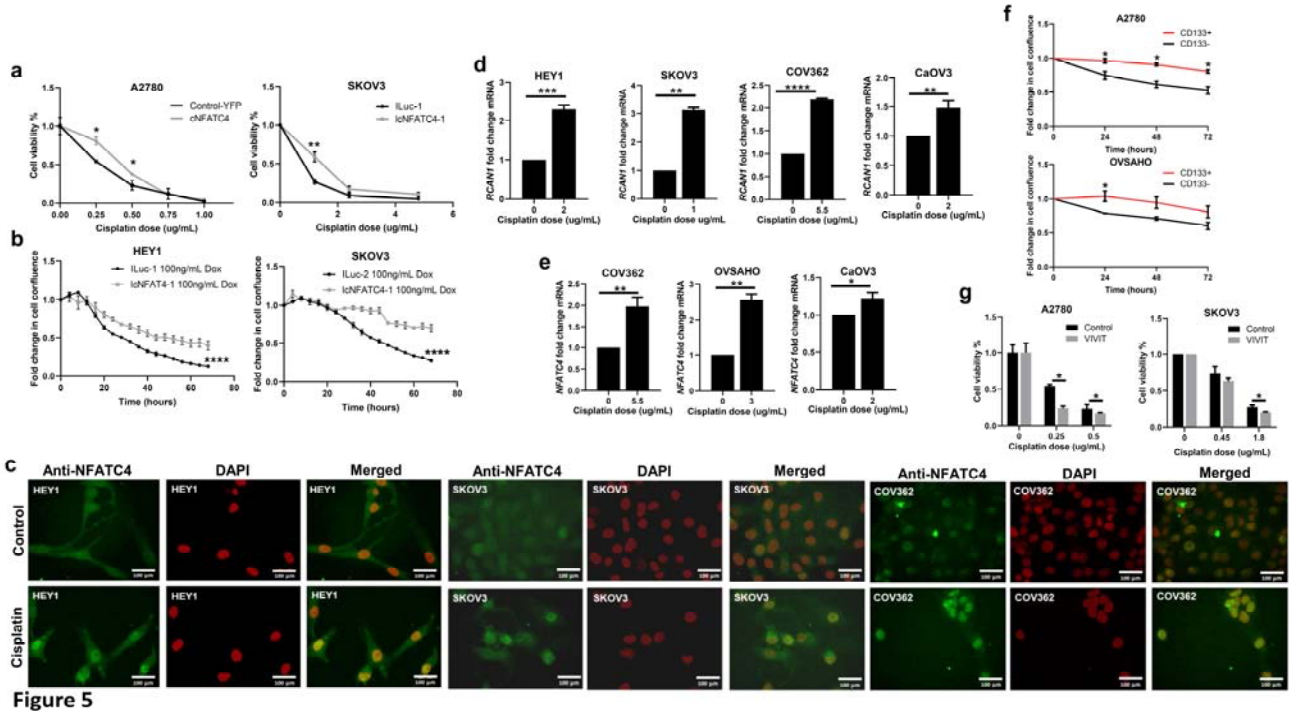

Figure 5

Figure 4. NFATC4 promotes chemoresistance in vitro and is activated by cisplatin. **a** Viability of cells expressing construct pairs (cNFATC4/Control-YFP or IcNFATC4/ILuc) treated with various concentrations of cisplatin. **b** IncuCyte confluence growth curves of IcNFATC4/ILuc expressing cells co-treated with cisplatin and doxycycline. **c** NFATC4 immunofluorescence of cells lines treated with or without cisplatin. **d** *RCAN1* mRNA expression levels of cells treated with or without cisplatin. **e** *NFATC4* mRNA expression of cell lines treated with a high concentration of cisplatin for 72h. **f** IncuCyte confluence growth curves of $CD133^-$ vs $CD133^+$ cells treated with cisplatin. **g** Cell viability following co-treatment with cisplatin and the pan-NFAT inhibitor VIVIT. T-tests and one-way ANNOVARs were performed to determine significance. All experiments were repeated a minimum of 3 times. *p<0.05, **p<0.01, ***p<0.001.

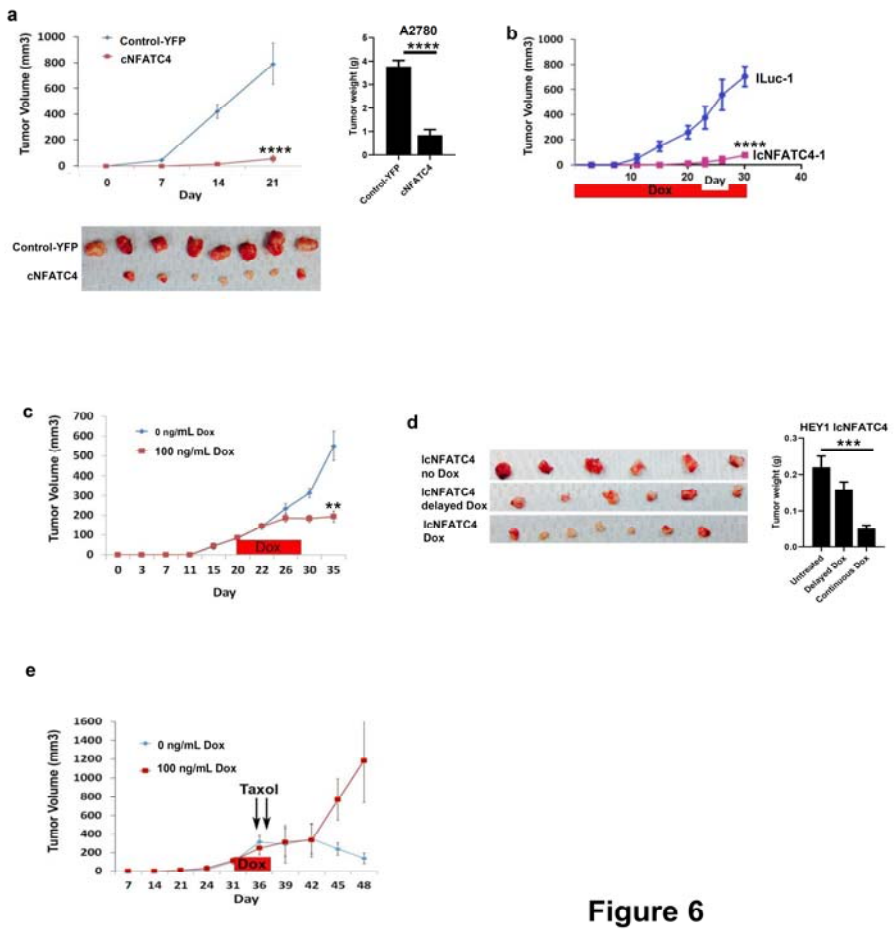

Figure 6

Figure 5. NFATC4 inhibits tumor growth and promotes chemoresistance in vivo. **a** Tumor growth of A2780 cells expressing cNFATC4 or Control-YFP. **b** Tumor growth of HEY1 cells expressing IcNFATC4 or ILuc control constructs in the presences of doxycycline. **c** Tumor growth of IcNFATC4 HEY1 cells treated with delayed doxycycline or vehicle. **d** Tumor weights of HEY1 IcNFATC4 xerographs treated with vehicle, delayed or continuous doxycycline. **e** Tumor growth of HEY1 IcNFATC4 cells treated with doxycycline for 5 days or vehicle, then both treated with 16 mg/kg paclitaxel, intraperitoneally. T-tests and one-way ANNOVARs were performed to determine significance. All experiments were repeated a minimum of 3 times. *p<0.05, **p<0.01, ***p<0.001.

III. Assess mechanisms of chemoresistance—*see Iyengar et.al. Oncotarget 2018*

a. <u>To determine the role of CDK6 in NFAT3 mediated cellular quiescence.</u> We have now demonstrated NFAT3 induces expression of CDK6. Based upon this we have completed extensive studies with the CDK4/6 inhibitor LEE011. We have demonstrated that this drug induces pseudosenescence in cancer cells to induce a partial growth arrest. However, combination of CDK4/6 inhibitor and chemotherapy is highly synergistic (Fig 4). CDK4/6 inhibitor is active in vivo as an effective consolidative therapy and works in platinum resistant disease. We are currently preparing a manuscript on this work.

b. <u>To determine the role of NFAT3 in regulating direct mediators of chemotherapy resistance.</u> While NFAT is reported to regulate regulators of chemotherapy resistance such as ABCB MDR pumps, direct analysis of numerous targets has not shown clear regulation of

c. <u>To identify additional NFAT3 targets</u>**:** RNAseq on the HEY1 IcNFAT, SKOV3 IcNFAT and A2780 cNFAT line has been completed. We have confirmed numerous targets of NFAT as putative drivers of quiescence and chemotherapy resistance. Excitingly one of the targets, follistatin (FST), is a known regulator of ovarian function. We have now shown that high follistatin expression in patient samples (TCGA) corelates with poor outcome (Fig 6A). Induction of NFAT3 expression in ovarian cancer cells is associated with a strong induction of FST. Similarly, suggesting this is part of a quiescence response to chemotherapy, FST is induced in multiple ovarian cancer cell lines in response to either cisplatin or taxol (Fig 6C-D). Furthermore addition of FST to ovarian cancer cell line culture was associated with a ~2-fold increase in resistance to both cisplatin and taxol in multiple high grade serous ovarian cancer cell lines. Ongoing work aims to establish the mechanism of FST driven chemoresistance and determine if targeting FST in vivo can overcome/reduce chemotherapy resistance.

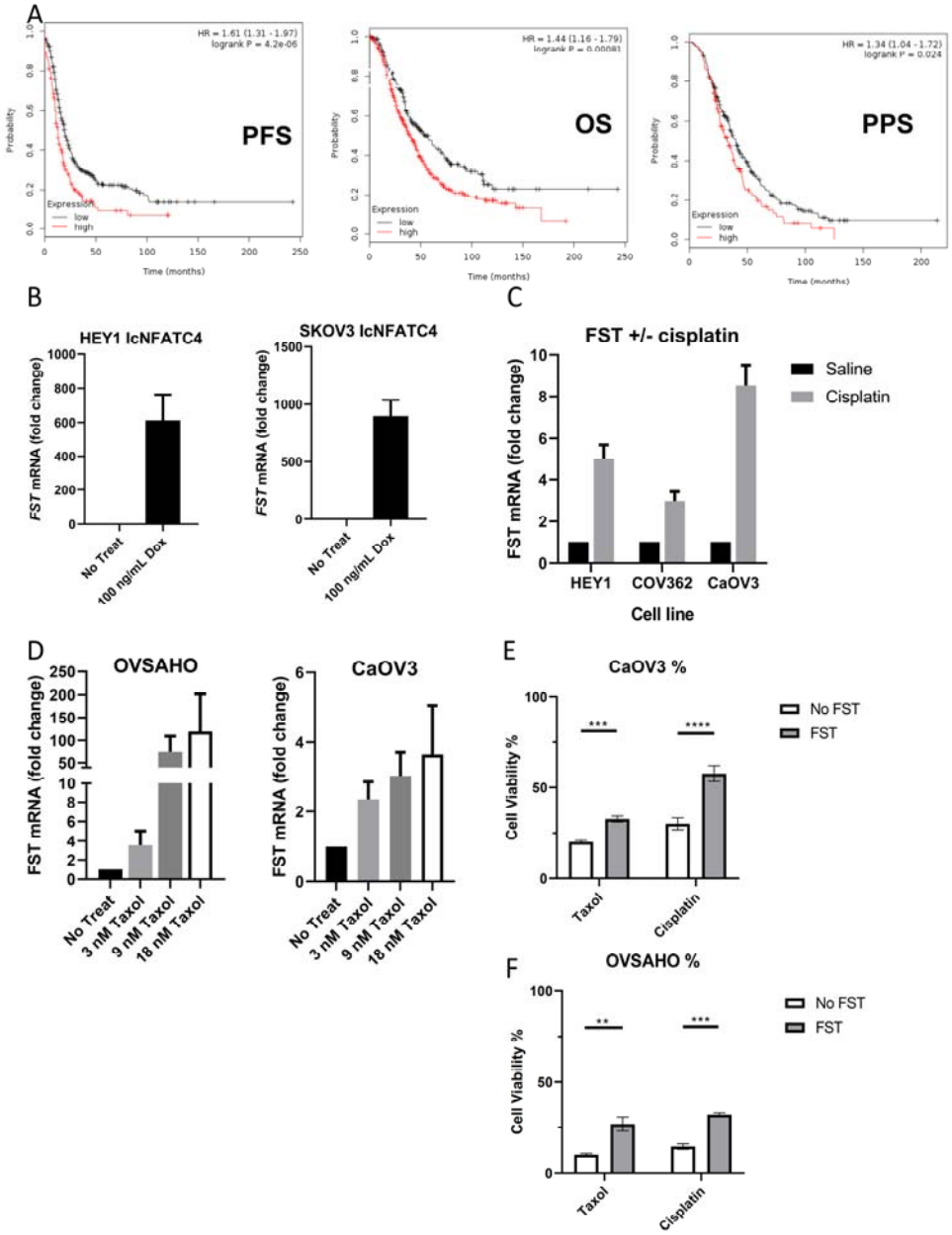

Figure 6. NFAT3 drives FST expression and FST drives chemotherapy resistance. A Overall survival, Progression free survival and post-progression survival based on high/low FST expression in the TCGA dataset. B. FST expression following doxycycline induced expression of NFAT3. C. FST induction in ovarian

cancer cell lines by cisplatin. D FST induction in response to Taxol. E-F. Cell viability in response to taxol or cisplatin therapy in the presence of FST.

Major Task 3: Determine prognostic implications of NFAT3 expression in primary ovarian cancer specimens. This aim been completed. A tissue TMA has been stained and for the impact of NFAT3 expression on overall survival. Interestingly in our array expression of NFAT3 in primary tissue did not impact prognosis, however expression of NFAT3 in tumors taken from patients at the time of chemoresistance predicted better prognosis suggesting NFAT3 may help maintain a quiescent cellular phenotype. Analysis of NFAT3 expression and prognosis in the TCGA data set suggested NFAT3 is a prognostic biomarker (Fig 1e). Confirming NFAT3 – the NFAT3 taraget RCAN shows a similar OS/PFS/PPS curve (not shown), as does the newly identified NFAT3 target FST.

Opportunities for Training.

1. MSTP Student Mangala Iyengar MD, PhD worked on the initial studies and portion related to CDK4/6 which was the basis of her graduate thesis. She is now a Medical Resident at the University of Colorado.
2. Alex Cole PhD – post-doctoral fellow was trained on this award and will continue his work on cancer quiescence on his return to an academic position in Australia
3. Santiago Panesso MD, is volunteer from Columbia, has work with Dr. Cole and will continue this work after Dr. Cole's departure this spring. Dr. Panesso has been assisting on the work on FST. This allowed the training of an under-represented minority population in science and will assist in his application for an a US medical residency training.

4. IMPACT:

- To date we have clearly demonstrated a role for NFAT3 in driving a quiescent ovarian cancer phenotype.
- We have demonstrated that NFAT3 translocates to the nucleus in response to chemotherapy. IcNFAT3 is associated with chemotherapy resistance and treatment of cells with the NFAT inhibitor VIVIT reverses chemotherapy resistance.
- We have performed an extensive study of CDK4/6inhibitors in a short time an demonstrated a role for these agents as consolidative therapy and potentially (surprisingly) as chemosensitizers.
- We have initiated a clinical trial "**Phase I trial of ribociclib (ribociclib (LEE-011)) with platinum-based chemotherapy in recurrent platinum sensitive ovarian cancer"**
- We have identified FST as an autocrine mediator of chemotherapy resistance
- Alex Cole – OCRA Ann Schreiber Fellowship Award.
- Based on this work we have a new R01 being prepared for submission to the NIH

5. CHANGES/PROBLEMS:

We were unable to obtain inducible IcNFAT3 contruct expression in many of the preferred HGSC cell lines. For HGSC lines we therefore used the cNFAT construct. Similarly, shRNA constructs have been ineffective and CRISPR cells were similarly non-viable. We used VIVIT inhibitor instead.

6. PRODUCTS:

A. Manuscripts

CDK4/6 inhibition as maintenance and combination therapy for high grade serous ovarian cancer Iyengar et.al. Oncotarget 2018.

NFATC4 Promotes Quiescence and Chemotherapy Resistance in Ovarian Cancer Cells – BioRx and under second review JCI Insight.

FST drives ovarian cancer cell resistance to chemotherapy – in preparation

B. Abstracts/Posters:

Date: September 2015
Authors: Mangala Iyengar, Lan Coffman, Kun Yang, and Ronald Buckanovich
Title: CDK4/6 Inhibition as a Maintenance Therapy in Ovarian Cancer
Meeting: AACR Advances in Ovarian Cancer: Exploiting Vulnerabilities
Location: Orlando Florida

October 2015
Authors: Mangala Iyengar, Shoumei Bai, Lan Coffman, Kun Yang, and Ronald Buckanovich
Title: NFAT3 Promotes Ovarian Cancer Quiescence and Chemotherapy Resistance
Meeting: University of Michigan Cancer Center Fall Research Symposium

C. Presentations

Date: April 2016
Speaker: Ronald Buckanovich
Title: Novel Therapeutics Targeting Cancer Stem Cells
Meeting: Mayo Clinic, Oncology Grand Rounds
Location: Rochester, MN

Date: May 2016
Speaker: Ronald Buckanovich
Title: A Hierarchical Model of Ovarian Cancer and Why it Matters
Meeting: Cancer Center Research Seminal
Location: Salt Lake City, Utah

Date: Jan 4 2017
Speaker: Ronald Buckanovich
Title: Novel therapeutics targeting ovarian cancer stem cells.
Meeting: NYU Research Seminar
Location: NY, NY

Date: March 2017
Speaker: Ronald Buckanovich
Title: NFAT3 in Ovarian Cancer Quiescence and Chemotherapy Resistance
Meeting: MWRI Women's Cancer Research Seminar

Location: Pittsburgh, Pa

Date: September 2018
Speaker: Alex Cole
Title: NFAT3 in Ovarian Cancer Quiescence and Chemotherapy Resistance
Meeting: Rivken/AACR 12th Biennial Ovarian Cancer Research Symposium
Location: Seattle, WA

D. Inventions, Patents and Licenses
None

E. Other Achievements:
Based upon our work on the CDK4/K inhibitor LEE-011, we have initiated a clinical trial to evaluate the role of CDK4/6 inhibitors as concurrent and maintenance therapy for patients with recurrent platinum sensitive disease. This trial has currently enrolled 32 of 38 anticipated patients.

7. PARTICIPANTS AND OTHER COLLABORATING INSTITUTIONS:

Name:	Ronald J. Buckanovich
Project Role:	PD/PI
Researcher Identifier (e.g. ORCID ID):	W81XWH-15-1-0083
Nearest person month worked:	.5 **(5/15/19 – 10/15/19)**
Contribution to Project:	Dr. Buckanovich was responsible for overseeing all project activities and supervising research staff.
Funding Support:	NA
Name:	Shoumei Bai
Project Role:	Research Associate
Researcher Identifier (e.g. ORCID ID):	W81XWH-15-1-0083
Nearest person month worked:	5 **(5/15/19 – 10/15/19)**
Contribution to Project:	Dr. Bai was responsible for the derivation of all CA-MSC lines from patient samples. She performed all cell line generation to create multiple cell lines with IcNFAT3 and NFAT3shRNA cell lines to validate current studies.
Funding Support:	NA

Has there been a change in the active other support of the PD/PI(s) or senior/key personnel since the last reporting period? Yes, Ronald Buckanovich: since last annual report (5/14/19)

- Two new awards as a co-investigator
- One award ended

New Award: W81XWH-18-OCRP-OMCDA Levine & Buckanovich (PI)
Title: Omics Consortium to Study the Origins of Ovarian Cancer
Effort: 0.24 calendar months
Sponsor Agency: Department of Defense/Subcontract from New York University
Contracting/Grants Officer: Abigail Strock, abigail.l.strock.civ@mail.mil
Address of Funding Agency: USA MRAA, 820 Chandler St, Fort Detrick MD 21702
Performance Period: 06/15/2019 – 06/14/2020
Level of Funding: $100,000
Specific Aims/Project Goals: Aim 1. To develop the consortium infrastructure and a multi-institutional research team of scientists, clinicians, and ovarian cancer consumer advocates to establish new collaborations, initiate a research and communication plan, and formalize the organizational structure.
Aim 2. To conduct a preliminary research project using multi-omic platforms to study the tumor microenvironment (TME) of normal fallopian tube epithelium and precursor (STIC) lesions compared to established ovarian cancers. Aim 3. To establish additional research plans for the FY20 OCRP Omics Consortium Award including studies of cancer stem cell, circulating and shed biomarkers, and drivers of transition between precursor (STIC) lesions and established cancers.
Overlap: No scientific or budgetary overlap

New Award: Research Scholar Grant Mehta (PI)
Title: Ovarian Cancer Tumoroids to Study Heterogeneity and Chemoresistance
Effort: 0.24 calendar months
Sponsor Agency: American Cancer Society/Subaward from University of Michigan
Contracting/Grants Officer: grants@cancer.org
Address of Funding Agency: 250 Williams Street NW, Atlanta, GA 30303
Performance Period: 07/01/2019 – 06/30/2023
Level of Funding: $53,424
Specific Aims/Project Goals: The goal of this research will provide a modular platform for the study of CSC-TME interactions in the ascites and help understand the individual and collective role of MSCs, ECs, MPs in CSC enrichment and chemoresistance. In the long term, using this platform to gain a comprehensive understanding of these interactions will be crucial in the development of novel therapeutics and treatment strategies to improve clinical outcomes of ovarian cancers.
Overlap: No scientific or budgetary overlap

Expired Award: W81XWH-13-1-0134 Mehta (PI)
Title: High-Throughput Platform for Patient-Derived, Small Cell Number, Three-Dimensional Ovarian
Cancer Spheroids
Effort: 0.78 calendar months
Sponsor Agency: Department of Defense/Subaward from University of Michigan
Contracting/Grants Officer: Abigail Strock, abigail.l.strock.civ@mail.mil
Address of Funding Agency: USA MRAA, 820 Chandler St, Fort Detrick MD 21702
Performance Period: 09/01/2018 – 08/31/2019
Level of Funding: $25,533
Specific Aims/Project Goals: Dr. Buckanovich Mentors Dr. Mehta and will review her final research reports and provide guidance on the final stage of her research project as well as assist

and or review manuscripts prepared by Dr. Mehta. An extensive mentoring plan has been put in place to provide Dr. Mehta with the tools and experience to promote her success.
Overlap: No scientific or budgetary overlap

What other organizations were involved as partners? Nothing to Report.

8. APPENDICES:

CDK4/6 inhibition as maintenance and combination therapy for high grade serous ovarian cancer

Mangala Iyengar[1,2,*], Patrick O'Hayer[1,2,*], Alex Cole[4], Tara Sebastian[3], Kun Yang[4], Lan Coffman[4,#] and Ronald J. Buckanovich[4,5,#]

[1]University of Michigan Department of Cellular and Molecular Biology, 2966 Taubman Medical Library, 1150 W. Medical Center Drive, Ann Arbor, Michigan 48109

[2]University of Michigan Medical Scientist Training Program, 2965 Taubman Medical Library, 1150 W. Medical Center Drive Ann Arbor, MI 48109-5619

[3]University of Michigan School of Literature, Science and the Arts, Ann Arbor, MI 48109

[4]University of Michigan Division of Hematology and Oncology, Department of Internal Medicine, 1500 E. Medical Center Drive Cancer Center, Ann Arbor, MI 48109

[5]Magee Women's Research Institute, University of Pittsburgh Department of Internal Medicine, Pittsburgh, PA 15213

[*]Co-first authors

[#]Co-senior authors

***Correspondence to**: Ronald J. Buckanovich, **email:** ronaldbu@med.umich.edu*

***Keywords:** ovarian cancer; Ribociclib; CDK 4/6 inhibitor; chemotherapy resistance; cell cycle*

***Abbreviations:** LEE-011: Ribociclib; CDK: Cyclin Dependent Kinase; HGSOC: high grade serous ovarian cancer; TCGA: The Cancer Genome Atlas*

***Received:** February 20, 2018 **Accepted:** February 21, 2018 **Published**: February 26, 2018*

ABSTRACT

High grade serous ovarian cancer (HGSOC) is a disease with a high relapse rate and poor overall survival despite good initial responses to platinum-based therapy. Cell cycle inhibition with targeted CDK4/6 inhibitors is a new therapeutic approach showing promise as a maintenance therapy in cancer. As multiple genes in the CDK4/6 pathway are commonly mutated or dysregulated in ovarian cancer, we evaluated the efficacy of the CDK4/6 inhibitor Ribociclib alone, in combination with chemotherapy, and as maintenance therapy in several models of HGSOC. Ribociclib restricted cellular proliferation in multiple ovarian cancer cell lines. Restricted proliferation was associated with a pseudo-senescent cellular phenotype; Ribociclib-treated cells expressed markers of senescence, but could rapidly re-enter the cell cycle with discontinuation of therapy. Surprisingly, concurrent Ribociclib and cisplatin therapy followed by Ribociclib maintenance was synergistic. Evaluation of the cell cycle suggested that Ribociclib may also act at the G2/M check point via dephosphorylation of ATR and CHK1. Consistent with this mechanism, Ribociclib demonstrated clear activity in both platinum-resistant and platinum-sensitive tumor models *in vivo*. This work supports clinical trials using Ribociclib in combination with cisplatin and as a maintenance therapy in ovarian cancer.

INTRODUCTION

High grade serous ovarian cancer (HGSOC) is the most lethal gynecological cancer in the United States and is characterized by a high recurrence rate [1]; 70% of patients relapse and succumb to their disease despite initially successful chemotherapy. This is largely because most patients present with disseminated disease (stages III/IV) at diagnosis [2]. Patients with recurrent ovarian cancer inevitably develop resistance to standard platinum-based chemotherapy and additional chemotherapy does not offer significant survival benefit [3]. Therefore, non-

cytotoxic maintenance therapies which could extend disease-free survival may improve a patient's quality of life and potentially prolong survival.

CDK4/6 inhibition is an emerging cytostatic therapy targeting cell cycle progression. A heterotrimeric complex of Cyclin D1, CDK4, and CDK6 is required to phosphorylate RB1, which eventually leads to the transcription of genes required for S phase. Therefore, CDK4/6 inhibition blocks the G1-S phase transition, forcing G1 arrest (reviewed in [4]). CDK4/6 inhibitors have shown promise in many tumors *in vitro*, such as neuroblastoma [5], liposarcoma [6], breast cancer [7], mantle cell lymphoma [8], non-small cell lung cancer [9], and germ cell tumors [10]. Importantly, there are also positive clinical results in patients. In metastatic breast cancer, Palbociclib in combination with letrozole doubled progression-free survival from 10 to 20 months compared to letrozole alone in a Phase II trial [11] and from 19.3 to 30.4 months in a Phase III trial [12]. Similarly, Ribociclib showed a significant impact in breast cancer [13], and both Palbociclib and Ribociclib are now FDA-approved in combination with an aromatase inhibitor as frontline treatment in $ER^+/HER2^-$ metastatic breast cancer.

In ovarian cancer, CDK4/6 inhibitors have shown promise *in vitro*. Response to CDK4/6 inhibitors has been linked to the mutational status of p16 and Rb [14]. CDK4/6 inhibitors have also been linked to targeting cancer stem cells [15]. However, resistance mechanisms have also been reported [16]. Clinical data regarding CDK4/6 inhibition in ovarian cancer are sparse. While Phase 1 (NCT03294694, NCT02897375) and Phase 2 (NCT02657928) trials of CDK4/6 inhibition in combination with other therapies in ovarian cancer have recently opened, no data is available yet from these studies. However, the CDK4/6 inhibitor abemaciclib as monotherapy did produce stable disease in two patients and a CA-125 response in a third patient [17]. Importantly, CDK4/6 inhibitors have generally been well-tolerated and side effects have been successfully managed by dose-reduction [18]. Therefore, these compounds could be useful as maintenance therapies or combination therapies in patients with chemotherapy-resistant disease.

We mined the TCGA database [19] and found that ~40% of patients with HGSOC have mutations/dysregulation of various genes which regulate the G1 to S phase cell cycle transition, which is consistent with previous literature (reviewed in [20]) . We therefore tested CDK4/6 inhibition with Ribociclib both *in vitro* and *in vivo* and demonstrated a significant delay in ovarian cancer cell growth via the induction of a pseudo-senescent state. The combination of Ribociclib and cisplatin led to growth-arrest *in vitro* and significantly delayed tumor growth *in vivo*; therefore, Ribociclib appears to be a promising therapeutic for ovarian cancer treatment.

RESULTS

Mutations and dysregulation of genes in the CDK4/6 pathway are common in ovarian cancer

The cBioPortal browser was used to mine data from The Cancer Genome Atlas (TCGA, [19]) to perform mutational analysis of genes in the CDK4/6 pathway. Mutations and significant dysregulation of mRNA expression (z-score < –2 or >2) were common in patients with HGSOC (Figure 1A). CDKN2A (also known as $p16^{INK4a}$) is a tumor suppressor that normally serves as a brake on cell cycle progression by inhibiting CDK4 and CDK6 [21]. Interestingly, 21% of ovarian cancer patients showed CDKN2A deletions or significant downregulation. Another 16% showed significant amplifications or increases in mRNA expression of CDK4, CDK6, and/or Cyclin D1 expression; both these classes of mutations would contribute to an aberrantly overactive cell cycle and, presumably, tumor growth. Of note, RB1 was deleted or significantly downregulated in 17% of HGSOC patients; these patients may be less likely to respond to CDK4/6 inhibition. Overall, our data (Figure 1A) show that there is a large subset of HGSOC patients who would likely benefit from therapy with a CDK4/6 inhibitor. Therefore, we investigated the CDK4/6 inhibitor Ribociclib (LEE-011)(Novartis) in HGSOC.

Ribociclib affects growth in multiple ovarian cancer cell lines

A2780, Hey1, COV362, COV504, PEO1, and OVSAHO ovarian cancer cell lines were treated with increasing doses of Ribociclib for 3 days as detailed in Figure 1B and cell proliferation was quantified by cell counts with trypan blue exclusion. The $RB1^{WT}$ cell lines A2780, Hey1, COV504, and PEO1 showed dose-dependent growth inhibition (Figure 1B). As RB1 is a core downstream target of CDK4 and CDK6, $RB1^{null}$ cells should be resistant to CDK4/6 inhibition. To verify on-target effects, the $RB1^{null}$ lines COV362 and OVSAHO were also treated with Ribociclib and were unresponsive (Figure 1B). For more detailed analysis, we treated the Rb^{WT} cell line Hey1 and the Rb^{null} line COV362 with Ribociclib and analyzed cell counts and viability daily. Relative to control treatment, Ribociclib decreased the number of Hey1 cells in a dose-dependent manner (Figure 1C) without affecting Hey1 cell viability (Figure 1E), suggesting that treatment leads to growth-arrest rather than cell death in this RB^{WT} cell line. However, Ribociclib did not affect Rb^{null} COV362 cell proliferation (Figure 1D) or viability (Supplementary Figure 1A) even at the highest doses, suggesting that decreased proliferation is an on-target effect of Ribociclib.

Ribociclib decreases cell proliferation by arresting cells in G1 in a 'pseudo-senescent' state

Cell cycle phase analysis with propidium iodide showed that Ribociclib treatment led to a dose-dependent accumulation of Hey1 cells in the G1/G0 phase of the cell cycle, with a concomitant decrease in the number of cells in the S and G2/M phases (Figure 2A–2B). This is consistent with the known role of CDK4 and CDK6 in regulating the G1-S transition [4]. We also observed a decrease in BrdU incorporation in Hey1 ovarian cancer cells during this treatment (Figure 2C), confirming a decrease in proliferation. The Rb^{null} line COV362 showed no cell cycle changes in response to Ribociclib, regardless of dose (Supplementary Figure 1B).

CDK4/6 inhibitors have been reported to induce senescence in cancer cells [22, 23]. We therefore evaluated the expression of Senescence Associated β-Galactosidase

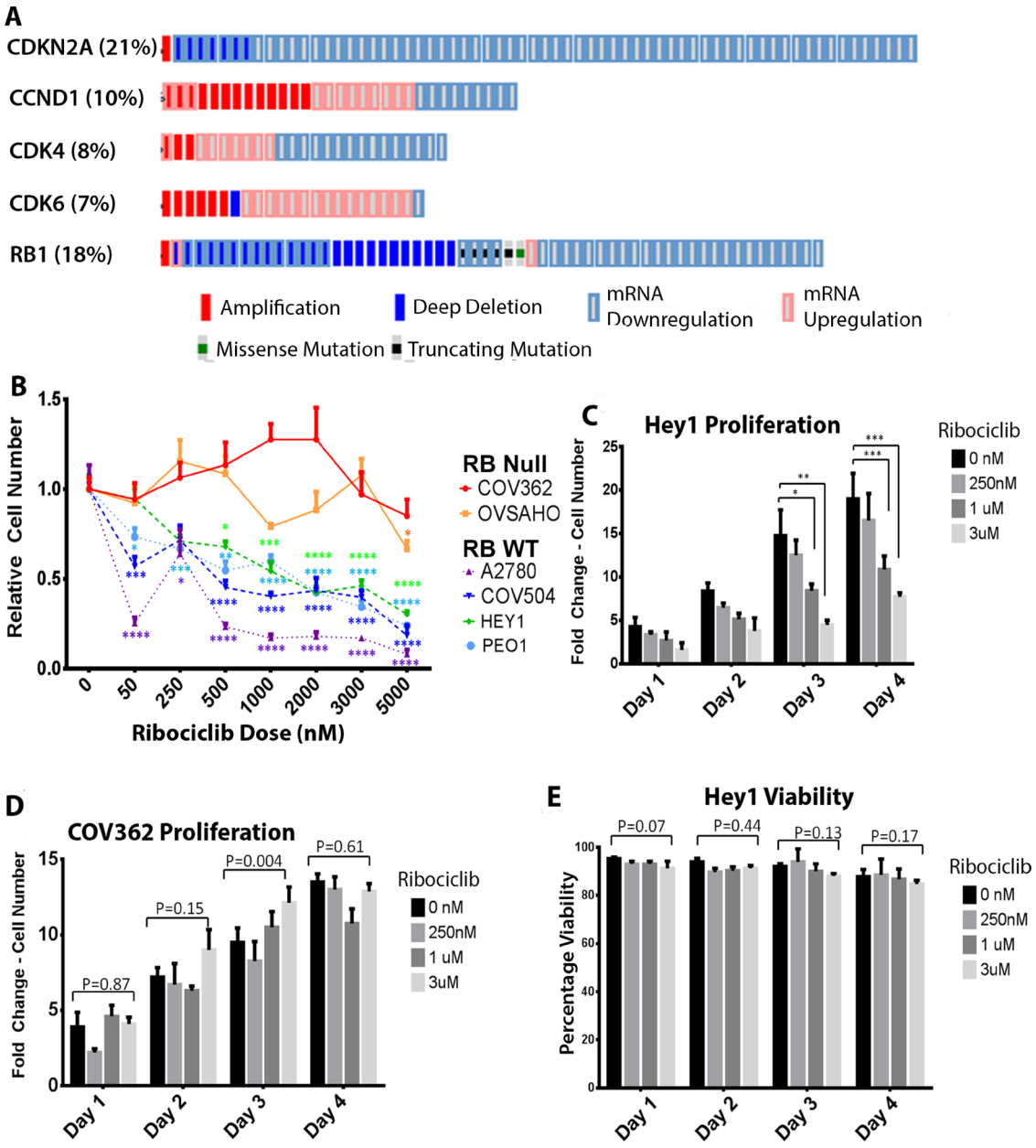

Figure 1: Ribociclib is a rational target in ovarian cancer. (**A**) Analysis of 316 tumors from the TCGA database showing mutations and mRNA dysregulation of genes known to regulate the G1-S phase transition. (**B**) Cell numbers as a proportion of untreated control cell numbers in the indicated cell lines after 72 hours of treatment with the indicated doses of Ribociclib. (**C**) Fold-change in cell number over time in Hey1 cells (Rb^{WT}) treated with the indicated doses of Ribociclib. (**D**) Fold-change in cell number over time in COV362 cells (Rb^{null}) treated with the indicated doses of Ribociclib. (**E**) Analysis of cellular viability in Hey1 cells treated with the indicated doses of Ribociclib. All samples were analyzed at least in triplicate with each experiment performed three times. $^{*}p < 0.05$, $^{**}p < 0.01$, $^{***}p < 0.001$, $^{****}p<0.0001$ by two-sample, two-tailed *t*-tests comparing the indicated values in C and D and one-way ANOVA comparing groups in B.

(SAβG) with Ribociclib treatment. Consistent with prior reports, we observed a clear increase in SAβG staining in treated Hey1 cells with increasing concentrations of Ribociclib (Figure 3Ai), with >95% of cells showing strong SAβG staining after three days of treatment (Figure 3Aii). Senescent cells are also reported to increase expression of numerous secretory proteins including CSF2, IL1A, IL6, ANG, HRG, and SERPINB1 (reviewed in [24]). However, Ribociclib treatment of Hey1 cells led to mRNA induction in only three of the six selected genes encoding senescence associated secretory proteins (Figure 3B).

Truly senescent cells are believed to permanently exit the cell cycle and should be unable to resume proliferation [25]. Even though cells treated with high-dose Ribociclib for 3 days demonstrate >95% SABG staining (Figure 3Ai-ii), cells demonstrate a stable albeit slow proliferation rate during treatment (Figure 1C). In addition, cells treated with Ribociclib for 5 days and then allowed to grow without the drug (termed "recovery") resumed cycling after the drug washout, indicating a lack of true senescence (Figure 3C). Continued cell growth could be related to either a subpopulation of resistant cells or slower proliferation in the majority of cells. To evaluate this, we performed time lapse microscopy of (i) control cells, (ii) cells treated with high dose Ribociclib (3 μM) for 5 days followed by drug washout (incubation without drug in control growth medium), or (iii) cells with continuous Ribociclib (3 μM) treatment. After normalization for cell numbers, control cells and cells treated with Ribociclib followed by washout demonstrated similar proliferation rates (Figure 3Di). Image analysis confirmed proliferation of >70% of cells in each group, demonstrating that most cells can resume proliferation following Ribociclib washout. Furthermore, image analysis of cells maintained in continuous Ribociclib treatment demonstrated that >70% of cells were actively proliferating, but at a slower

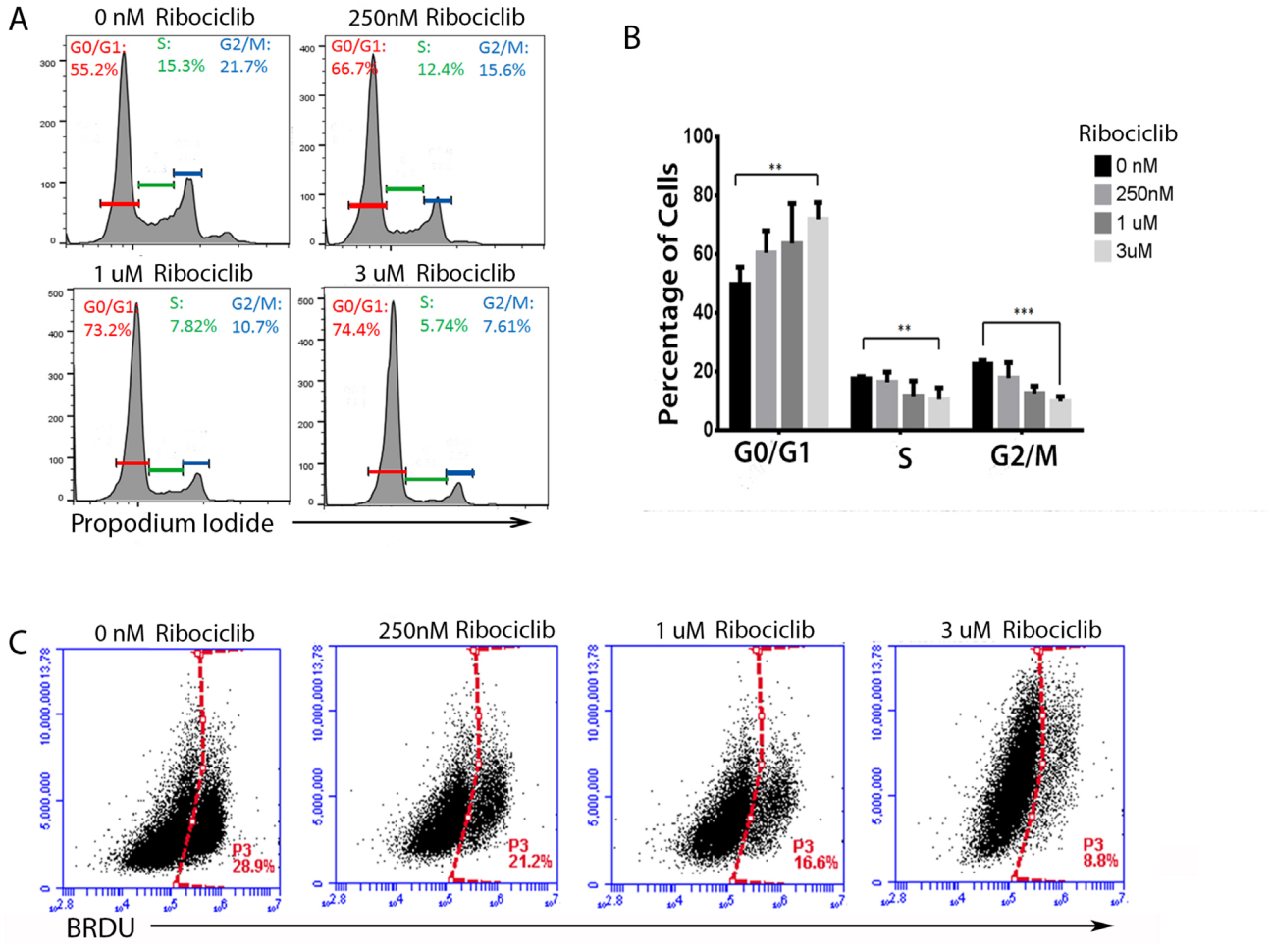

Figure 2: Ribociclib treatment leads to G1 arrest and decreased BrdU incorporation. (**A**) Representative cell cycle profiles of Hey1 ovarian cancer cells treated with Ribociclib for 72 h and (**B**) summary of cell cycle phase shifts. (**C**) BrdU incorporation in Hey1 ovarian cancer cells after 72 h of treatment with the indicated doses of Ribociclib. All samples were analyzed in triplicate with each experiment replicated at least once. FACS samples counted at least 10,000 events. $^{*}p < 0.05$, $^{**}p < 0.01$, $^{***}p < 0.001$ by two-sample, two-sided *t*-test.

rate compared to the control and Ribociclib washout groups (Figure 3Dii). Therefore, it appears that rather than rapid proliferation of a small, resistant subpopulation, most cells continue to cycle at a slow rate when treated with Ribociclib, rather than entering a state of complete growth arrest. Together, these data suggest that CDK4/6 inhibition does not induce a truly senescent state in ovarian cancer cells.

Ribociclib potentiates the impact of cisplatin

Platinum-based chemotherapy is the standard of care for first-line treatment in ovarian cancer. We therefore investigated the combined impact of treatment with Ribociclib and cisplatin. We treated Hey1 ovarian cancer cells with 1ug/mL cisplatin alone or cisplatin in combination with Ribociclib (0 nM, 250 nM, 1 uM, or

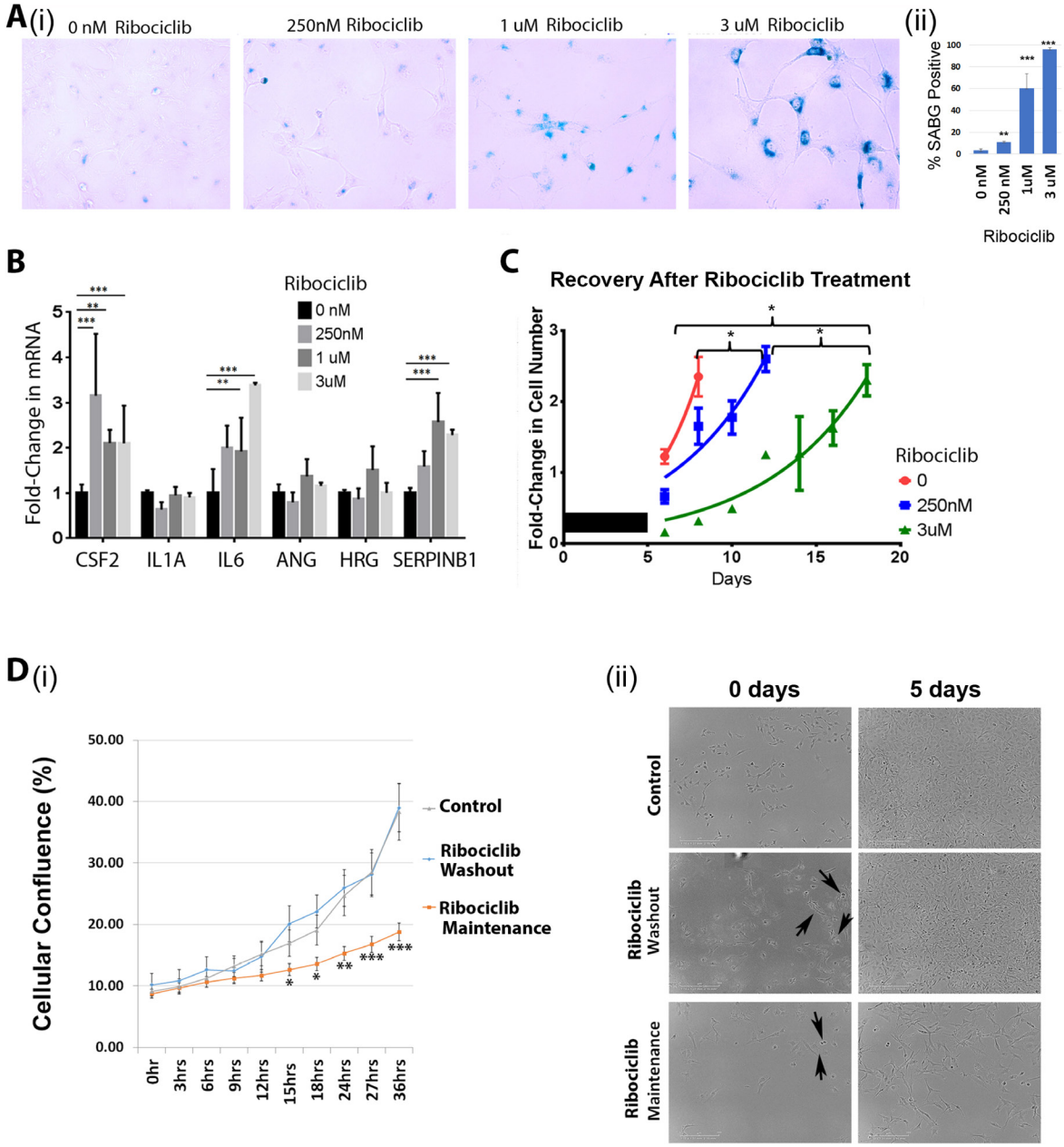

Figure 3: Ribociclib induces a pseudosenescent state in ovarian cancer cells. (**A**) Senescence-associated β-galactosidase staining (i) and quantification (ii) following a 72 h treatment of Hey1 cells with the indicated dose of Ribociclib. (**B**) qRT-PCR analysis of mRNA expression of senescence-associated secretory genes after a 72 h treatment with the indicated dose of Ribociclib. (**C**) Fold-change in cell numbers of Hey1 cells after 5 days of treatment with the indicated dose of Ribociclib or vehicle (black bar) followed by discontinuation of treatment. (**D**)(i) Graph of confluence of control cells and cells treated continuously with Ribociclib for 5 days and then either maintained on therapy or washed and given fresh media 24 hours prior to monitoring. (ii) Representative photomicrographs from representative wells of the indicated treatment conditions in panel (i) at the start and end of imaging. Arrows indicate cells observed to be dividing. All samples were analyzed in triplicate with each experiment replicated at least once. $^{*}p < 0.05$, $^{**}p < 0.01$, $^{***}p < 0.001$ by two-sample, two-sided *t*-tests.

3 uM). Consistent with previous reports and the known mechanism of cisplatin-induced DNA damage preventing cell cycle progression [26, 27], we observed that cisplatin treatment led to accumulation of cells in the S/G2/M phases of the cell cycle 24–48 hours after treatment (Figure 4A–4B). Cells treated with cisplatin alone recovered, with normalization of the cell cycle in surviving cells at 72 hours (Figure 4C). In contrast, the addition of Ribociclib to cisplatin significantly decreased the ability of cancer cells to move past the G2/M restriction point and back into a normal cell cycling pattern in a dose-dependent manner (Figure 4A–4C). 72 hours after treatment, the majority of cells treated with cisplatin and 3 uM Ribociclib remained in the G2/M peak (Figure 4C).

Given these results, we next used MTT assays to quantify the effects of Ribociclib on absolute and relative cell numbers remaining after cisplatin chemotherapy. Concurrent treatment with Ribociclib and cisplatin for 72 hours led to a decrease in the absolute number of surviving Hey1 cells (Supplementary Figure 2Ai). Normalization for the impact of Ribociclib on cell proliferation demonstrated a similar rate of cellular kill (Supplementary Figure 2Bi). Conversely, while pre-treatment with Ribociclib for 24 hours before chemotherapy led to a decrease in the absolute number of cells (Supplementary Figure 2Aii), normalization of cell numbers to adjust for cell number decrease related to Ribociclib exposure suggested that cell cycle arrest with Ribociclib prior to cisplatin exposure resulted in a higher proportion of surviving cells (Supplementary Figure 2Bii). When pre-treatment with Ribociclib was followed by a 24 hr washout period before cisplatin treatment, this effect disappeared (Supplementary Figure 2Aiii, 2Biii).

We further evaluated the timing of therapy and the addition of Ribociclib maintenance therapy using cancer cell recovery assays. Ribociclib maintenance therapy (initiated 72 hrs after initial treatment with cisplatin), potently synergized with cisplatin in the COV504, PEO1, and Hey1 ovarian cancer cell lines; in fact, control cells recovered effectively after cisplatin therapy, while cells treated with 1 uM or 3 uM Ribociclib as maintenance after cisplatin therapy remained unable to proliferate throughout the two-week observation period (Figure 4D; Supplementary Figure 3A). Combination indices for TD50 doses of cisplatin and doses of Ribociclib 250 nm–3 uM ranged from 0.2–0.39. Co-treatment for 3 days with Ribociclib and cisplatin, followed by no maintenance therapy (Figure 4E; Supplementary Figure 3C) effectively delayed cell growth, but the Hey1 and PEO1 cells resumed proliferation in the absence of continued Ribociclib treatment. Continued therapy with 1 uM or 3 uM Ribociclib effectively prevented cells from proliferating (Figure 4F; Supplementary Figure 3B). As seen in the MTT assays, pretreatment of cells with Ribociclib prior to cisplatin therapy was not an effective therapeutic regimen (Supplementary Figure 3D).

Ribociclib and Ribociclib + Cisplatin treatment decreases pCHK1

To verify on-target activity of Ribociclib, Hey1, COV504, and PEO1 cells were treated with increasing doses of Ribociclib either alone or combined with cisplatin, and lysates were collected for Western blot analysis of p-Rb. As predicted, Ribociclib treatment resulted in dose-dependent inhibition of Rb phosphorylation (Figure 5A–5C). Interestingly, co-treatment with Ribociclib and cisplatin decreased both pRB and total RB.

The potentiation of the impact of cisplatin with extended arrest of cells in the G2/M phase of the cell cycle data, as seen in Figure 4, suggests that CDK4/6 inhibition may have an unappreciated impact on the DNA damage response. We therefore evaluated the impact of Ribociclib on pATR and pChk1, which are known to participate in the DNA damage response. We found that in all three tested cell lines, Ribociclib decreased p-Chk1 in a dose dependent manner in the presence of cisplatin (Figure 5A–5C). pATR was similarly decreased in Hey1 cells (Figure 5A).

Ribociclib is effective alone and in combination with cisplatin *in vivo*

We next evaluated Ribociclib activity *in vivo* using platinum-sensitive PEO1 cell line xenografts. Ribociclib treatment (5 days on + 2 days off, as described in the dosing schedule in Figure 6A) was started three days after tumor initiation. Ribociclib treatment was as effective as cisplatin in slowing tumor growth in the PEO1 xenografts (Figure 6B). Cisplatin treatment, either as a single agent or concurrent with Ribociclib, followed by maintenance with Ribociclib, further restricted disease growth (Figure 6B; $p < 0.01$). No clear benefit of concurrent versus sequential therapy with cisplatin and Ribociclib was observed.

As platinum-resistance is an important clinical problem, we next evaluated the impact of single agent Ribociclib in the platinum-resistant Hey1 cell line. Compared to vehicle treatment, treatment with Ribociclib significantly delayed tumor growth ($p < 0.01$) (Figure 6Ci). Then, we tested the impact of Ribociclib as a maintenance therapy following cisplatin in Hey1 cells. Dosing schedules were established such that all treatment groups received two doses of cisplatin weekly and five doses of Ribociclib weekly (Figure 6A). The addition of Ribociclib maintenance therapy after cisplatin resulted in a ~40% increase in time to tumor endpoint (defined as a total tumor burden >2,000 mg per mouse, >10% weight loss, tumor ulceration, or poor health of the animal) (Figure 6Cii). We also evaluated the impact of concurrent cisplatin+Ribociclib followed by Ribociclib maintenance vs. cisplatin alone followed by Ribociclib maintenance therapy. In this platinum-resistant cell line, there was

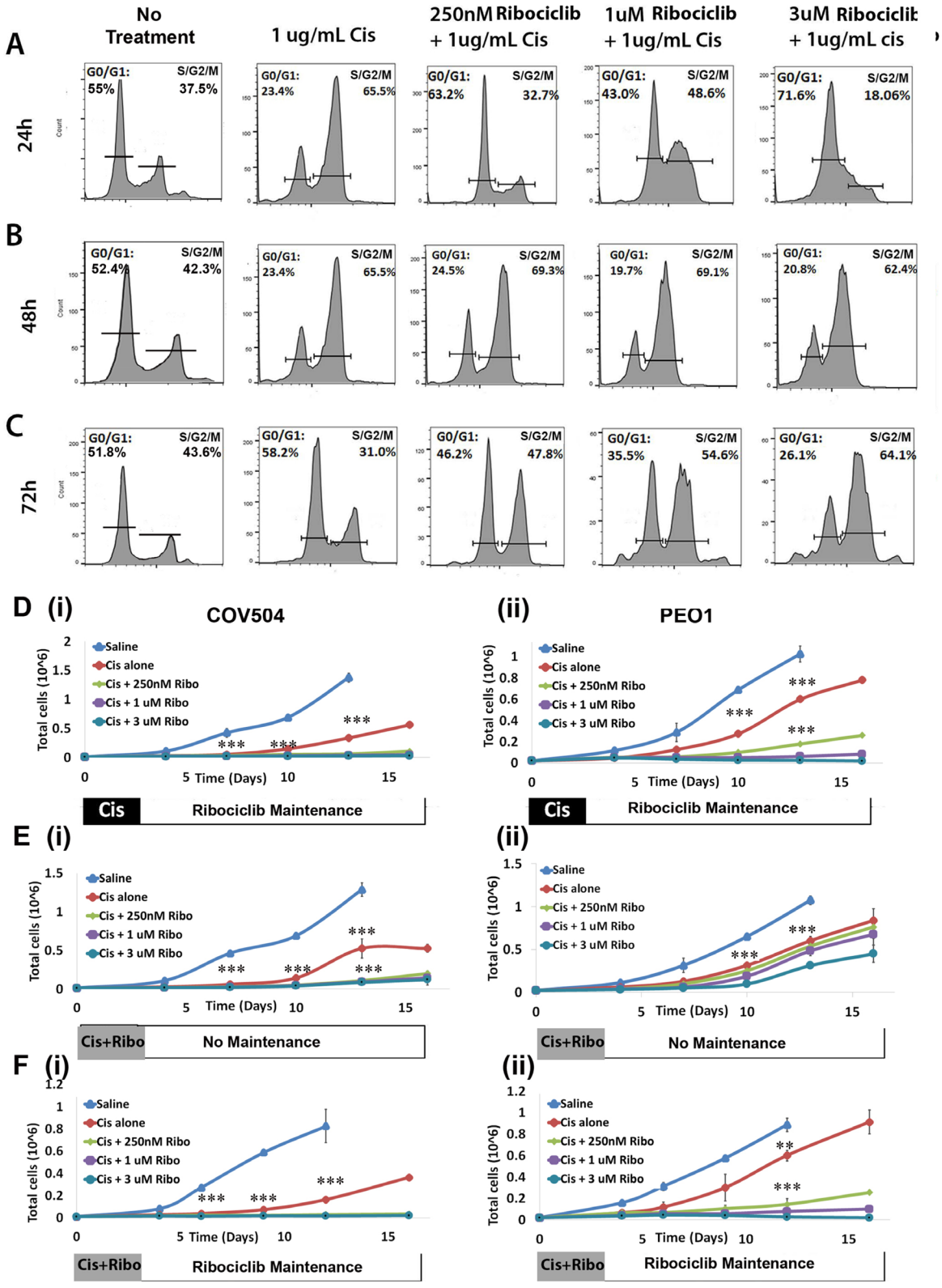

Figure 4: Ribociclib enhances cisplatin-induced G2/M arrest. Cell cycle phase diagrams after 24 h (**A**), 48 h (**B**), and 72 h (**C**) of treatment with cisplatin alone or concurrent 1ug/mL cisplatin and the indicated dose of Ribociclib, or no treatment. (**D**) Absolute cell counts in (i) COV504 and (ii) PEO cells after treatment with cisplatin followed by maintenance Ribociclib. (**E**) Absolute cell counts in (i) COV504 and (ii) PEO cells after concurrent treatment with cisplatin and Ribociclib without maintenance Ribociclib. (**F**) Absolute cell counts in (i) COV504 and (ii) PEO1 cells after concurrent treatment with cisplatin and Ribociclib followed by maintenance Ribociclib. All samples were analyzed in triplicate with each experiment replicated at least once. $^{*}p < 0.05$, $^{**}p < 0.01$, $^{***}p < 0.001$ by two-sided, two-tailed *t*-tests.

no additional benefit of concurrent therapy versus maintenance alone (Figure 6Ciii).

Finally, we performed immunohistochemical analysis of the treated PEO1 xenografts. Cisplatin+ Ribociclib-treated tumors demonstrated large acellular regions (Figure 6Di–ii). Immunohistochemical analysis of PEO1 tumors demonstrated a clear decrease in both p-Rb and Ki67 (Figure 6Di–iii) in Ribociclib-treated tumors, indicating on-target activity and efficacy. The greatest decrease in pRb was observed in tumors treated with cisplatin and Ribociclib.

DISCUSSION

We investigated the effects of Ribociclib as combination and maintenance therapy for high grade serous ovarian cancer (HGSOC). Given that multiple previous reports have shown dysregulated cell cycle gene expression within the known CDKN2A/Cyclin D1-CDK4-CDK6/Rb axis, CDK4/6 inhibition represents a promising approach in ovarian cancer. The tumor suppressor CDKN2A has been shown to be dysregulated through multiple mechanisms, including promoter methylation

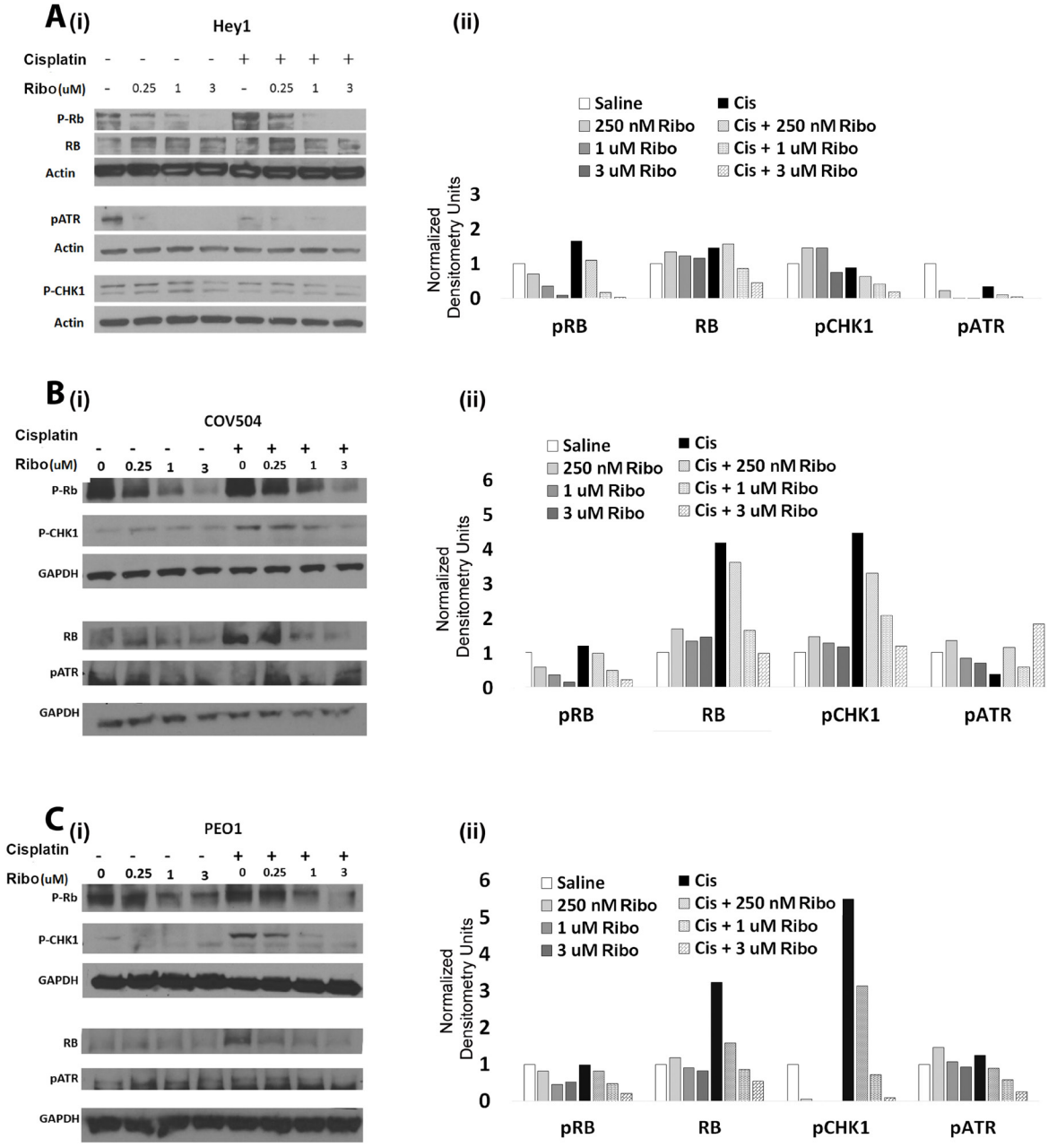

Figure 5: Ribociclib decreases pRb, ATR, and Chk1 alone and in combination with cisplatin. (i) Western blot evaluation and (ii) densitometric quantification of total Rb, p-Rb, p-Chk1, and p-ATR in Hey1 (**A**), COV504 (**B**), and PEO1 (**C**) cells after 72 hours of the indicated doses of Ribociclib or a single dose of cisplatin followed by three days of Ribociclib. Gels have been cropped for clarity. All samples were analyzed in triplicate with each experiment replicated at least once for each cell line.

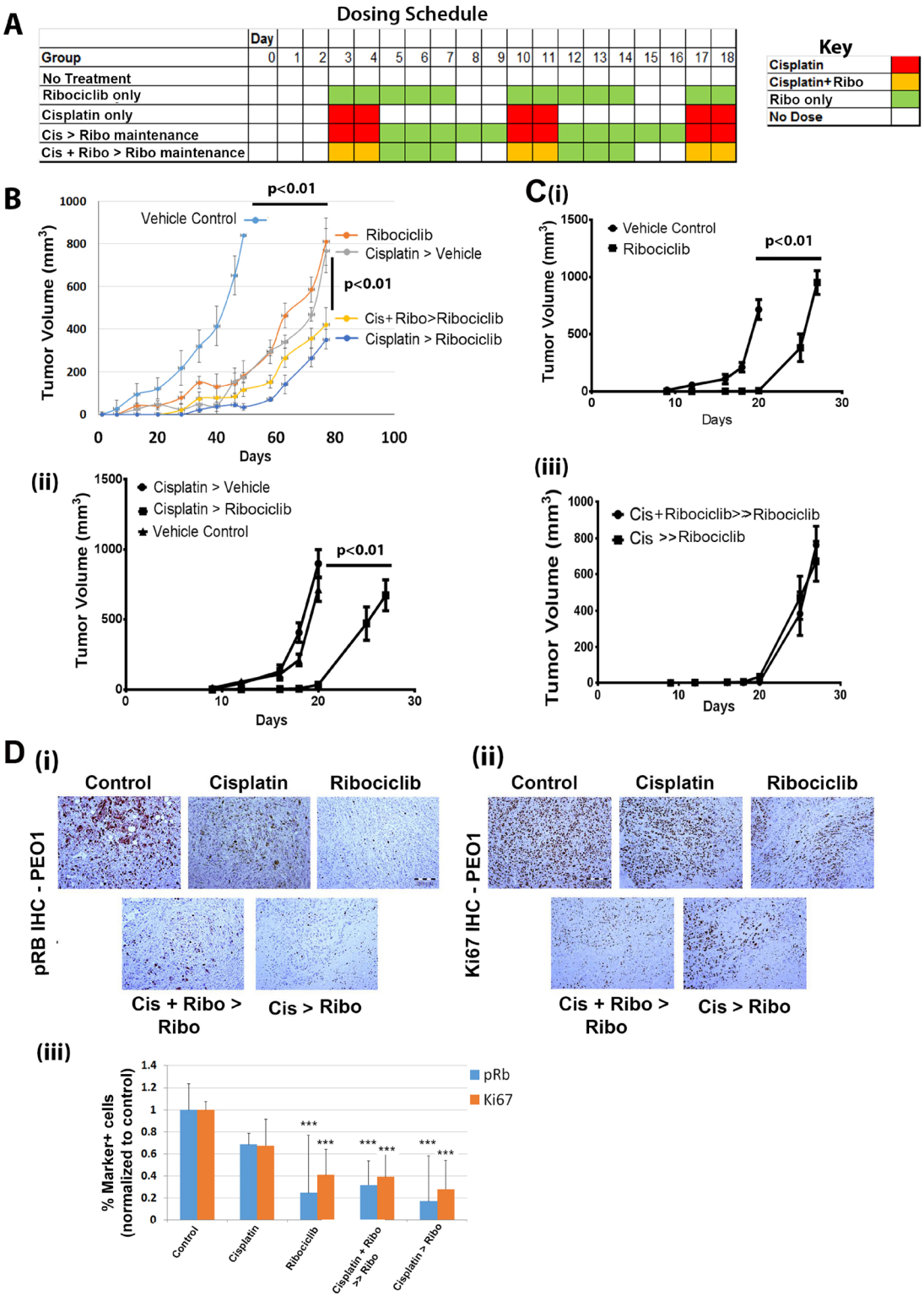

Figure 6: Ribociclib decreases Hey1 and PEO1 ovarian cancer tumor xenograft growth in combination with cisplatin. (**A**) Sample dosing schedule for Ribociclib-only maintenance therapy and various combinations of sequential and concurrent treatment with cisplatin and Ribociclib. (**B**) Tumor growth in platinum-sensitive PEO1 xenografts treated with the indicated combinations of cisplatin with or without concurrent Ribociclib treatment and with or without Ribociclib maintenance therapy. (**C**) Hey1 tumorxenograft growth when treated with (i) vehicle vs. Ribociclib, (ii) vehicle control vs. cisplatin followed by vehicle (Cisplatin > vehicle) vs. cisplatin followed by Ribociclib maintenance (Cisplatin > Ribociclib), or (iii) cisplatin concurrent with Ribociclib followed by Ribociclib maintenance (Cis + Ribociclib > Ribociclib) vs. cisplatin alone followed by Ribociclib maintenance (Cis > Ribociclib). (**D**) IHC analysis of (i) pRB and (ii) Ki67 in tumors from the indicated treatment groups, and (iii) quantification of pRB and Ki67 marker-positive cells in the in the indicated treatment groups. Five high power fields from three sections of three tumors in each group were scored. $^{***}p < 0.001$ relative to the control.

in 40% of cases in one series [28] and homozygous deletions in 18% of another series [29]. Abnormal CDK4 expression was found in 14–16% of patients in one series and did not differ by tumor stage [30], consistent with a 14% aberrant CDK4 expression rate found through Northern blot analysis in another study [31]. Cyclin D1 was found to be overexpressed in 19% of ovarian tumors in one study, which was correlated with poor prognosis [32]. Rates of RB loss or aberrant expression vary widely, and have ranged from 8–78%, (reviewed in [20]). In our study, mutational analysis of TCGA ovarian cancer data has shown that a significant percentage of patients have mutations or dysregulated expression of CDKN2A, CDK4, CDK6, or CCND1 that would likely make them good candidates for CDK4/6 inhibitor therapy (Figure 1A). However, 17% of ovarian cancer patients in the TCGA database also have homozygous deletions or significantly downregulated RB1; these patients are less likely to receive significant benefit from CDK4/6 inhibitor therapy. Consistent with this mechanism, previous reports have shown that CDKN2A-low/RB1-proficient ovarian cancer cells were most responsive to CDK4/6 inhibition [14] and that RB1 loss was a mechanism of resistance to CDK4/6 inhibition. The correlations between mutational status and response to CDK4/6 inhibition are also clear in breast cancer, where downregulation of CDKN2A and amplification of CDK4 or CDK6 were correlated with sensitivity to CDK4/6 inhibition [7]. This is also concordant with our data showing that ovarian cancer cell lines carrying RB deletions are insensitive to Ribociclib as single-agent therapy.

Several studies have reported that CDK4/6 inhibition can induce cellular senescence [33–35]. Traditionally, senescence is considered to be irreversible exit from the cell cycle into the G0 phase with expression of a suite of senescence-associated secretory markers (reviewed in [24]). Through these secretory factors, senescent cells can promote malignant progression without actively dividing. Despite the traditional association of senescence with the G0 phase, one known mechanism of senescence begins with the tumor suppressor $p16^{Ink4a}$ (CDKN2A), which inhibits Rb inactivation by CDK4 and CDK6, leading to failure to transition from G1 phase into S phase [36, 37]. Therefore, it is possible that CDK4/6 inhibition by Ribociclib could lead to replicative senescence. In our study, Ribociclib treatment was associated with a pseudo-senescent-phenotype *in vitro*; cells showed strong induction of SAβG with partial mRNA induction of some known senescence associated secretory proteins. However, cells continued to proliferate after drug washout, even after a long exposure. Indeed, the majority of cells could proliferate even in the presence of high-dose Ribociclib, albeit more slowly. Based on our data, cell cycle retardation delays tumor growth and can serve as an effective treatment. Given that cells do not truly senesce, continuous therapy will be necessary. However, given the pro-inflammatory and pro-tumorigenic nature of senescence-associated secretory proteins, further investigation is required to better characterize this pseudo-senescent state.

Interestingly, we have observed significant synergy (CI 0.2–0.4) between Ribociclib and cisplatin. While Ribociclib alone retards but does not completely block cell proliferation, the combination of concurrent and maintenance Ribociclib with and after cisplatin *in vitro* arrested cell growth. This was associated with a prolonged arrest of cells in G2/M phase (Figure 4A-C). We hypothesize that this arrest may be related to the known functions of CDKs in the DNA damage response (reviewed in [38, 39]), which is essential for response to and recovery from cisplatin exposure [40]. In particular, cells can become sensitized to cisplatin after ATR depletion [41]; a recent report shows that CDK6 regulates transcription of ATR, and that CDK6 inhibition therefore sensitizes epithelial ovarian cancer cells to death from cisplatin due to an impaired DNA damage response [42]. We found that Ribociclib treatment was associated with a decrease in p-Chk1 in all tested ovarian cancer cells and in ATR in the Hey1 cell line. ATR or Chk-1 mediated dysregulation of the DNA damage response may help to explain the prolonged growth arrest seen with the combination of Ribociclib and cisplatin.

We observed that Ribociclib significantly delayed tumor growth in *in vivo* xenograft experiments when used as a single agent and after cisplatin treatment. Interestingly, Ribociclib therapy was as effective as cytotoxic cisplatin therapy *in vivo* in platinum-sensitive cells, and it had significant activity in platinum-resistant cells. In platinum-sensitive cells, cisplatin + Ribociclib followed by Ribociclib maintenance therapy was not superior to cisplatin alone followed by maintenance therapy. This may be partly because tumor volume measurements were misleading due to large regions of acellular tissues. Previous studies have suggested that concurrent CDK4/6 inhibition with platinum may decrease chemotherapeutic effectiveness [14, 43] as it decreases the cell cycling rate. However, we find that the timing of drug administration is critical, with pre-administration of Ribociclib increasing resistance to cisplatin, but concurrent therapy enhancing efficacy. Given the competing roles of Ribociclib during initial cisplatin therapy in the cytostatic G1-arrest response vs. recovery after cisplatin and the DNA damage response, further studies are necessary to investigate this balance.

In conclusion, CDK4/6 inhibition with Ribociclib showed significant activity against both platinum-sensitive and platinum-resistant cell lines both *in vitro* and *in vivo*. This drug shows significant combinatorial effects with cisplatin, resulting in prolonged times to cellular recovery *in vitro* and restriction of tumor growth *in vivo*. Further research regarding specific mechanisms by which

this drug combination affects cell cycling and the DNA damage response as well as clinical impacts is required.

MATERIALS AND METHODS

Cell lines

The A2780 cell line (Rb^{WT}; platinum-sensitive) was obtained from Dr. Susan Murphy at Duke and was used at passages 12–14. COV504 (Rb^{WT}; platinum-sensitive) and OVSAHO (Rb^{null}; platinum-sensitive) lines were obtained from Dr. Deborah Marsh at the University of Sydney and were used from passages 5–10. The COV362 (Rb^{null}; platinum-sensitive) line was obtained from ATCC and used from passages 6–12. The PEO1 cell line (Rb^{WT}; platinum-sensitive) was purchased from Sigma-Aldrich in 12/2016, which uses STR profiling for cell line authentication. The Hey1 cell line (Rb^{WT}; platinum-resistant) was obtained from Rebecca Liu at the University of Michigan. The A2780, COV504, Hey1, OVSAHO, and COV362 lines underwent STR profiling in 2/2017 with the American Type Culture Collection (ATCC) for validation; the PEO1 line was not profiled as it had been purchased two months previously. In 2016, the A2780, Hey1, and OVSAHO cell lines tested positive for mycoplasma and were successfully treated with the MycoZap-5 kit (Lonza) and monitored every six months using the MycoAlert detection kit (Lonza) with no subsequent evidence of infection. Hey1, A2780, and COV504 lines were cultured in RPMI-1640 media with 10% FBS and 1% Penicillin/Streptomycin at 37° C and 5% CO2. OVSAHO, PEO1, and COV362 lines were cultured in DMEM with 10% FBS and 1% Penicillin/Streptomycin at 37° C and 5% CO_2.

Cell cycle analysis

Hey1 and COV362 cells were grown in 6-well plates in triplicate and treated for 72 hours with 0, 250 nM, 1 uM, or 3 uM Ribociclib (initially purchased from Selleckchem, later generously provided by Novartis) for three days. Cells were then harvested, fixed dropwise in 70% ethanol, and incubated with 0.1 ug/mL RNAse for 1h at 37° F. 1 ug/mL propidium iodide was added and then cells were run on the BD Accuri C6 flow cytometer (Becton Dickinson) and analyzed with FlowJo Version 10. 10,000 events were used for each sample.

Senescence analysis

Hey1 cells were grown in 6-well dishes in triplicate and treated for three days with 0, 250 nM, 1 uM, or 3 uM Ribociclib. Each well was stained overnight for senescence-associated β-galactosidase with the Senescence β-galactosidase Assay Kit (Cell Signaling) according to the manufacturer's instructions. Images were quantified as described in the Statistics section.

Western blots

Western blots were performed as previously described [44]. Briefly, Hey1, COV504, or PEO1 cells were cultured with various concentrations of Ribociclib (clinical grade provided by Novartis) and cisplatin (clinical grade purchased from the University of Michigan Pharmacy) for 3 days, lysed in RIPA buffer (Pierce) with complete protease inhibitor (Roche), and quantified by Bradford assay (Pierce) per the manufacturer's instructions. Then, 100 ug of protein were loaded onto a 4–12% NuPAGE SDS gel (Thermo Fisher) and transferred to a PVDF membrane (Thermo Fisher). Membranes were incubated overnight with 1:1000 anti-RB, 1:1000 anti-pRB-S807/811, 1:1000 anti-pCHK1, or 1:1000 anti-pATR (all from Cell Signaling) at room temperature and then washed and incubated for 1h with 1:10,000 anti-mouse HRP or anti-rabbit HRP (Cell Signaling). Visualization was performed with ECL Plus Western Blotting Substrate (Pierce). Densitometry and quantification were subsequently performed with ImageJ.

qRT-PCR

Hey1 cells were grown in 6-well dishes and treated for three days with 0, 250 nM, 1 uM, or 3 uM Ribociclib. Total RNA was extracted with an RNeasy Mini Kit (Qiagen) and quantified with a Nanodrop 1000 (Thermo Scientific). 1 ug RNA was converted to cDNA with a SuperScript III Reverse Transcriptase cDNA Kit (Life Technologies) per the manufacturer's instructions, and 10 ng of cDNA was used for each reaction. qRT-PCR was performed for 40 cycles using SYBR dye (Applied Biosystems) as recommended by the manufacturer, with primers at 100 nM concentrations each.

Primers for senescence-associated qRT-PCR genes are as follows: CSF2, F-5′-GCTGTCTACGTCGG GATGC-3′, R-5′- GACCATGCGATCCACCTCTC-3′; IL 1A, F-5′- TGGTAGTAGCAACCAACGGGA-3′, R-5′- ACTTTGATTGAGGGCGTCATTC-3′; IL6, F-5′- ACT CACCTCTTCAGAACGAATTG-3′, R-5′- CCATCTTT GGAAGGTTCAGGTTG-3′; ANG F-5′- AGCGCC GAAGTCCAGAAAAC-3′, R-5′- TACTCTCACGACAGT TGCCAT-3′; HRG F-5′- CGGTGTCCATGCCTTCCAT-3′, R-5′- GCGAGTTTCTTAACAGGCTCT-3′; and SERP INB1 F-5′- TTCCTGGCGTTGAGTGAGAAC-3′, R-5′- CTGCCGTGTTACCTCTGGTC-3′. Melt curves were performed to ensure a uniform product, and expression was then normalized to B-Actin with the ΔΔCT method.

MTT assays

2,000 Hey1 cells were plated into each well of a 96-well plate and treated with various combinations of 1 ug/mL cisplatin and 0, 250 nM, 1 uM, and 3 uM Ribociclib for up to five days, as described in Supplementary Figure 2. Then, media was removed and cells were incubated with

MTT and SDS using the Vybrant MTT Cell Proliferation Assay Kit (ThermoFisher Scientific) as described in the manufacturer's protocol. Absorbance was read at 570 nM and was normalized for the impact of Ribociclib on cell proliferation for analysis.

Recovery assays

20,000 Hey1, PEO1, or COV504 cells were plated in 12-well dishes and treated with various combinations of Ribociclib and cisplatin. Thereafter, cells were counted every 2–3 days in triplicate with trypan blue exclusion and the recovery of cell number was plotted. Experiments were terminated when cells reached confluence.

Tumor xenograft experiments

All animal experiments were approved by the University of Michigan Institutional Review Board and the University of Michigan Institutional Animal Cases and Use Committee (IACUC). Nod/SCID/Gamma (NSG) mice were raised under SPF conditions with a 12 hr dark/light cycle and ad-libitum chow and drinking water. Mice were injected subcutaneously with 100,000 Hey1 or PEO1 cells on Day 0 of each experiment. Three days later, mice were treated with PBS, vehicle (1% methylcellulose), cisplatin, Ribociclib, or cisplatin + Ribociclib, according to the dosing schedule provided in Figure 6A. Tumors were measured twice a week with calipers and tumor volumes were calculated using the modified ellipsoid formula: volume = $(L*W^2)/2$. Tumor weights were collected when mice were sacrificed at the tumor endpoint, which was defined in our IACUC protocol as a tumor burden >2000 mm^3 per mouse, >10% weight loss, poor health of the animal, or tumor ulceration. Mice were euthanized when they reached any of these tumor endpoints, and growth curves were plotted for each drug or drug combination. Three animals in each group were sacrificed when animals reached 400–500 mm^3 for IHC analysis of tumors during active treatment.

IHC

IHC for Ki67 and pRb was performed by the UMCC histology core on tumors harvested at a volume of 400-500 mm^3 to minimize central tumor necrosis and better define tumor histology. Ki67 staining was performed as previously described [45]. For pRB, formalin-fixed paraffin-embedded sections were cut at 5-micron thickness and rehydrated with water. Heat induced epitope retrieval was performed with FLEX TRS High pH Retrieval buffer (9.0) for 20 minutes for pRB (Ser 807/811, 1:400) (Cell Signaling, D20B12) and Ki-67 (rabbit monoclonal, Cell Marque 1:2:50). The Dako EnVision+ Rabbit or Mouse System, as appropriate, was used for detection per the manufacturer's protocol. DAB chromagen was then applied for 10 minutes. Slides were counterstained with Harris Hematoxylin for 5 seconds and then dehydrated and coverslipped.

Statistical analysis

In vitro experiments were repeated independently at least three times with triplicate samples in each experiment, unless indicated otherwise. All mouse studies were performed with $n = 10$ tumors per group, based on a final tumor volume of ~1000 mm^3 in control animals and an expected standard deviation of 30%. For SABG analysis, five high power fields from three technical replicates in each treatment group were scored. Similarly, for tumor IHC analysis, five high power fields from three sections of three tumors in each group were scored as previously described [45, 46]. Statistical significance for continuous variables was evaluated using a 2-sided student's *T*-test or one-way ANOVA, as appropriate, with *p*-values < 0.05 denoting significance. Error bars in figures represent standard error of the mean unless denoted otherwise. Synergy analysis was performed using 12 day time points using the Chou-Tataly median effects method [47] and calculated using Compusyn software (http://www.combosyn.com).

Author contributions

Mangala Iyengar—Designed and performed experiments, drafted manuscript; Patrick O'Hayer—Designed and performed experiments, edited manuscript; Alex Cole—Designed and performed experiments, edited manuscript; Tara Sebastian–Performed experiments; Kun Yang- Performed experiments; Lan Coffman–Designed experiments, experimental interpretation, edited manuscript; Ronald J Buckanovich–Designed experiments, experimental interpretation, edited manuscript, provided funding.

CONFLICTS OF INTEREST

The authors declare no potential conflicts of interest.

FINANCIAL INFORMATION

This work was supported by the Department of Defense award #W81XWH-15-1-0083. M Iyengar was supported by NIH F30 CA189316-01 award and a University of Michigan Rackham Graduate Student Research grant. We would like to thank the UMCC histology core for assistance with IHC. UMCC cores were supported by NIH P30 CA046592. Ribociclib was provided by Novartis.

Editorial note

This paper has been accepted based in part on peer-review conducted by another journal and the authors' response and revisions as well as expedited peer-review in Oncotarget.

REFERENCES

1. Aletti GD, Gallenberg MM, Cliby WA, Jatoi A, Hartmann LC. Current Management Strategies for Ovarian Cancer. Mayo Clinic Proceedings. 2007; 82:751–70. http://doi.org/10.4065/82.6.751.
2. Siegel RL MK, Jemal A. Cancer statistics, 2015. CA Cancer J Clin. 2015; 65:5–29.
3. Markman M, Bookman MA. Second-Line Treatment of Ovarian Cancer. The Oncologist. 2000; 5:26–35. https://doi.org/10.1634/theoncologist.5-1-26.
4. Sherr CJ, Beach D, Shapiro GI. Targeting CDK4 and CDK6: From Discovery to Therapy. Cancer Discovery. 2016; 6:353–67. https://doi.org/10.1158/2159-8290.cd-15-0894.
5. Rader J, Russell MR, Hart LS, Nakazawa MS, Belcastro LT, Martinez D, Li Y, Carpenter EL, Attiyeh EF, Diskin SJ, Kim S, Parasuraman S, Caponigro G, et al. Dual CDK4/CDK6 Inhibition Induces Cell Cycle Arrest and Senescence in Neuroblastoma. Clinical cancer research : an official journal of the American Association for Cancer Research. 2013; 19:10.1158/078-0432.CCR-13-1675. https://doi.org/10.1158/1078-0432.CCR-13-1675.
6. Zhang YX, Sicinska E, Czaplinski JT, Remillard SP, Moss S, Wang Y, Brain C, Loo A, Snyder EL, Demetri GD, Kim S, Kung AL, Wagner AJ. Antiproliferative Effects of CDK4/6 Inhibition in CDK4-Amplified Human Liposarcoma *In Vitro* and *In Vivo*. Molecular Cancer Therapeutics. 2014; 13:2184–93. https://doi.org/10.1158/1535-7163.mct-14-0387.
7. Finn RS, Dering J, Conklin D, Kalous O, Cohen DJ, Desai AJ, Ginther C, Atefi M, Chen I, Fowst C, Los G, Slamon DJ. PD 0332991, a selective cyclin D kinase 4/6 inhibitor, preferentially inhibits proliferation of luminal estrogen receptor-positive human breast cancer cell lines *in vitro*. Breast Cancer Research : BCR. 2009; 11:R77–R. https://doi.org/10.1186/bcr2419.
8. Leonard JP, LaCasce AS, Smith MR, Noy A, Chirieac LR, Rodig SJ, Yu JQ, Vallabhajosula S, Schoder H, English P, Neuberg DS, Martin P, Millenson MM, et al. (2012). Selective CDK4/6 inhibition with tumor responses by PD0332991 in patients with mantle cell lymphoma.
9. Priya Kadambi Gopalan MCP, Alberto Chiappori, Alison Marguerite Ivey, Andres Gordillo Villegas, Frederic J. Kaye; University of Florida, Gainesville, FL; H. Lee Moffitt Cancer Center & Research Institute, Tampa, FL. A phase II clinical trial of the CDK 4/6 inhibitor palbociclib (PD 0332991) in previously treated, advanced non-small cell lung cancer (NSCLC) patients with inactivated CDKN2A. J Clin Oncol. 2014 ASCO Annual Meeting; 32.
10. Vaughn DJ, Hwang WT, Lal P, Rosen MA, Gallagher M, O'Dwyer PJ. Phase 2 trial of the cyclin-dependent kinase 4/6 inhibitor palbociclib in patients with retinoblastoma protein-expressing germ cell tumors. Cancer. 2015; 121:1463–8. https://doi.org/10.1002/cncr.29213.
11. Finn RS, Crown JP, Lang I, Boer K, Bondarenko IM, Kulyk SO, Ettl J, Patel R, Pinter T, Schmidt M, Shparyk Y, Thummala AR, Voytko NL, et al. The cyclin-dependent kinase 4/6 inhibitor palbociclib in combination with letrozole versus letrozole alone as first-line treatment of oestrogen receptor-positive, HER2-negative, advanced breast cancer (PALOMA-1/TRIO-18): a randomised phase 2 study. The Lancet Oncology. 2015; 16:25–35. http://dx.doi.org/10.1016/S1470-2045(14)71159-3.
12. Finn RS, Martin M, Rugo HS, Jones S, Im SA, Gelmon K, Harbeck N, Lipatov ON, Walshe JM, Moulder S, Gauthier E, Lu DR, Randolph S, et al. Palbociclib and Letrozole in Advanced Breast Cancer. New England Journal of Medicine. 2016; 375:1925–36. https://doi.org/10.1056/NEJMoa1607303.
13. Hortobagyi GN, Stemmer SM, Burris HA, Yap YS, Sonke GS, Paluch-Shimon S, Campone M, Blackwell KL, André F, Winer EP, Janni W, Verma S, Conte P, et al. Ribociclib as First-Line Therapy for HR-Positive, Advanced Breast Cancer. New England Journal of Medicine. 2016; 375:1738–48. https://doi.org/10.1056/NEJMoa1609709.
14. Konecny GE, Winterhoff B, Kolarova T, Qi J, Manivong K, Dering J, Yang G, Chalukya M, Wang HJ, Anderson L, Kalli KR, Finn RS, Ginther C, et al. Expression of p16 and retinoblastoma determines response to CDK4/6 inhibition in ovarian cancer. Clin Cancer Res. 2011; 17:1591–602. https://doi.org/10.1158/1078-0432.ccr-10-2307.
15. Bonuccelli G, Peiris-Pages M, Ozsvari B, Martinez-Outschoorn UE, Sotgia F, Lisanti MP. Targeting cancer stem cell propagation with palbociclib, a CDK4/6 inhibitor: Telomerase drives tumor cell heterogeneity. Oncotarget. 2017; 8:9868–84. https://doi.org/10.18632/oncotarget.14196.
16. Taylor-Harding B, Aspuria PJ, Agadjanian H, Cheon DJ, Mizuno T, Greenberg D, Allen JR, Spurka L, Funari V, Spiteri E, Wang Q, Orsulic S, Walsh C, et al. Cyclin E1 and RTK/RAS signaling drive CDK inhibitor resistance via activation of E2F and ETS. Oncotarget. 2015; 6:696–714.
17. Patnaik A, Rosen LS, Tolaney SM, Tolcher AW, Goldman JW, Gandhi L, Papadopoulos KP, Beeram M, Rasco DW, Hilton JF, Nasir A, Beckmann RP, Schade AE, et al. Efficacy and Safety of Abemaciclib, an Inhibitor of CDK4 and CDK6, for Patients with Breast Cancer, Non–Small Cell Lung Cancer, and Other Solid Tumors. Cancer Discovery. 2016; 6:740–53. https://doi.org/10.1158/2159-8290.cd-16-0095.

18. DeMichele A, Clark AS, Tan KS, Heitjan DF, Gramlich K, Gallagher M, Lal P, Feldman M, Zhang P, Colameco C, Lewis D, Langer M, Goodman N, et al. CDK 4/6 Inhibitor Palbociclib (PD0332991) in Rb^+ Advanced Breast Cancer: Phase II Activity, Safety, and Predictive Biomarker Assessment. Clinical Cancer Research. 2015; 21:995–1001. https://doi.org/10.1158/1078-0432.ccr-14-2258.

19. Integrated genomic analyses of ovarian carcinoma. Nature. 2011; 474:609–15. https://doi.org/10.1038/nature10166.

20. Corney DC, Flesken-Nikitin A, Choi J, Nikitin AY. Role of p53 and Rb in Ovarian Cancer. Advances in experimental medicine and biology. 2008; 622:99–117. https://doi.org/10.1007/978-0-387-68969-2_9.

21. Ruas M, Peters G. The p16INK4a/CDKN2A tumor suppressor and its relatives. Biochimica et Biophysica Acta (BBA) - Reviews on Cancer. 1998; 1378:F115–F77. http://doi.org/10.1016/S0304-419X(98)00017-1.

22. Rader J, Russell MR, Hart LS, Nakazawa MS, Belcastro LT, Martinez D, Li Y, Carpenter EL, Attiyeh EF, Diskin SJ, Kim S, Parasuraman S, Caponigro G, et al. Dual CDK4/CDK6 Inhibition Induces Cell-Cycle Arrest and Senescence in Neuroblastoma. Clinical Cancer Research. 2013; 19:6173.

23. Liu G, Sun Y, Ji P, Li X, Cogdell D, Yang D, Parker Kerrigan BC, Shmulevich I, Chen K, Sood AK, Xue F, Zhang W. MiR-506 suppresses proliferation and induces senescence by directly targeting the CDK4/6–FOXM1 axis in ovarian cancer. The Journal of Pathology. 2014; 233:308–18. https://doi.org/10.1002/path.4348.

24. Coppé JP, Desprez PY, Krtolica A, Campisi J. The Senescence-Associated Secretory Phenotype: The Dark Side of Tumor Suppression. Annual review of pathology. 2010; 5:99–118. https://doi.org/10.1146/annurev-pathol-121808-102144.

25. Heinrichs A. Cell division: Back and forth. Nat Rev Cancer. 2008; 8:740–.

26. Sorenson CM, Barry MA, Eastman A. Analysis of Events Associated With Cell Cycle Arrest at G 2 Phase and Cell Death Induced by Cisplatin. JNCI: Journal of the National Cancer Institute. 1990; 82:749–55. https://doi.org/10.1093/jnci/82.9.749.

27. Sorenson CM, Eastman A. Mechanism of cis-Diamminedichloroplatinum(II)-induced Cytotoxicity: Role of G2 Arrest and DNA Double-Strand Breaks. Cancer Research. 1988; 48:4484–8.

28. Katsaros D, Cho W, Singal R, Fracchioli S, Rigault de la Longrais IA, Arisio R, Massobrio M, Smith M, Zheng W, Glass J, Yu H. Methylation of tumor suppressor gene p16 and prognosis of epithelial ovarian cancer. Gynecologic Oncology. 2004; 94:685–92. https://doi.org/10.1016/j.ygyno.2004.06.018.

29. Kudoh K, Ichikawa Y, Yoshida S, Hirai M, Kikuchi Y, Nagata I, Miwa M, Uchida K. Inactivation of p16/CDKN2 and p15/MTS2 is associated with prognosis and response to chemotherapy in ovarian cancer. International Journal of Cancer. 2002; 99:579–82. https://doi.org/10.1002/ijc.10331.

30. Kusume T, Tsuda H, Kawabata M, Inoue T, Umesaki N, Suzuki T, Yamamoto K. The p16-Cyclin D1/CDK4-pRb Pathway and Clinical Outcome in Epithelial Ovarian Cancer. Clinical Cancer Research. 1999; 5:4152–7.

31. Masciullo V, Scambia G, Marone M, Giannitelli C, Ferrandina G, Bellacosa A, Benedetti Panici P, Mancuso S. Altered expression of cyclin D1 and CDK4 genes in ovarian carcinomas. International Journal of Cancer. 1997; 74:390–5. https://doi.org/10.1002/(SICI)1097-0215(19970822)74:4<390::AID-IJC5>3.0.CO;2-Q.

32. Bali A, O'Brien PM, Edwards LS, Sutherland RL, Hacker NF, Henshall SM. Cyclin D1, p53, and p21 Waf1/Cip1 Expression Is Predictive of Poor Clinical Outcome in Serous Epithelial Ovarian Cancer. Clinical Cancer Research. 2004; 10:5168–77. https://doi.org/10.1158/1078-0432.ccr-03-0751.

33. Valenzuela CA, Vargas L, Martinez V, Bravo S, Brown NE. Palbociclib-induced autophagy and senescence in gastric cancer cells. Exp Cell Res. 2017; 360:390–6. https://doi.org/10.1016/j.yexcr.2017.09.031.

34. Yoshida A, Diehl JA. CDK4/6 inhibitor: from quiescence to senescence. Oncoscience. 2015; 2:896–7. https://doi.org/10.18632/oncoscience.256.

35. Yoshida A, Lee EK, Diehl JA. Induction of Therapeutic Senescence in Vemurafenib-Resistant Melanoma by Extended Inhibition of CDK4/6. Cancer Res. 2016; 76:2990–3002. https://doi.org/10.1158/0008-5472.can-15-2931.

36. Alcorta DA, Xiong Y, Phelps D, Hannon G, Beach D, Barrett JC. Involvement of the cyclin-dependent kinase inhibitor p16 (INK4a) in replicative senescence of normal human fibroblasts. Proceedings of the National Academy of Sciences of the United States of America. 1996; 93:13742–7.

37. Takahashi A, Ohtani N, Yamakoshi K, Iida S-i, Tahara H, Nakayama K, Nakayama KI, Ide T, Saya H, Hara E. Mitogenic signalling and the p16INK4a-Rb pathway cooperate to enforce irreversible cellular senescence. Nat Cell Biol. 2006; 8:1291–7. http://www.nature.com/ncb/journal/v8/n11/suppinfo/ncb1491_S1.html.

38. Johnson N, Shapiro GI. Cyclin-dependent kinases (cdks) and the DNA damage response: rationale for cdk inhibitor–chemotherapy combinations as an anticancer strategy for solid tumors. Expert opinion on therapeutic targets. 2010; 14:1199–212. https://doi.org/10.1517/14728222.2010.525221.

39. Trovesi C, Manfrini N, Falcettoni M, Longhese MP. Regulation of the DNA Damage Response by Cyclin-Dependent Kinases. Journal of Molecular Biology. 2013; 425:4756–66. https://doi.org/10.1016/j.jmb.2013.04.013.

40. Basu A, Krishnamurthy S. Cellular Responses to Cisplatin-Induced DNA Damage. Journal of Nucleic Acids. 2010; 2010:16. https://doi.org/10.4061/2010/201367.

41. Wagner JM, Karnitz LM. Cisplatin-Induced DNA Damage Activates Replication Checkpoint Signaling Components that Differentially Affect Tumor Cell Survival. Molecular Pharmacology. 2009; 76:208–14. https://doi.org/10.1124/mol.109.055178.

42. Dall'Acqua A, Sonego M, Pellizzari I, Pellarin I, Canzonieri V, D'Andrea S, Benevol S, Sorio R, Giorda G, Califano D, Bagnoli M, Militello L, Mezzanzanica D, et al. CDK6 protects epithelial ovarian cancer from platinum-induced death via FOXO3 regulation. EMBO Molecular Medicine. 2017; 9:1415–33. https://doi.org/10.15252/emmm.201607012.

43. Konecny GE, Winterhoff B, Kolarova T, Qi J, Manivong K, Dering J, Yang G, Chalukya M, Wang HJ, Anderson L, Kalli KR, Finn RS, Ginther C, et al. Expression of p16 and Retinoblastoma Determines Response to CDK4/6 Inhibition in Ovarian Cancer. Clinical cancer research : an official journal of the American Association for Cancer Research. 2011; 17:1591–602. https://doi.org/10.1158/1078-0432.CCR-10-2307.

44. Coffman LG, Choi YJ, McLean K, Allen BL, di Magliano MP, Buckanovich RJ. Human carcinoma-associated mesenchymal stem cells promote ovarian cancer chemotherapy resistance via a BMP4/HH signaling loop. Oncotarget. 2016; 7:6916–32. https://doi.org/10.18632/oncotarget.6870.

45. Bai S, Ingram P, Chen YC, Deng N, Pearson A, Niknafs Y, O'Hayer P, Wang Y, Zhang ZY, Boscolo E, Bischoff J, Yoon E, Buckanovich RJ. EGFL6 Regulates the Asymmetric Division, Maintenance, and Metastasis of ALDH+ Ovarian Cancer Cells. Cancer Res. 2016; 76:6396–409. https://doi.org/10.1158/0008-5472.CAN-16-0225.

46. Pulaski HL, Spahlinger G, Silva IA, McLean K, Kueck AS, Reynolds RK, Coukos G, Conejo-Garcia JR, Buckanovich RJ. Identifying alemtuzumab as an anti-myeloid cell antiangiogenic therapy for the treatment of ovarian cancer. J Transl Med. 2009; 7:49. https://doi.org/10.1186/1479-5876-7-49.

47. Chou TC, Talalay P. Analysis of combined drug effects: a new look at a very old problem. Trends in Pharmacological Sciences. 1983; 4:450–4. https://doi.org/10.1016/0165-6147(83)90490-X.

NFATC4 Promotes Quiescence and Chemotherapy Resistance in Ovarian Cancer

Alexander J. Cole[1*], Mangala Iyengar[2*], Patrick O'Hayer[2], Daniel Chan[1], Greg Delgoffe[3], Katherine M. Aird[4], Euisik Yoon[5], Shoumei Bai[1¥], and Ronald J. Buckanovich[1,6¥]

1. Department of Internal Medicine and Magee-Womens Research Institute, University of Pittsburgh, Pittsburgh, PA, USA;, Pittsburgh, PA, USA.
2. University of Michigan, Department of Cellular and Molecular Biology, Ann Arbor, MI 48109, USA.
3. Tumor Microenvironment Center, UPMC Hillman Cancer Center, Pittsburgh, PA 15232, USA; Department of Immunology, University of Pittsburgh, Pittsburgh, PA 15213, USA
4. Department of Cellular & Molecular Physiology, Penn State College of Medicine, Hershey, PA 17033, USA
5. Department of Electrical Engineering and Computer Science, University of Michigan, Ann Arbor, MI 48109
6. Division of Gynecologic Oncology, Department of Obstetrics and Gynecology, Hillman Cancer Center, University of Pittsburgh, Pittsburgh, Pennsylvania, USA.

* These authors contributed equally to this work.

¥ Co-senior authors

The authors have declared that no conflict of interest exists.

Abstract

Development of chemotherapy resistance is a major problem in ovarian cancer. One understudied mechanism of chemoresistance is the induction of quiescence, a reversible non-proliferative state. Unfortunately, little is known about regulators of quiescence. Here we identify the master transcription factor NFATC4 as a regulator of quiescence in ovarian cancer. NFATC4 is enriched in ovarian cancer stem-like cells (CSC) and correlates with decreased proliferation and poor prognosis. Treatment of cancer cells with cisplatin results in NFATC4 nuclear translocation and activation of NFATC4 pathway, while inhibition of the pathway increased chemotherapy response. Induction of NFATC4 activity results in a marked decrease in proliferation, G0 cell cycle arrest and chemotherapy resistance, both *in vitro* and *in vivo*. Finally, NFATC4 drives a quiescent phenotype in part via downregulation of MYC. Together these data identify that NFATC4 as a driver of quiescence and a potential new target to combat chemoresistance in ovarian cancer.

Introduction

Every year approximately 240,000 women are diagnosed with ovarian cancer worldwide, and 140,200 succumb to the disease [1]. Among all cancers in developed countries, ovarian cancer has the third highest incidence:mortality ratio. Although initial response rates to cytoreductive surgery and primary chemotherapy can be as high as 70%, the vast majority of patients experience a cancer relapse, develop chemotherapy-resistant disease, and die of their cancer [2]. Consequently, identifying and understanding mechanisms of chemotherapy resistance in ovarian cancer are essential for the development of new therapeutics to prevent relapse and improve overall survival.

Quiescence is defined as a reversible non-dividing state in which cells arrest in the G0 phase of the cell cycle. Adult stem cells are typically maintained in G0 until stimulated to enter the cell cycle and proliferate [3]. As chemotherapy targets rapidly dividing cells, quiescent stem cells are innately resistant to these therapies [4]. A striking example of this mechanism can be observed in the hair follicle, where the Nuclear Factor of Activated T-cells (NFAT) family member, NFAT1, drives Cyclin Dependent Kinase 4 (CDK4) downregulation in the stem cell pool to induce a quiescent state [5]. During chemotherapy, the rapidly dividing follicular cells die resulting in hair loss; however, due to the NFAT1 induced quiescence, the stem cells survive allowing hair re-growth following cessation of therapy.

The role of quiescence in cancer is new area of research. Quiescent cancer stem-like cells (CSC) have been reported in leukemia, medulloblastoma and colon cancers [6–8]. In some cases, the quiescence is niche dependent, driving CSCs resistance to chemotherapeutics and tumor recurrence [6–8]. Consequently, successful targeting of quiescent CSCs may be essential for

improving cancer cure rates. To date, little is known about regulators of quiescence in ovarian cancer.

We previously reported the identification of ovarian CSC populations defined by the expression of the stem cell makers aldehyde dehydrogenase (ALDH) and CD133 [9]. Meeting the definition for CSCs proposed by Weinberg and colleagues [10], these cells had enhanced tumor initiation capacity, and the ability to both self-renew and asymmetrically divide [9,11]. In addition, these cells exhibit increased resistance to chemotherapy [9]. Here, we demonstrate that the NFAT family member NFATC4 (coding for the NFATC4 protein) is upregulated in ovarian CSCs and in response to chemotherapy undergoes cytoplasm to nuclear translocation and with subsequent activation of known NGATC4 target genes. Using two constitutively active NFATC4 constructs, we demonstrate that NFATC4 drives the induction of a quiescent state characterized by (i) decreased proliferation rates, (ii) smaller cell size, and (iii) and arrest of cells in G0 [12]. Furthermore, induction of NFATC4 conveyed growth arrest and chemoresistance both *in vitro* and *in vivo*. Suggesting, that NFATC4 driven quiescence is in part related to suppressed MYC activity, activation of NFATC4 results in suppression MYC expression, and overexpression of MYC following induction of NFATC4 can partially rescue the quiescent phenotype.

Results

NFATC4 mRNA and activity are enriched in a population of slowly dividing CSC

NFAT family members have been linked with quiescence in hair follicle stem cells [5]. We therefore evaluated the expression of NFAT family members in ovarian cancer stem-like cells (CSC). We previously identified a subset of ovarian CSC marked by expression of ALDH and

CD133 [9]. Evaluation of NFAT family mRNAs in $ALDH^+/CD133^+$ ovarian CSC and $ALDH^-/CD133^-$ ovarian cancer bulk cells identified *NFATC4* as upregulated (4-200 fold, $p<0.05$-0.001) in 3 independent late stage (III-IV) High-Grade Serous Carcinoma (HGSC) patient-derived $ALDH^+/CD133^+$ samples (**Fig. 1a**). While not as prominent, *NFATC4* expression is also enriched in slower growing $CD133^+$ CSC populations from OVSAHO and A2780 cell lines (cell lines chosen to have distinct $CD133^+$ cell populations) (**Fig. 1b, c**).

To agnostically determine if *NFATC4* was enriched in slower proliferating cells, we used evaluated NFATC4 expression in slowly proliferating/vital dye retaining cells [13] in multiple ovarian cancer cell lines. Slow growing/dye retaining cells (Bright), demonstrated a significant enrichment for *NFATC4* mRNA expression compared to the fast-growing (dim – dye dilute) cells in all four cell lines tested (HEY1 $p<0.05$, OVSAHO $p<0.001$, CaOV3 $p<0.01$, COV362 $p<0.05$) (**Fig. 1d**). These slow dividing cells were also shown to be enriched for ovarian CSC markers (**Fig. 1e**).

Suggesting these findings may have clinical relevance, i*n silico* analysis of the impact of NFATC4 expression on patient prognosis was performed using publicly available data [14,15]. Analyses of microarray data from 1287 HGSC ovarian-cancer patients [15] suggested higher expression of *NFATC4* is correlated with worse Overall Survival (OS), Progression Free Survival (PFS) and Post Progression Survival (PPS) (**Fig. 1f**, $p<0.01$, $p<0.0001$, $p<0.05$). Similarly, analysis of 376 samples in the The Cancer Genome Atlas (TCGA) ovarian cancer data set, demonstrated that dysregulation of the NFATC4 pathway correlated with poor patient outcome (**Supplementary Fig. 1**, $p<0.05$). Parallel analysis of NFATC4 target gene RCAN1, also showed a correlation between elevated expression and OS, PFS, and PPS (**Fig. 1g**, $p<0.051$,

p<0.0001, p<0.05). The impact of RCAN on prognosis was less prominent but is likely complicated by RCAN expression in T cells.

NFATC4 activity induces a quiescent state

To directly interrogate the function of NFATC4 in ovarian cancer cells, we used two distinct previously generated NFATC4 expression constructs, a constitutively active (cNFATC4) [16] and an inducible (IcNFATC4) [17].NFAT proteins are primarily regulated through phosphorylation regulated cytoplasmic retention (dephosphorylation results in nuclear translocation and activation of transcription various binding partners [18,19]). One construct (cNFATC4) lacks the regulatory phosphorylation domain and is therefore constitutively nuclear/active (**Fig. 2a**). Transfection of this construct into A2780 cells demonstrated clear expression of the *NFATC4* mRNA relative to Control-YFP transfected cells (**Fig. 2b**). Confirming cNFATC4 is transcriptionally active, expression of cNFATC4 resulted in a strong induction of the known NFAT target genes *RCAN1* (regulator of calcineurin-1) [20], and Follistatin (FST) [21] (**Fig. 2b**). **To confirm the was broadly applicable, we repeated this experiment and found similar results using** multiple ovarian cancer cell lines (CaOV3, COV362 and OVSAHO) (Fig 2b).

We also generated an inducible nuclear NFATC4 (IcNFATC4) with a puromycin selection cassette. As deletion of the regulatory domain could lead to unexpected changes in function, we used a previously developed construct with point mutations that change the regulatory serines to alanines, leaving the remaining protein intact [17]. Due to the lack of serine phosphorylation, this NFATC4 protein has an exposed nuclear localization sequence and is

therefore constitutively nuclear. An inducible luciferase (ILuc) was used as a control. Disappointingly and inexplicably, despite clear presence of the construct, we were unable to show any inducible expression in multiple HGSC cell lines including OVSAHO, OVCAR3 and OVCAR4 (**Supplemental Fig. 2a**). However, we were able to generate inducible expression of *NFATC4* mRNAs in the HGSC cell line HEY1 [22], and the endometriod ovarian cancer SKOV3 line (**Fig. 2c)**. Once again, confirming transcriptional activity, the NFAT target genes *RCAN1* and *FST* were induced following NFATC4 induction (**Fig. 2c**).

Using these constructs, we tested the effects of NFATC4 activity on ovarian cancer cell growth. Compared to control-YFP lines, cNFATC4 overexpression was associated with a 2-fold (A2780) decrease in total cell number over four days ($p<0.0001$) (**Fig. 3a**). Similarly, cNFATC4 overexpression in HGSC cell lines resulted in a 60% (COV362, $P<0.001$), 50% (OVSAHO, $P<0.05$) and 70% (CaOV3, $P<0.01$) decrease in total cell number compared to Control-YFP lines (**Fig. 3b**).

For the IcNFATC4 constructs, doxycycline induction of two independent HEY1 IcNFATC4 cell clones and two independent SKOV3 cell clones showed 1.5-3 fold and 2-4 fold ($p<0.01$) decrease in cell number at 3 and 6 days after doxycycline treatment, respectively (**Fig. 3c**). In contrast, doxycycline had no impact on ILuc cell growth for either cell line (**Fig. 3c**). Explaining the more profound suppression of growth with the IcNFATC4 construct, we noted that, despite multiple rounds of FACS enrichment, cNFATC4 expression was rapidly lost/selected against over time in cell culture which selects for rapidly growing cells (**Supplemental Fig. 2b**).

Given the significant reduction in cell numbers and links between NFAT proteins and apoptosis [23], we evaluated the effects of NFATC4 on cellular viability. Trypan blue staining of

A2780 and SKOV3 cells indicated that total viability did not change with the expression of cNFATC4 or IcNFATC4 (with or without dox) compared to their respective controls (**Fig. 3d**). We also analyzed apoptosis rates in the HEY1 IcNFATC4 cells vs ILuc control with Annexin-V FACS. We observed no significant increase in Annexin stain in IcNFATC4 cells vs. ILuc controls (**Fig. 3e**). Thus, it does not appear that increased apoptosis rates account for the significant reduction in proliferation of NFATC4 overexpressing ovarian cancer cells.

Another explanation for a reduction in growth following overexpression of NFATC4 could be an increase in cellular senescence [24]. Senescent cells demonstrate an increase in senescence-associated β-galactosidase (SABG). SABG staining demonstrated no increase in SABG expression in control or cNFATC4 cells compared with controls (**Supplementary Fig. 3b**). Therefore, it appears that NFATC4 expression decreases cell division without inducing death, apoptosis, or senescence.

We next evaluated the impact of NFATC4 expression on cellular division. Suggesting a reduction in the percentage of dividing cells, immunofluorescent evaluation of BrdU incorporation demonstrated a reduction of BrdU incorporation in cNFATC4 cells ($p=0.058$) (**Fig. 4a**). We then evaluated cellular proliferation at a single cell level. We monitored cell divisions of cells expressing cNFATC4 or Control-YFP in single cell microfluidic culture chips (**Fig. 4b**), described previously [11]. Over four days, 39% of control cells and 20% of cNFATC4 cells underwent at least one cell division. 41% of dividing control cells underwent a second cell division while only 4% of the cNFATC4 cells underwent a second division; this resulted in a final >3-fold decreased total cell number in the cNFATC4 cells vs. Control-YFP cells (**Fig. 4b**). We also evaluated the impact of NFATC4 on growth rates of SKOV3 and HEY1 cell lines. Cells lines expressing the construct IcNFATC4 or ILuc were evaluated in the presence of doxycycline

for 96 hours using real-time imaging. Doxycycline treated IcNFATC4 expressing cells had significantly slower proliferation rates than doxycycline treated ILuc controls (HEY1 $p<0.0001$, SKOV3 $p<0.001$), with near complete arrest at 96 hours (**Fig. 4c**) ($p<0.0001$).

An explanation for restricted cell proliferation, in the absence of cell death or senescence, is the induction of quiescence. Quiescent cells typically exit the cell cycle and reside in G0. To directly evaluate the impact of NFATC4 activity on G0 cells, we transduced HEY1 cells expressing the IcNFATC4 and ILuc constructs with the mVenus-p27K- and mCherry-CDT1 vectors [12]. This system can be used to define the G0/G1 transition; briefly, cells expressing high levels of each fusion protein (yellow) are in G0, cells with low or no mVenus-p27K- and high mCherry-CDT1 (red) are transitioning into G1 or in the G1/S phase, and cells with no/low expression of either construct are in S/G2/M. ILuc and IcNFATC4 cells were labeled with the two reporters and the cells expressing both reporter constructs were FACS isolated (**Fig. 4d**). Purified cells were then treated with doxycycline, plated at ~10% confluency, allowed to adhere overnight before real-time imaging was performed over 90 hours. At the conclusion of the experiment, we scored the number of cells in each phase of the cell cycle found IcNFATC4 cells had a >4-fold increase in the number of cells in G0 (**Fig. 4d,** $P<0.01$).

To determine if a subset of cells were cycling while a distinct subset was arresting in G0, we FACS isolated ILuc and IcNFATC4 cells in the G1/S phase of the cell cycle (mCherry-CDT1$^{(+)}$, mVenus-p27K-$^{(-)}$) of the cell cycle, re-plated and FACS analyzed after 72 hours. FACs analysis showed that while ILuc cells redistributed appropriately through the cell cycle with 39% of cells in G1/S, nearly 90% of the IcNFATC4 cells were in the S/G2/M and G0 phases of the cell cycle with only 7% of cells in the G1/S phase of the cell cycle (**Fig. 4e**).

In addition to G0 arrest, quiescent cells have a unique phenotype which includes a reduction in cell size [25]. Light microscopic evaluation of doxycycline treated HEY1 and SKOV3 IcNFATC4 and ILuc controls, controlled for cell confluences (**Supplemental Fig 4a**) demonstrated IcNFATC4 cells became significantly smaller with doxycycline treatment (HEY1 $p<0.01$, SKOV3 $p<0.001$) (**Fig. 4f**). FACS analyses of forward-scatter as another measure of size confirmed these results in A2780 cNFATC4 cells and doxycycline treated HEY1 IcNFATC4 cells (**Supplementary Fig. 4b-d**).

NFATC4 overexpression promotes chemotherapy resistance in vitro

Multiple groups have reported that quiescent/slower-cycling cells are more chemotherapy resistant [26–28]. We therefore tested the effects of constitutive NFATC4 expression on chemoresistance. We co-treated A2780 cells expressing the cNFATC4 or Control-YFP construct and SKOV3 expressing the IcNFATC4 or ILuc constructs with doxycycline and varying concentrations of cisplatin for 72h (for IC 50 values, see **Supplementary Table 1**). We then quantitated cell number and normalized to the untreated cells. cNFATC4 and IcNFATC4 cells demonstrated significantly increased survival ($p<0.001$ and $p<0.01$ respectively) in response to cisplatin chemotherapy when compared to Control-YFP and doxycycline treated ILuc (**Fig. 5a**). SKOV3 expressing IcNFATC4 treated with and without doxycycline also showed a similar effect (**Supplementary Fig. 5a,** left graph $P<0.01$), while ILuc untreated vs doxycycline showed no difference (**Supplementary Fig. 5a,** right graph). To confirm these results, we co-treated HEY1 and SKOV3 cells expressing the IcNFATC4 or ILuc control construct with doxycycline and cisplatin (9.5 ug/ml) for 72h and measured cell confluency using the IncuCyte real time

imaging (**Fig. 5b**). IcNFATC4 cells were significantly more resistant to chemotherapy than ILuc cells for both HEY1 ($p<0.0001$) and SKOV3 ($p<0.0001$) cell lines.

To determine if chemotherapy exposure could induce NFATC4 nuclear translocation, we performed immunofluorescence on cisplatin treated ovarian cancer cell lines. Cisplatin demonstrated clear nuclear translocation of native NFATC4 in all tested ovarian cancer cell lines (**Fig. 5c**). Confirming transcriptional activity of NFAT with cisplatin induced nuclear translocation, cisplatin treatment resulted in increases in both *RCAN1* mRNA (COV362 $p<0.0001$, SKOV3 $P<0.01$, HEY1 $p<0.001$, CaOV3 $p<0.01$) (**Fig. 5d**), and *FST* mRNA (COV362 $p<0.01$, HEY1 $p<0.1$, CaOV3 $p<0.01$) (**Fig. 5e**). We also observed a significant enrichment of NFATC4 mRNA expression (COV362 $p<0.01$, OVSAHO $P<0.01$, CaOV3 $P<0.05$), following prolonged treatment of a high dose of cisplatin for 72h (**Fig. 5f**). Whether this relates to an increase in NFAT gene expression in platinum treated cells, or selection for cells expressing NFATC4 remains to be determined.

Supporting these results, slower growing/NFATC4 enriched $CD133^+$ A2780 and OVSAHO CLSCs (**Fig. 1c**), demonstrated resistance to cisplatin treatment (**Fig. 5g**). A2780 $CD133^+$ cells which had the highest levels of NFATC4 were most cisplatin resistant. To functionally link NFATC4 activity and chemotherapy resistance, we co-treated cell lines with the pan-NFAT inhibitor VIVIT [29] and various concentrations of cisplatin for 72 hours. Cells co-treated with VIVIT and cisplatin showed a significant decrease in cell viability when compared to cells treated with cisplatin alone (A2780 $p<0.05$, SKOV3 $p<0.05$) (**Fig. 5h**). Taken together, our *in vitro* data demonstrates NFATC4 promotes quiescence and chemoresistance in ovarian cancer cells and ovarian CSCs in vitro.

With NFATC4 clearly being activated by cisplatin, we wished to investigate if this response was specific to cisplatin or a general response to cellular stress. To test this, we Taxol treated ovarian cancer cell lines for 72h (for IC50 values see, **Supplementary Table 1**) and looked at expression of the same genes (**Supplementary Fig. 6**). We demonstrated a mild increase in both *RCAN1* and *NFATC4* expression following Taxol treatment.

cNFATC4 expression suppresses tumor growth and drives chemotherapy resistance *in vivo*

We next examined the effect of NFATC4 expression on tumor xenograft growth. A2780 cNFATC4 tumors demonstrated significant growth delay relative to controls ($p<0.0001$), with essentially no growth for three weeks and with 2/10 cNFATC4 tumors failing to initiate (**Fig. 6a**). After three weeks, cNFATC4 tumors resumed normal growth; however, suggesting a requirement for loss of cNFATC4 for resumption of growth, analysis of these tumors demonstrated complete loss of cNFATC4 transgene expression (**Supplementary Fig. 7**).

We similarly evaluated the impact of IcNFATC4 expression on tumor growth. In the presence of continuous doxycycline treatment, tumors expressing IcNFATC4 were >13 fold smaller than their ILuc controls ($p<0.0001$) (**Fig. 6b**). To confirm this was not related to unequal cell inoculation or altered tumor initiation, we repeated this experiment, but did not initiate doxycycline treatment until tumors were 100mm3. Control-Luc and IcNFATC4 tumors initiated and grew similarly. However, ~5 days after the initiation of treatment with doxycycline, IcNFATC4 tumors showed growth arrest (**Fig. 6c-d)**. Confirming reversibility of the phenotype, on withdrawal of doxycycline, after a slight delay, tumors resumed normal growth.

We next tested the impact of IcNFATC4 induction on chemotherapy resistance. We allowed IcNFATC4 tumors to grow until they were ~150mm^3. Tumor bearing mice were then randomized and half were then treated with doxycycline for 5 days to induce NFATC4 expression. Due to the low sensitivity of HEY1 to cisplatin at baseline, animals were treated with 2 daily doses of high-dose paclitaxel (16 mg/kg). While control tumors demonstrate a complete response to chemotherapy, tumors in which IcNFATC4 expression was transiently induced demonstrated growth arrest in response to doxycycline, and then ~8 days after doxycycline discontinuation, tumors resumed normal growth without any evidence of response to therapy ($p<0.001$) (**Fig. 6e**).

NFATC4 downregulates MYC and MYC overexpression can partially inhibit early NFATC4 mediated quiescence

It has been reported by multiple studies that NFAT family members can regulate the proto-oncogene MYC [30–32]. MYC is a master regulator of growth-promoting signal transduction pathways and a well-defined pro-proliferation gene [33]. To determine if NFATC4, like other family NFAT family members, can regulate MYC expression and if this could be a mechanism for NFATC4 mediated quiescence, we examined the effect of cNFATC4 on MYC mRNA expression. HEY1 and SKOV3 cells demonstrated a significant reduction in MYC expression following NFATC4 induction, $p<0.0001$ and $p<0.05$ respectively (**Fig. 7a**). Furthermore, we conducted doxycycline recovery experiments, where we induced the construct by treating cells with doxycycline for 72h, then removed the doxycycline and recorded cell number (**Supplementary Fig 8**) and mRNA expression of NFATC4 target genes (**Supplementary Fig 9**) as the cells resumed cell cycle. We were then able to re-induce the quiescent state via additional

doxycycline treatment. These experiments demonstrated MYC, along with the NFATC4 target genes RCAN1 and FST, cycled with the induction and loss of quiescence, supporting their role in inducing this quiescent state.

To investigate if this downregulation in MYC following NFATC4 induction could affect cell proliferation, we transfected lcNFATC4 expressing SKOV3 and HEY1 cells with a MYC overexpression construct [34] or PCDNA3 vector control. MYC overexpression resulted in a significant increase in MYC mRNA expression (SKOV3 $p<0.05$, HEY1 $p<0.01$) (**Fig.7b**). To determine if early induction of MYC expression was able to prevent NFATC4 induced quiescence, induced IcNFATC4 cells for 6 hours then transfected cells with PCDNA3 (control) or cMYC. We continued doxycycline for 72 h before and then evaluated cell growth. Cells transfected with MYC 6 h after NFATC4 induction demonstrated cell growth which was not statistically significantly different from control iLuc cells (**Fig.7c**).

To determine if MYC expression could overcome growth suppression in established NFATC4 driven quiescent cells we repeated the above experiment, in cells in which NFATC4 had been induced for 72 h to ensure the cells had already establish a quiescent phenotype before transfecting with PCDNA3 or cMYC. Doxycycline treatment was continued for an additional 72 h before and cell proliferation evaluated. Interestingly, MYC expression in established quiescent cells was unable reverse the quiescent phenotype (**Fig.7c**).

Discussion

The Nuclear Factor of Activated T-Cells (NFAT) family of transcription factors act as master regulators of numerous cellular processes. In normal cells, NFAT family members can

impact both proliferation [35–39] and quiescence [5]. NFAT proteins have been directly implicated in the regulation of stem cell proliferation [40]. We report here a critical role for NFATC4 in the regulation of cellular quiescence in ovarian cancer. Expression of constitutively nuclear NFATC4 suppresses cellular proliferation, reduces cell size and arrested tumor growth. Furthermore, consistent with previous reports [41,42], we find that NFATC4 activity contributes to chemotherapy resistance, both *in vitro* and *in vivo*. Finally, NFATC4 induction represses MYC which contributes to a quiescent state.

NFAT family members and regulation of quiescence: We identified NFATC4 as a potential regulator of quiescence in ovarian cancer. Previously NFATC1 was identified as regulating quiescence in the hair follicle. More recently, a study of NFATC3 in the brain [43] observed significant changes in cell proliferation and vital dye retention with NFATC3 inhibition. These studies implicate the NFAT family of transcription factors as regulators of quiescence.

The complete mechanism through which NFAT regulates proliferation/quiescence is unclear. In the hair follicle, NFAT regulates the cyclin dependent kinase CDK4 to arrest cell cycle progression [5]. We did not observe similar mechanisms here; however, we did observe NFATC4 expression correlated with a down regulation of MYC, while MYC overexpression was able to partially rescue the quiescent phenotype following early, but not late, induction of NFATC4. This observation suggests that although downregulation MYC could be an important part of the induction of a quiescent phenotype, there are secondary mechanisms downstream of NFATC4 which are critical in the maintenance of the quiescent state. Future work is required to elucidate the mechanism responsible for NFATC4 induced quiescence.

NFATC4 and chemotherapy resistance: NFATC4 has been poorly studied in cancer. In normal physiologic states, NFATC4 appears to function partly as a general stress response protein, as it serves a protective role in cardiomyocytes in response to radiation [44], is activated by mechanical stress in the heart [45] and bladder [46], and serves as a protective factor during hypoxia [47]. NFATC4 may serve as a similar stress regulator in cancer cells to promote survival. We have shown that NFATC4 translocates to the nucleus and initiates transcription in response to cisplatin chemotherapy and drives chemotherapy resistance. Similarly, NFATC4 expression was linked with therapeutic response in gastric cancer [48]. Taxol's partial induction the NFATC4 pathway of may be a result of its limited ability to increase intracellular calcium [49], while increasing intracellular calcium is a key mechanism by which cisplatin functions [50].

Consistent with a role for NFATC4 in cancer stem-like cells, NFATC4 plays a role in pancreatic cell plasticity and tumor initiation [51]. Consistent with the data above, survival data demonstrating dysregulation or high expression of NFATC4 leads to worse prognosis of ovarian cancer patients, suggest NFATC4 may be an important therapeutic target in ovarian cancer to overcome the chemotherapy resistance associated with slow-cycling cells. This hypothesis is supported by studies on cyclosporine, a commonly used immunosuppressant which inhibits the NFAT family. Cyclosporine has shown activity as a chemo-sensitizer in a phase II clinical trial, demonstrating that cyclosporine could improve response to therapy in patients with chemotherapy-refractory disease [52,53]. However, this has not been reproducible [54] and has not been tested in patients with chemotherapy naïve disease, who may benefit the most from the elimination of slow cycling cells. Furthermore, as cyclosporine impacts all NFAT family members, and is not selective for cancer cells, suppression of immunity may limit efficacy. NFATC4 is the only core NFAT family member that is not expressed in the immune system [55],

thus the development of specific NFATC4 inhibitors could allow chemosensitization of the NFATC4-expressing CSC without concomitant immunosuppression.

In summary, we have found that the master transcriptional regulator NFATC4 induces a quiescent state in ovarian cancer and translocates to the nucleus in response to chemotherapy. Constitutively nuclear NFATC4 is associated with a reduction in cellular size and proliferation and the induction of chemotherapy resistance. NFATC4 promotes the quiescent phenotype by early downregulation of MYC; however other mechanisms are responsible for maintaining an established quiescent phenotype. Taken together, this data suggest NFATC4 is an important therapeutic target in ovarian cancer that warrants significant further investigation.

Materials and Methods

Cell Culture

The A2780 cell line was obtained from Dr. Susan Murphy at Duke University. SKOV3, CaOV3 and HEY1 lines were purchased from ATCC (2018). OVSAHO cells were gifted from Dr. Deborah Marsh from the University of Sydney. COV362 were purchased from Sigma- Aldrich (2018). All cells were cultured in RPMI-1640 media with 10% FBS, 1% Penicillin/Streptomycin at 37^0C and 5% CO_2.

Constructs

Both constructs used in this study were designed to result in constitutively nuclear NFATC4. A constitutively nuclear NFATC4-YFP fusion (cNFATC4) with the phospho-regulatory domain deleted or a YFP-only control (Control-YFP) were cloned into a pGIPZ lentiviral vector and

transduced into the A2780, CaOV3, OVSAHO and COV362 ovarian cancer cell lines. A second, phospho-specific mutant constitutively active NFATC4 [17] was also cloned into the doxycycline-inducible Tet-One expression system (Clontech) to create an inducible and constitutive NFATC4 (IcNFATC4) in the HEY1 ovarian cancer line. This was paired with an inducible luciferase control (ILuc) to control for overexpression. Details regarding the structure and validation of all constructs are presented in the results section (**Fig. 2**). Because the only known function of NFAT proteins are transcription, the phospho-mutants used are constitutively nuclear and therefore constitutively active. A pcDNA3-cmyc construct was purchased from Addgene (Cat# 16011).

Patient samples

Fresh High-grade Serious Ovarian Carcinomas (HGSOC) were acquired from the University of Michigan's Comprehensive Cancer Center. Fresh tumor samples were dissociated using a Tumor Dissociation Kit (Miltenyi Biotec) and cultured using standard conditions. HGSOC diagnosis was confirmed using immunohistochemistry.

Carboxyfluorescein succinimidyl ester (CFSE) Assay

HEY1, COV362, OVSAHO and CaOV3 cell lines were stained with 2.5 uM of CellTrace™ CFSE Cell Proliferation Kit (Thermo Fisher) for 20 mins at 37^0C, washed and then grown for 5-7 days. The top 4% bright cells, 10% medium cells and bottom 4% dim cells were FACS isolated. RNA was extracted, and qPCR performed to validate NFATC4 expression (as below).

Quantitative PCR

RNA was extracted using RNeasy Mini Kit (Qiagen) and cDNA was made using SuperScript™ III Reverse Transcriptase kit (Theremofisher). qPCR was performed using SYBR™ Green PCR

Master Mix (Applied Biosystems) using standard cycling conditions. The primers used for this study are available in supplemental material (**Supplementary Table 2**).

Cell counting

Cell counts were performed using the Moxi Z automated counting system (ORLFO Technologies) and the Cassettes Type S. For trypan blue staining, the Countess automated cell counter (Invitrogen) was used with Countess Cell Counting Chamber Slides.

BrdU labeling

A2780 cells were treated with 10 µM BrdU labeling solution and incubated for 4 hours at 37ºC in a CO2 incubator. Cell were washed with PBS, fixed with 4% paraformaldehyde and permeabilized with 0.1% Triton X. Standard ICC was followed. Cells were then incubated in 2.5 M HCL for 30 mins at room temperature, then washed with PBS. Standard immunocytochemistry protocol was then followed.

Micro Fluidics

A2780 Control-YFP or cNFATC4 cells were loaded into single cell capture microfluidic chips from collaborator Dr. Yoon (University of Michigan). Cells mitoses were tracked using a microscope over a three-day period and results were recorded. Cell viability was confirmed using LIVE/DEAD cell staining at the termination of the experiment.

Size Analysis

HEY1 and SKOV3 cells expressing the ILuc and IcNFATC4 constructs were pre-treated with doxycycline, then plated into a 96 well plate at 300 and 1000 cell/well respectively and placed into the IncuCyte. Cells were treated with or without doxycycline and grown for 36 h. Images we

taken at 36 hours making sure the confluency was comparable between the doxycycline treated and untreated control cells (**Supplementary Fig. 4a**). Images were imported into ImageJ and cell size was calculated by drawing around cells and quantifying their area.

Fluorescence ubiquitination cell cycle indicator (FUCCI)

HEY1 cells expressing the IcNFATC4 or ILuc constructs were transduced with the p27-mVenus and CDT1-mCherry FUCCI cell cycle reporter constructs [12]. Cells expressing both constructs were isolated using FACS and plated in the IncuCyte and grown for 90 hours. Fluorescence was measured, and percentages of green, red, yellow, and unstained cells were quantitated. G1-S phase cells expressing the constructs were FACS isolated and grown for 3 additional days to determine if they retained the cell cycle phases as a result of the NFACTC4 overexpression.

Annexin V staining

For apoptosis detection via annexin staining, HEY1 ILuc and IcNFATC4 cells were grown in 6 well dishes with or without doxycycline for 72 hrs. Cells were stained with the Annexin-V FITC apoptosis kit (BD Biosciences) according to the manufacturer's instructions and at least 10,000 events were analyzed on the Mo Flo Astrios flow cytometer (BD Biosciences). The percentage of Annexin V^+, PI^+, Annexin V^+/PI^+, and Annexin V^-/PI^- cells was quantified.

Senescence-associated beta galactosidase (SABG) staining

Cells were plated on tissue culture coverslips, allowed to grow for 96 hours , fixed, and then SABG staining was done as previously described [56].

IncuCyte growth curves

HEY1 and SKOV3 cells expressing the ILuc or IcNFATC4 constructs were seeded at 300 and 1000 cells per well respectively, in a 96 well plate. For growth curves, cells were treated with or without 100 ng/mL doxycycline for 96 h. For cisplatin curves, cells were treated with 9.5 ug/mL cisplatin for 72h with or without co-treatment with 100 ng/mL dox. IncuCyte images were taken every 4 h and cell confluence was recorded.

Immunofluorescence

HEY1, COV362 and SKOV3 ovarian cancer cell lines were grown on glass coverslips and treated with various concentrations of cisplatin based on their respective IC50s. Coverslips were fixed with 4% paraformaldehyde and permeabilized with 0.1% Triton X. Cells were blocked with 10% horse serum and incubated with 1:50 mouse anti-NFATC4 antibody (Novus Biologicals) in 5% horse serum for 2 hours. Slides were washed 3 x 5 mins with PBS, cells were incubated with an Alexa Fluor 488 anti-mouse secondary antibody, mounted with DAPI mounting medium (Vector Labs), and then imaged on an Olympus BX41 microscope.

In vivo xenografts

NOD/SCID/IL2R^{KO} or nude mice were injected with 500,000 Control-YFP or cNFATC4 cells or 300,000 ILuc or IcNFATC4 cells for tumor xenograft experiments. Animals were maintained at 12 hour light/dark cycles under SPF conditions with free access to food and water. For induction, 2 mg/mL doxycycline was administered in the water along with 5% sucrose to mask its bitter taste. Tumors were monitored once a week initially and twice a week after tumors reached 1000 mm^3, and animals were sacrificed at protocol endpoints. All experiments were conducted in accordance with the animal care and use committee from the University of Michigan.

Statistical analysis

Statistically analysis was conducted using GraphPad Prism (8.0.2) and http://vassarstats.net/. All data was analyzed using two tailed student's t-tests or one-way ANNOVARs. A minimum of 3 replicate experiments ($n \geq 3$) were used for each experiment.

Acknowledgements

Funding for this work was provided by Ann and Sol Schreiber Mentored Investigator Award (599997) from the Ovarian Cancer Research Alliance (OCRA), DOD Award #W81XWH-15-1-0083 and NIH RO1 award 1R01CA203810.

Contributions

A.C and M.I conducted the majority of the experiments. R.B and S.B conceived the project and planned the experiments. P.H, E.Y and D.H. helped with the experiments. G.D., K.A., E.Y reviewed the manuscript. A.C, M.I and R.B. wrote the manuscript.

Competing interests

The authors declare no competing interests.

Corresponding author

Ronald Buckanovich (buckanovichrj@mwri.magee.edu).

References

1. Siegel RL, Miller KD, Jemal A. Cancer statistics, 2018. *CA Cancer J Clin*. 2018;68(1):7-30. doi:10.3322/caac.21442

2. Ushijima K. Treatment for recurrent ovarian cancer-at first relapse. *J Oncol*. 2010;2010:497429. doi:10.1155/2010/497429

3. Yoshihara H, Arai F, Hosokawa K, et al. Thrombopoietin/MPL signaling regulates hematopoietic stem cell quiescence and interaction with the osteoblastic niche. *Cell Stem Cell*. 2007;1(6):685-697. doi:10.1016/j.stem.2007.10.020

4. Zeuner A, Francescangeli F, Contavalli P, et al. Elimination of quiescent/slow-proliferating cancer stem cells by Bcl-XL inhibition in non-small cell lung cancer. *Cell Death Differ*. 2014;21(12):1877-1888. doi:10.1038/cdd.2014.105

5. Horsley V, Aliprantis AO, Polak L, Glimcher LH, Fuchs E. NFATc1 balances quiescence and proliferation of skin stem cells. *Cell*. 2008;132(2):299-310. doi:10.1016/j.cell.2007.11.047

6. Jin K, Ewton DZ, Park S, Hu J, Friedman E. Mirk regulates the exit of colon cancer cells from quiescence. *J Biol Chem*. 2009;284(34):22916-22925. doi:10.1074/jbc.M109.035519

7. Saito Y, Uchida N, Tanaka S, et al. Induction of cell cycle entry eliminates human leukemia stem cells in a mouse model of AML. *Nat Biotechnol*. 2010;28(3):275-280. doi:10.1038/nbt.1607

8. Vanner RJ, Remke M, Gallo M, et al. Quiescent sox2(+) cells drive hierarchical growth and relapse in sonic hedgehog subgroup medulloblastoma. *Cancer Cell*. 2014;26(1):33-47. doi:10.1016/j.ccr.2014.05.005

9. Silva IA, Bai S, McLean K, et al. Aldehyde dehydrogenase in combination with CD133 defines angiogenic ovarian cancer stem cells that portend poor patient survival. *Cancer Res*. 2011;71(11):3991-4001. doi:10.1158/0008-5472.CAN-10-3175

10. Mani SA, Guo W, Liao M-J, et al. The epithelial-mesenchymal transition generates cells with properties of stem cells. *Cell*. 2008;133(4):704-715. doi:10.1016/j.cell.2008.03.027

11. Choi Y-J, Ingram PN, Yang K, et al. Identifying an ovarian cancer cell hierarchy regulated by bone morphogenetic protein 2. *Proc Natl Acad Sci USA*. 2015;112(50):E6882-8. doi:10.1073/pnas.1507899112

12. Oki T, Nishimura K, Kitaura J, et al. A novel cell-cycle-indicator, mVenus-p27K-, identifies quiescent cells and visualizes G0-G1 transition. *Sci Rep*. 2014;4:4012. doi:10.1038/srep04012

13. Deleyrolle LP, Rohaus MR, Fortin JM, Reynolds BA, Azari H. Identification and isolation of slow-dividing cells in human glioblastoma using carboxy fluorescein succinimidyl ester (CFSE). *J Vis Exp*. 2012;(62). doi:10.3791/3918

14. Cancer Genome Atlas Research Network. Integrated genomic analyses of ovarian carcinoma. *Nature*. 2011;474(7353):609-615. doi:10.1038/nature10166

15. Gyorffy B, Lánczky A, Szállási Z. Implementing an online tool for genome-wide validation of survival-associated biomarkers in ovarian-cancer using microarray data from 1287 patients. *Endocr Relat Cancer*. 2012;19(2):197-208. doi:10.1530/ERC-11-0329

16. Bai S, Kerppola TK. Opposing roles of FoxP1 and Nfat3 in transcriptional control of cardiomyocyte hypertrophy. *Mol Cell Biol*. 2011;31(14):3068-3080. doi:10.1128/MCB.00925-10

17. Graef IA, Mermelstein PG, Stankunas K, et al. L-type calcium channels and GSK-3 regulate the activity of NF-ATc4 in hippocampal neurons. *Nature*. 1999;401(6754):703-708. doi:10.1038/44378

18. Ruff VA, Leach KL. Direct demonstration of NFATp dephosphorylation and nuclear localization in activated HT-2 cells using a specific NFATp polyclonal antibody. *J Biol Chem*. 1995;270(38):22602-22607.

19. Beals CR, Clipstone NA, Ho SN, Crabtree GR. Nuclear localization of NF-ATc by a calcineurin-dependent, cyclosporin-sensitive intramolecular interaction. *Genes Dev*. 1997;11(7):824-834.

20. Lee MY, Garvey SM, Baras AS, et al. Integrative genomics identifies DSCR1 (RCAN1) as a novel NFAT-dependent mediator of phenotypic modulation in vascular smooth muscle cells. *Hum Mol Genet*. 2010;19(3):468-479. doi:10.1093/hmg/ddp511

21. Pisconti A, Brunelli S, Di Padova M, et al. Follistatin induction by nitric oxide through cyclic GMP: a tightly regulated signaling pathway that controls myoblast fusion. *J Cell Biol*. 2006;172(2):233-244. doi:10.1083/jcb.200507083

22. Anglesio MS, Wiegand KC, Melnyk N, et al. Type-specific cell line models for type-specific ovarian cancer research. *PLoS One*. 2013;8(9):e72162. doi:10.1371/journal.pone.0072162

23. Mognol GP, Carneiro FRG, Robbs BK, Faget DV, Viola JPB. Cell cycle and apoptosis regulation by NFAT transcription factors: new roles for an old player. *Cell Death Dis*. 2016;7:e2199. doi:10.1038/cddis.2016.97

24. Kuilman T, Michaloglou C, Mooi WJ, Peeper DS. The essence of senescence. *Genes Dev*. 2010;24(22):2463-2479. doi:10.1101/gad.1971610

25. Rumman M, Dhawan J, Kassem M. Concise review: quiescence in adult stem cells: biological significance and relevance to tissue regeneration. *Stem Cells*. 2015;33(10):2903-2912. doi:10.1002/stem.2056

26. Moore N, Lyle S. Quiescent, slow-cycling stem cell populations in cancer: a review of the evidence and discussion of significance. *J Oncol*. 2011;2011. doi:10.1155/2011/396076

27. Naumov GN, Townson JL, MacDonald IC, et al. Ineffectiveness of doxorubicin treatment on solitary dormant mammary carcinoma cells or late-developing metastases. *Breast Cancer Res Treat*. 2003;82(3):199-206. doi:10.1023/B:BREA.0000004377.12288.3c

28. Dembinski JL, Krauss S. Characterization and functional analysis of a slow cycling stem cell-like subpopulation in pancreas adenocarcinoma. *Clin Exp Metastasis*. 2009;26(7):611-623. doi:10.1007/s10585-009-9260-0

29. Roehrl MHA, Kang S, Aramburu J, Wagner G, Rao A, Hogan PG. Selective inhibition of calcineurin-NFAT signaling by blocking protein-protein interaction with small organic molecules. *Proc Natl Acad Sci USA*. 2004;101(20):7554-7559. doi:10.1073/pnas.0401835101

30. Singh G, Singh SK, König A, et al. Sequential activation of NFAT and c-Myc transcription factors mediates the TGF-beta switch from a suppressor to a promoter of cancer cell proliferation. *J Biol Chem*. 2010;285(35):27241-27250. doi:10.1074/jbc.M110.100438

31. Köenig A, Linhart T, Schlengemann K, et al. NFAT-induced histone acetylation relay switch promotes c-Myc-dependent growth in pancreatic cancer cells. *Gastroenterology*. 2010;138(3):1189-99.e1. doi:10.1053/j.gastro.2009.10.045

32. Buchholz M, Schatz A, Wagner M, et al. Overexpression of c-myc in pancreatic cancer caused by ectopic activation of NFATc1 and the Ca2+/calcineurin signaling pathway. *EMBO J*. 2006;25(15):3714-3724. doi:10.1038/sj.emboj.7601246

33. Dang CV. MYC on the path to cancer. *Cell*. 2012;149(1):22-35. doi:10.1016/j.cell.2012.03.003

34. Ricci MS, Jin Z, Dews M, et al. Direct repression of FLIP expression by c-myc is a major determinant of TRAIL sensitivity. *Mol Cell Biol*. 2004;24(19):8541-8555. doi:10.1128/MCB.24.19.8541-8555.2004

35. Bushdid PB, Osinska H, Waclaw RR, Molkentin JD, Yutzey KE. NFATc3 and NFATc4 are required for cardiac development and mitochondrial function. *Circ Res*. 2003;92(12):1305-1313. doi:10.1161/01.RES.0000077045.84609.9F

36. McCaffrey PG, Luo C, Kerppola TK, et al. Isolation of the cyclosporin-sensitive T cell transcription factor NFATp. *Science*. 1993;262(5134):750-754.

37. Northrop JP, Ho SN, Chen L, et al. NF-AT components define a family of transcription factors targeted in T-cell activation. *Nature*. 1994;369(6480):497-502. doi:10.1038/369497a0

38. Hoey T, Sun YL, Williamson K, Xu X. Isolation of two new members of the NF-AT gene family and functional characterization of the NF-AT proteins. *Immunity*. 1995;2(5):461-472.

39. Wilkins BJ, De Windt LJ, Bueno OF, et al. Targeted disruption of NFATc3, but not NFATc4, reveals an intrinsic defect in calcineurin-mediated cardiac hypertrophic growth. *Mol Cell Biol*. 2002;22(21):7603-7613.

40. Huang T, Xie Z, Wang J, Li M, Jing N, Li L. Nuclear factor of activated T cells (NFAT) proteins repress canonical Wnt signaling via its interaction with Dishevelled (Dvl) protein and participate in regulating neural progenitor cell proliferation and differentiation. *J Biol Chem*. 2011;286(43):37399-37405. doi:10.1074/jbc.M111.251165

41. Lin H, Sue Y-M, Chou Y, et al. Activation of a nuclear factor of activated T-lymphocyte-3 (NFAT3) by oxidative stress in carboplatin-mediated renal apoptosis. *Br J Pharmacol*. 2010;161(7):1661-1676. doi:10.1111/j.1476-5381.2010.00989.x

42. Gopinath S, Vanamala SK, Gujrati M, Klopfenstein JD, Dinh DH, Rao JS. Doxorubicin-mediated apoptosis in glioma cells requires NFAT3. *Cell Mol Life Sci*. 2009;66(24):3967-3978. doi:10.1007/s00018-009-0157-5

43. Serrano-Pérez MC, Fernández M, Neria F, et al. NFAT transcription factors regulate survival, proliferation, migration, and differentiation of neural precursor cells. *Glia*. 2015;63(6):987-1004. doi:10.1002/glia.22797

44. Coleman MA, Sasi SP, Onufrak J, et al. Low-dose radiation affects cardiac physiology: gene networks and molecular signaling in cardiomyocytes. *Am J Physiol Heart Circ Physiol*. 2015;309(11):H1947-63. doi:10.1152/ajpheart.00050.2015

45. Finsen AV, Lunde IG, Sjaastad I, et al. Syndecan-4 is essential for development of concentric myocardial hypertrophy via stretch-induced activation of the calcineurin-NFAT pathway. *PLoS One*. 2011;6(12):e28302. doi:10.1371/journal.pone.0028302

46. Chang AY, Sliwoski J, Butler S, et al. Calcineurin mediates bladder wall remodeling secondary to partial outlet obstruction. *Am J Physiol Renal Physiol*. 2011;301(4):F813-22. doi:10.1152/ajprenal.00586.2010

47. Moreno M, Fernández V, Monllau JM, Borrell V, Lerin C, de la Iglesia N. Transcriptional Profiling of Hypoxic Neural Stem Cells Identifies Calcineurin-NFATc4 Signaling as a Major Regulator of Neural Stem Cell Biology. *Stem Cell Rep*. 2015;5(2):157-165. doi:10.1016/j.stemcr.2015.06.008

48. Zhang X, Kang T, Zhang L, Tong Y, Ding W, Chen S. NFATc3 mediates the sensitivity of gastric cancer cells to arsenic sulfide. *Oncotarget*. 2017;8(32):52735-52745. doi:10.18632/oncotarget.17175

49. Zhang K, Heidrich FM, DeGray B, Boehmerle W, Ehrlich BE. Paclitaxel accelerates spontaneous calcium oscillations in cardiomyocytes by interacting with NCS-1 and the InsP3R. *J Mol Cell Cardiol*. 2010;49(5):829-835. doi:10.1016/j.yjmcc.2010.08.018

50. Kerkhofs M, Bittremieux M, Morciano G, et al. Emerging molecular mechanisms in chemotherapy: Ca2+ signaling at the mitochondria-associated endoplasmic reticulum membranes. *Cell Death Dis*. 2018;9(3):334. doi:10.1038/s41419-017-0179-0

51. Hessmann E, Zhang J-S, Chen N-M, et al. Nfatc4 regulates sox9 gene expression in acinar cell plasticity and pancreatic cancer initiation. *Stem Cells Int*. 2016;2016:5272498. doi:10.1155/2016/5272498

52. Morgan RJ, Synold TW, Gandara D, et al. Phase II trial of carboplatin and infusional cyclosporine in platinum-resistant recurrent ovarian cancer. *Cancer Chemother Pharmacol*. 2004;54(4):283-289. doi:10.1007/s00280-004-0818-x

53. Chambers SK, Davis CA, Chambers JT, Schwartz PE, Lorber MI, Hschumacher RE. Phase I trial of intravenous carboplatin and cyclosporin A in refractory gynecologic cancer patients. *Clin Cancer Res*. 1996;2(10):1699-1704.

54. Manetta A, Blessing JA, Hurteau JA. Evaluation of cisplatin and cyclosporin A in recurrent platinum-resistant ovarian cancer: a phase II study of the gynecologic oncology group. *Gynecol Oncol*. 1998;68(1):45-46. doi:10.1006/gyno.1997.4887

55. Mancini M, Toker A. NFAT proteins: emerging roles in cancer progression. *Nat Rev Cancer*. 2009;9(11):810-820. doi:10.1038/nrc2735

56. Iyengar M, O'Hayer P, Cole A, et al. CDK4/6 inhibition as maintenance and combination therapy for high grade serous ovarian cancer. *Oncotarget*. 2018;9(21):15658-15672. doi:10.18632/oncotarget.24585

Figure legends

Figure 1. NFATC4 is enriched in ovarian stem like cancer cells and expression correlates with a decrease in cellular proliferation and patient survival. **a** *NFATC4* mRNA expression in $ALDH^+/CD133^+$ ovarian cancer stem-like cells and bulk $ALDH^-/CD133^-$ cancer cells from 3 primary advanced stage (Stage III-IV) HGSC patients. **b** *NFATC4* mRNA expression in $CD133^+$ and $CD133^-$ ovarian cancer cell lines. **c** Representative growth curves of $CD133^+$ and $CD133^-$ ovarian cancer cell lines. **d** *NFATC4* mRNA expression levels in 4 cell lines stained with CFSE. CFSE intensity; bright=slowly dividing, medium=bulk cells, dim=rapidly dividing. **e** mRNA expression of the dominate ALDH genes (ALDH1A1/3) and CD133 in CFSE stain cell lines. Kaplan-meier survival plots displaying Overall Survival (OS), Progression Free Survival (PFS), Post Progression Survival (PPS) of TCGA HGSC patients expressing **f** high or low *NFATC4* ***g*** high and low *RCAN1*. All experiments were repeated a minimum of 3 times with 3 technical replicates per experiment. T-tests and one-way ANNOVARs were performed to determine significance. *p<0.05, **p<0.01, ****p<0.0001.

Figure 2. Characterization of NFATC4 overexpression constructs. **a** Schematic diagram of the two constitutive activation *NFTAC4* overexpression constructs; cNFATC4 (truncated regulatory domain and tagged with a yellow fluorescent protein (YFP)), and IcNFATC4 (NLS phosphorylation sites mutated). **b** cNFATC4, RCAN1 and FST mRNA expression in HGSC cells (CaOV3, OVSAHO and COV362) and A2780 cells expressing cNFATC4 or Control-YFP construct (n=2). **d** *NFATC4*, *RCAN1* and FST (n=3) mRNA expression in HEY1 and SKOV3 cells expressing IcNFATC4 or a ILuc control constructs treated with or without 100 ng/mL doxycycline for 72 h. T-tests and one-way ANNOVARs were performed to determine significance. All experiments were repeated a minimum of 3 times with at least 3 technical replicates per experiment. *p<0.05, **p<0.01, ***p<0.001.

Figure 3. NFATC4 overexpression significantly inhibits cell growth. Cell counts of **a** A2780 cell line or **b** HGSC cell lines (COV362, OVSAHO and CaOV3, at 6, 4 and 6 days respectively) expressing cNFATC4 or control-YFP constructs. **c** Cell counts of HEY1 and SKOV3 cells expressing IcNFATC4 or ILuc control constructs treated with or without doxycycline. **d** trypan blue viability staining of cells line expressing cNFATC4 or YFP control, or IcNFATC4 or ILuc control with or without 100 ng/mL doxycycline. **e** Annexin V/propidium iodine staining of A2780 cells expressing cNFATC4 or YFP control. T-tests and one-way ANNOVARs were performed to determine significance. All experiments were repeated a minimum of 3 times with at least 3 technical replicates per experiment. *p<0.05, **p<0.01, ***p<0.001.

Figure 4. NFATC4 promotes a quiescent phenotype. **a** Quantitation of BrdU incorporation of A2780 cells expressing control-YFP or cNFATC4. **b** Table displaying the number of first and second mitosis of A2780 cells expressing the cNFATC4 or control-YFP constructs, grown in single cell capture microfluidic chips. **c** IncuCyte growth curves of IcNFATC4 or ILuc cells treated with or without doxycycline. **d** FACS plots demonstrating the isolation and quantification of IcNFATC4 and ILuc HEY1 cells expressing the Fucci cell-cycle reporter vectors. Bar graph summarizing the cell cycle phase of cell expressing either construct. **e** Cell cycle analysis of G1-S phase enriched ILuc and IcNFATC4. **f** Representative images and quantification of cells size

changes in ILuc and IcNFATC4 cells following doxycycline treatment for 106 h. T-tests and one-way ANNOVARs were performed to determine significance. Microfluidics experiment and Fucci cell cycle experiments were performed twice, all other experiments were repeated a minimum of 3 times with at least 3 technical replicates per experiment. **p<0.01, ***p<0.001.

Figure 5. NFATC4 promotes chemoresistance in vitro and is activated by cisplatin. **a** Viability of cells expressing construct pairs (cNFATC4/Control-YFP or IcNFATC4/ILuc) treated with various concentrations of cisplatin. **b** IncuCyte confluence growth curves of IcNFATC4/ILuc expressing cells co-treated with cisplatin and doxycycline. **c** NFATC4 immunofluorescence of cells lines treated with or without cisplatin. **d** *RCAN1* mRNA expression levels of cells treated with or without cisplatin. **e** *FST* mRNA expression levels of treated with or without cisplatin. CaOV3 (2ug/mL), COV362 (5.5ug/mL), HEY (2.5 ug/mL). **f** *NFATC4* mRNA expression of cell lines treated with a high concentration of cisplatin for 72h. **f** IncuCyte confluence growth curves of $CD133^-$ vs $CD133^+$ cells treated with cisplatin. **g** Cell viability following co-treatment with cisplatin and the pan-NFAT inhibitor VIVIT. T-tests and one-way ANNOVARs were performed to determine significance. All experiments were repeated a minimum of 3 times. *p<0.05, **p<0.01, ***p<0.001.

Figure 6. NFATC4 inhibits tumor growth and promotes chemoresistance in vivo. **a** Tumor growth of A2780 cells expressing cNFATC4 or Control-YFP. **b** Tumor growth of HEY1 cells expressing IcNFATC4 or ILuc control constructs in the presences of doxycycline. **c** Tumor growth of IcNFATC4 HEY1 cells treated with delayed doxycycline or vehicle. **d** Tumor weights of HEY1 IcNFATC4 xerographs treated with vehicle, delayed or continuous doxycycline. **e** Tumor growth of HEY1 IcNFATC4 cells treated with doxycycline for 5 days or vehicle, then both treated with 16 mg/kg paclitaxel, intraperitoneally. T-tests and one-way ANNOVARs were performed to determine significance. All experiments were repeated a minimum of 3 times. *p<0.05, **p<0.01, ***p<0.001.

Figure 7. NFATC4 overexpression inhibits MYC, and cMYC overexpression partially rescues the quiescent phenotype at early, but not late, timepoints. **a** MYC mRNA expression following 24 h doxycycline treatment. **b** Validation of cMYC overexpression construct in SKOV3 and HEY1 cell lines. **c** The effect of MYC overexpression on cell number of IcNFATC4 cells transfected with PCDNA3 or cMYC and treated with doxycycline for 72 h or post treated for 72h with dox before transfection with PCDNA3 or cMYC and treated with doxycycline for an addition 72 h. T-tests and one-way ANNOVARs were performed to determine significance. All experiments were repeated a minimum of 3 times. n.s.= not significant, *p<0.05, **p<0.01, ****p<0.0001.

Supplementary Figure legends

Supplementary Figure 1. Kaplan-Meier survival plot. Survival probability of dysregulation of the NFATC4 pathway in ovarian cancer TCGA data set. *p<0.05.

Supplementary Figure 2. Evaluation of NFATC4 constructs. **a** NFATC4 and RCAN1 mRNA expression of 3 HGSOC cells lines transduced with IcNFATC4 or ILuc control. **b** Flow cytometry analysis of A2780 cells expressing Control-YFP or cNFATC4 constructs.

Supplementary Figure 3. No difference in apoptosis or SABG staining between NFATC4 and control constructs. **a** Annexin V PI apoptosis assay of HEY1 expressing ILuc or NFATC4 constructs. **b** SABG staining of A2780 cNFATC4 or Control-YFP. **c** Quantification of SABG staining; the cyclin D1/CDK4 and CDK6 inhibitor Ribociclib was used as a positive control for senescence.

Supplementary Figure 4. lcNFATC4 expressing cells have a reduction in cell size. **a** IncuCyte growth curves of IcNFATC4 or ILuc HEY1 and SKOV3 cells treated with or without doxycycline. Red box indicates the confluency used to validate changes in cell morphology. Forward scatter flow cytometry of; **b** A2780 cNFATC4 vs Control-YFP cells, **c** HEY1 ILuc and lcNFATC4 cells treated with or without doxycycline. **d** Quantitation HEY1 cell size. **p<0.01. ****p<0.0001.

Supplementary Figure 5. NFATC4 promotes chemoresistance. Cell viability ILuc and IcNFATC4 SKOV3 cells treated with or without doxycycline and co-treated with varying concentrations of cisplatin.**p<0.01.

Supplementary Figure 6. Taxol partially activates NFATC4 signaling in ovarian cancer cell lines. OVSAHO, COV362 and HEY1 cells were treated with or without 3 uM and 9 uM of Taxol for 72 h before RCAN1 and NFATC4 expression was validated using qPCR. Results were expressed as fold change to untreated control, n=2.

Supplementary Figure 7. NFATC4 constructs expression is lost in vivo. Flow cytometry analysis of control-YFP and cNFATC4 expression in tumors.

Supplementary Figure 8. Doxycycline recovery cell counts of NFATC4 expressing SKOV3 and HEY1 cells lines. **a** HEY1 and SKOV3 cells expressing the IcNFATC4 and ILuc constructs were treated for 72h with 100 ng/mL doxycycline. After 72h doxycycline was removed and cells were grown in doxycycline free media for 120-144 h. Cell counts were performed daily. **b** after recovering from quiescence, cells were treated with dox for 96 h, then re-plated at 30 K cells and grown in the presence of dox for an additional 72-96h. Cell counts were recorded daily. n=2.

Supplementary Figure 9. Doxycycline recovery qPCR of NFATC4 target genes in NFATC4 expressing SKOV3 and HEY1 cells lines. HEY1 and SKOV3 cells expressing the IcNFATC4 and ILuc constructs were treated for 72h with 100 ng/mL doxycycline. After 72h doxycycline was removed and cells were grown in doxycycline free media for 120 h. After recovering from quiescence, cells were treated with dox for another 144h. RNA was extract and qPCR performed for NFATC4, FST, RCAN1 and MYC at each of the listed time points. N=2.

Supplementary Table 1. Cisplatin and Taxol IC50 values for ovarian cancer cell lines used in this study.

Supplementary Table 2. qPCR primer sequences.

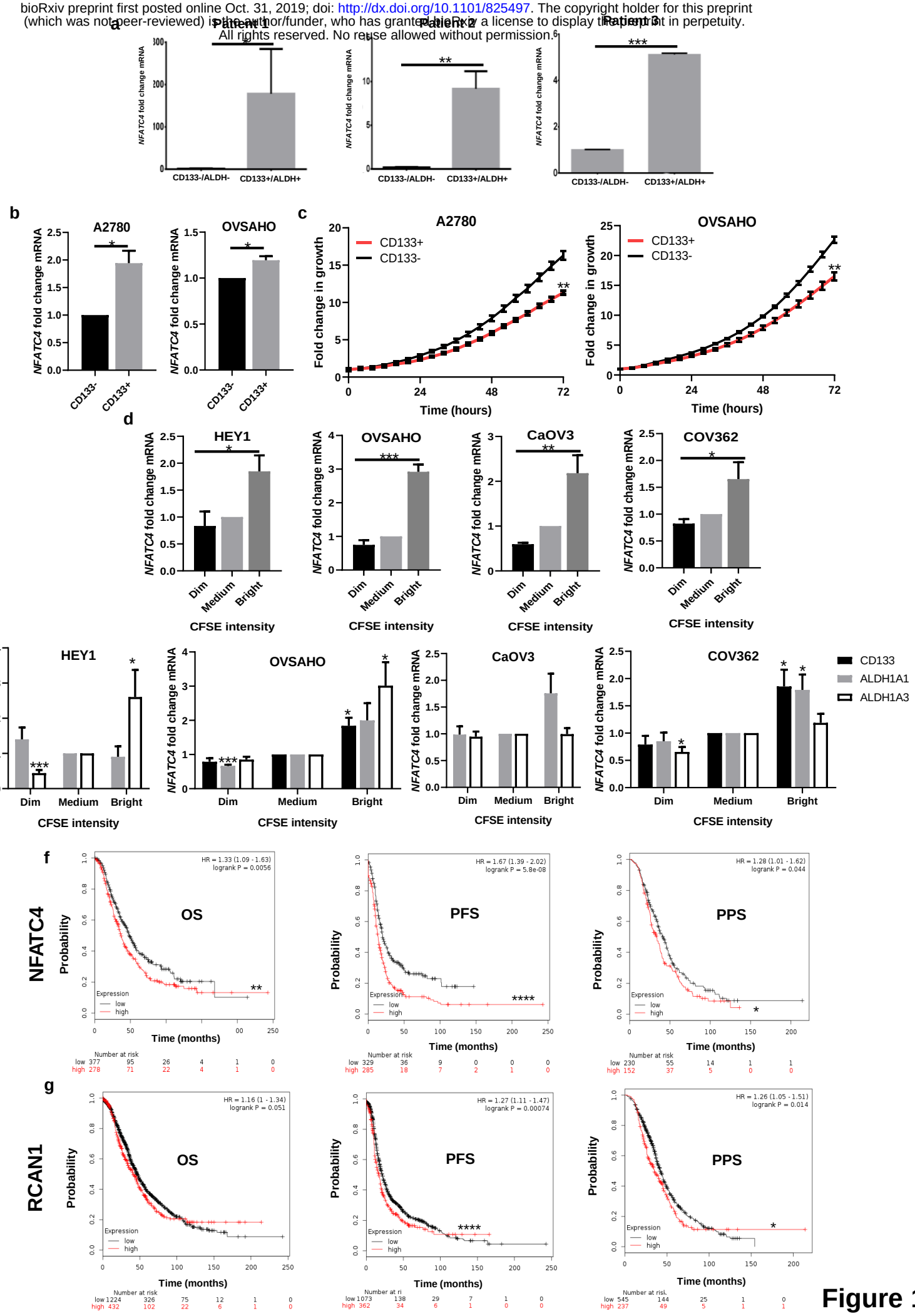

Figure 1

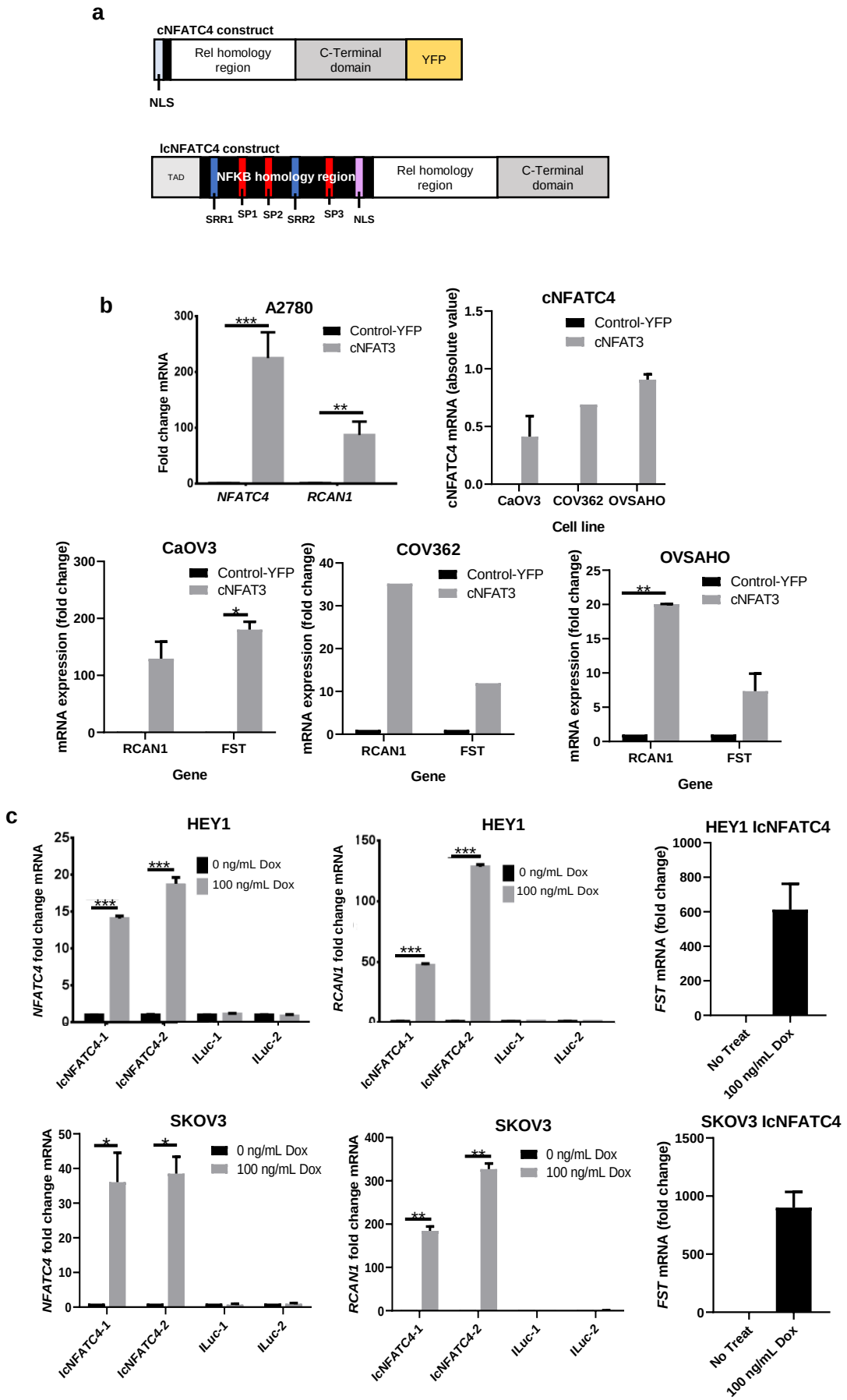

Figure 2

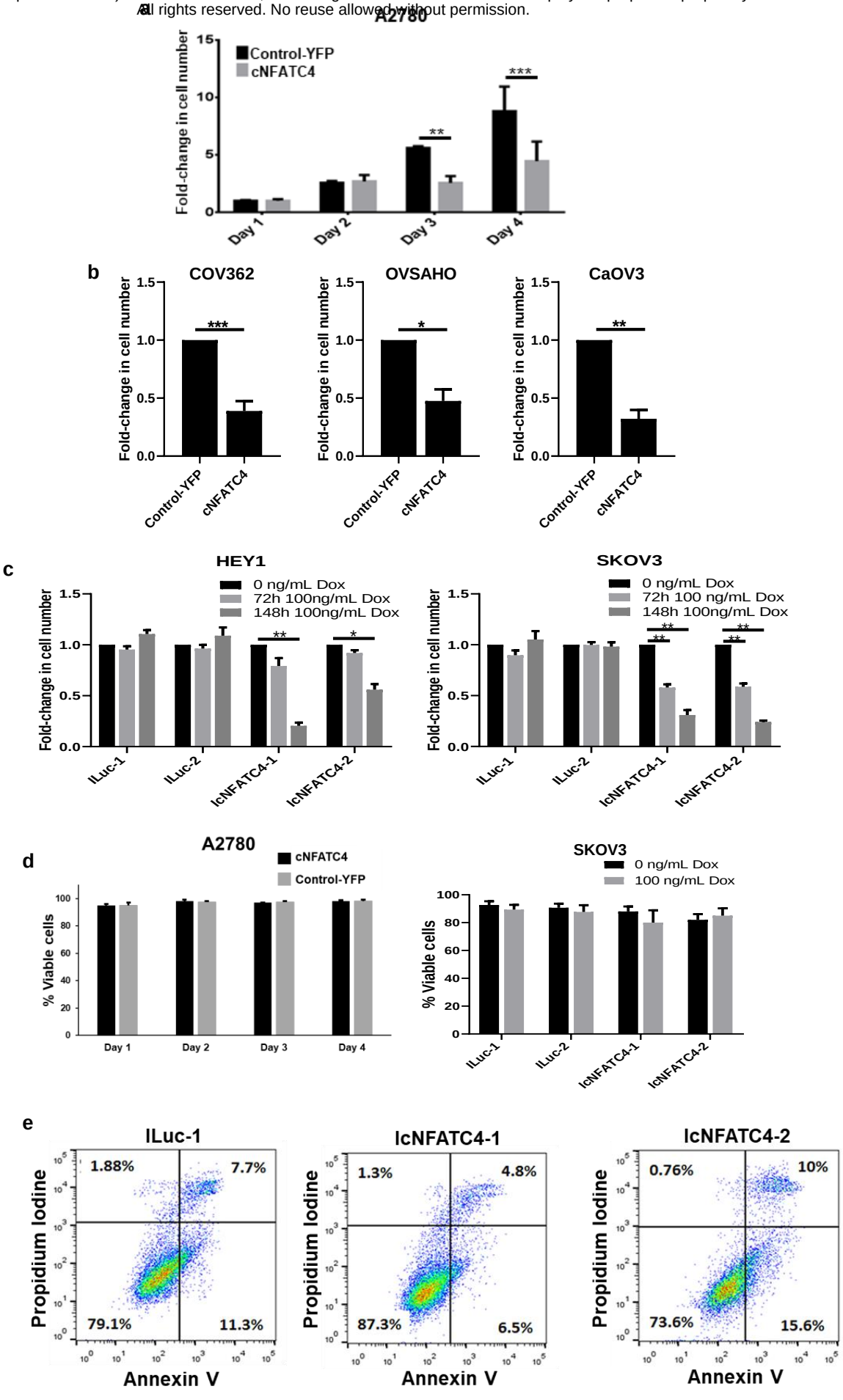

Figure 3

a

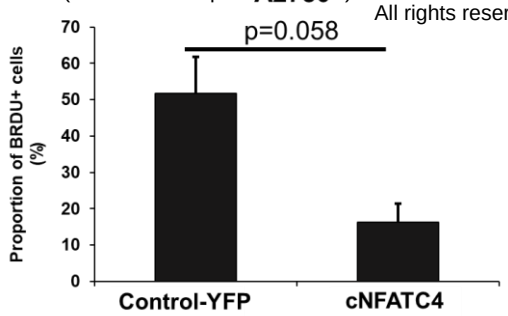

b

Number of first and second mitoses		
	Control-YFP	cNFATC4
Initial count	180	120
1st mitoses	71 (39%)	25 (20%)
2nd mitoses	29 (41%)	1 (4%)
Final count	605 (3.4-fold)	174 (1.4-fold)

c

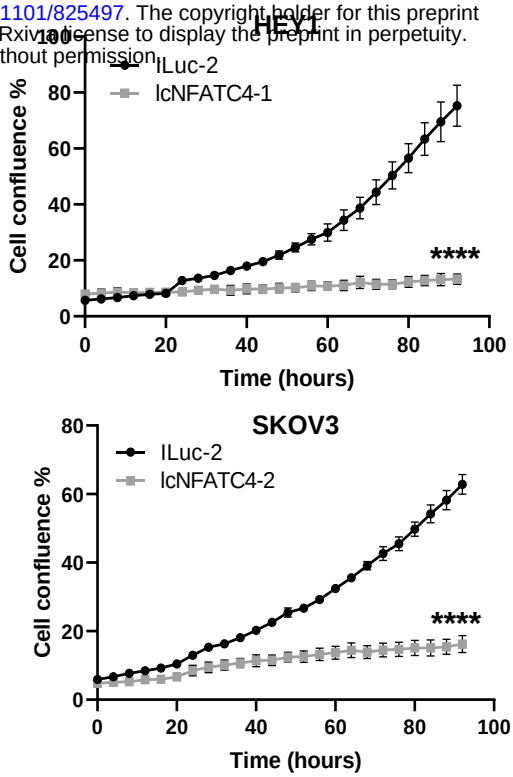

d

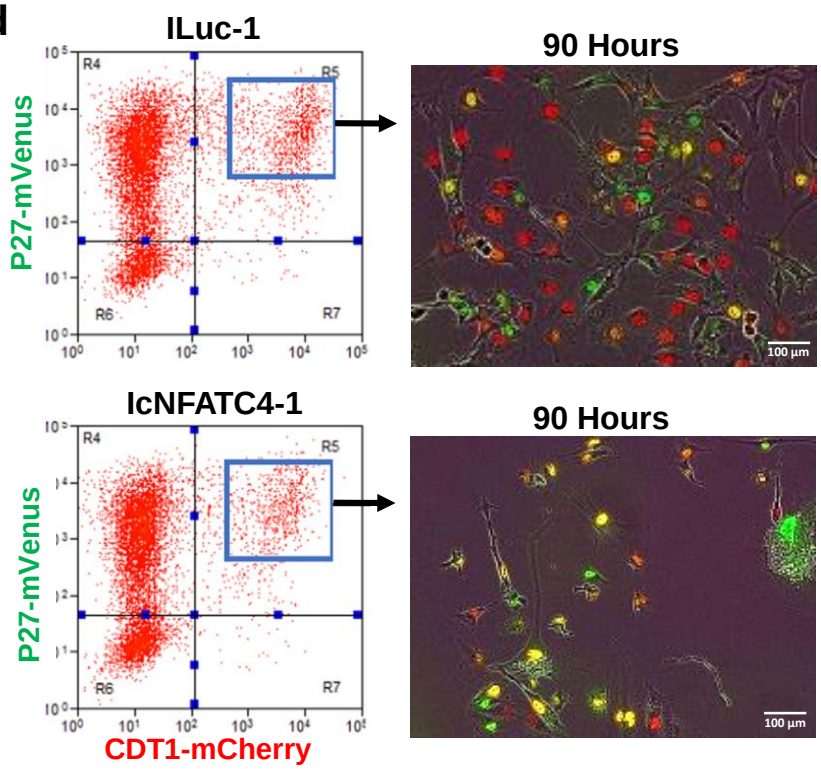

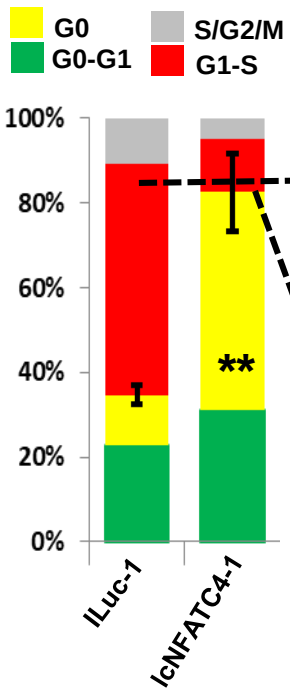

e

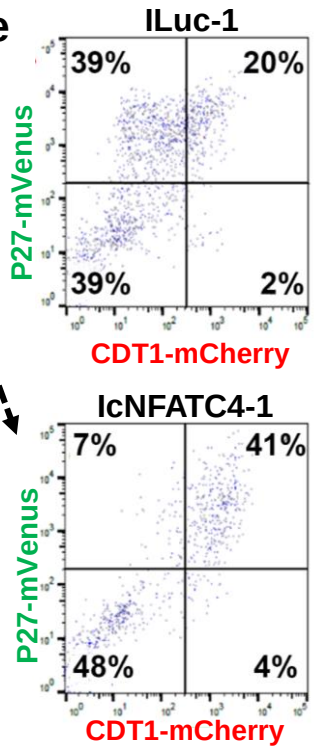

f

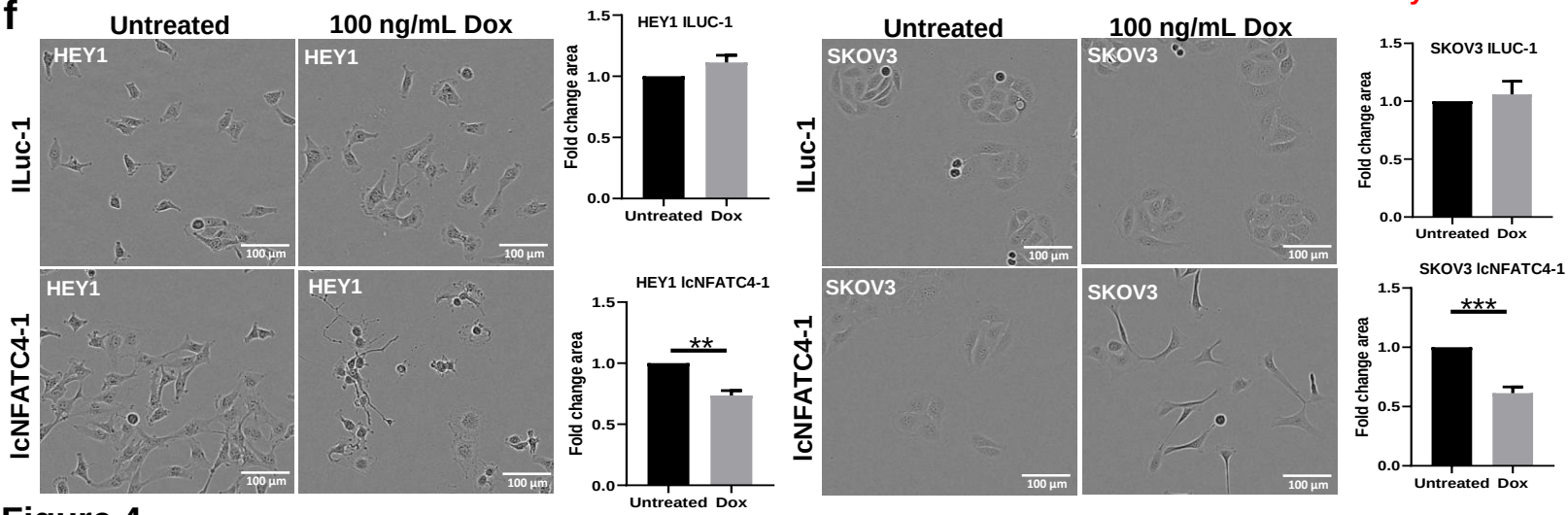

Figure 4

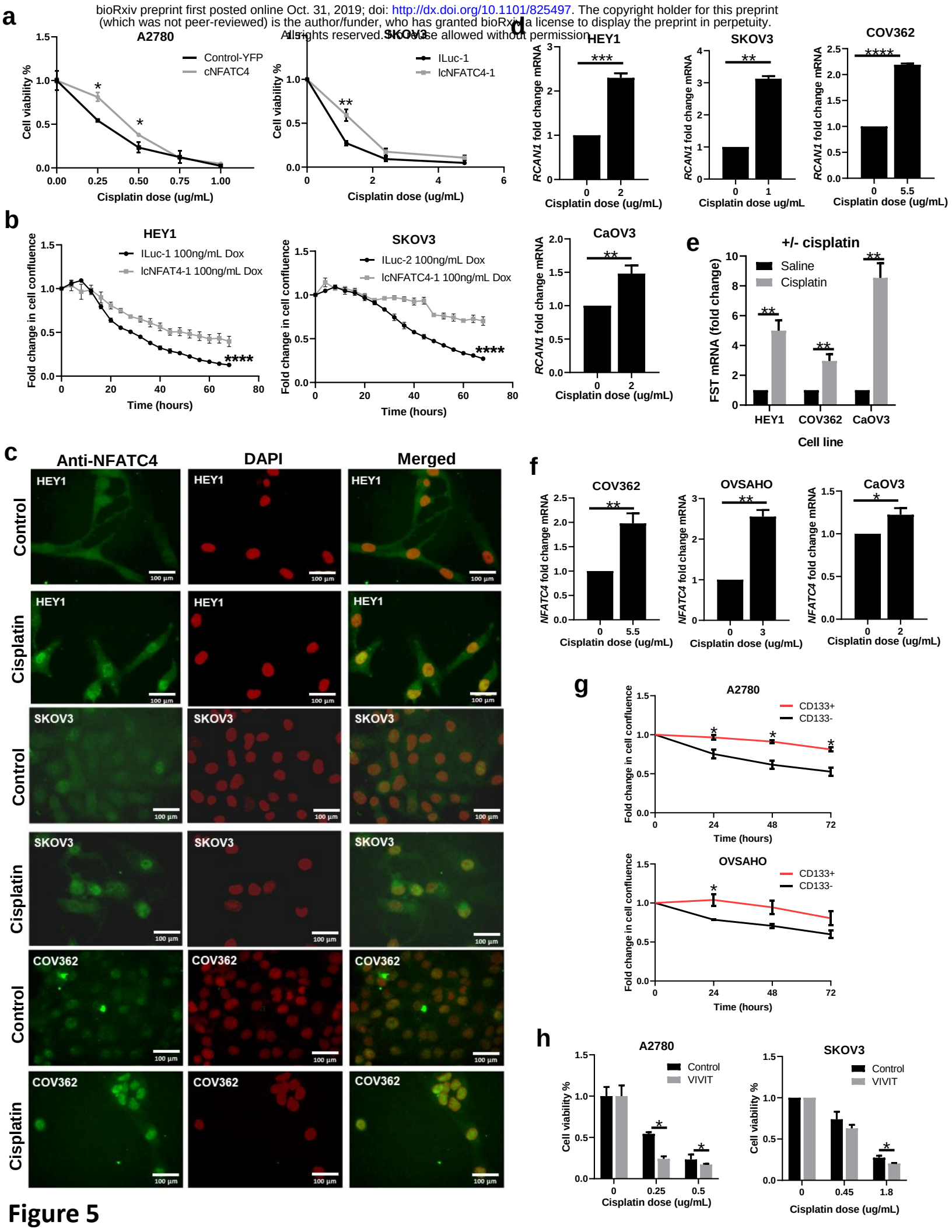

Figure 5

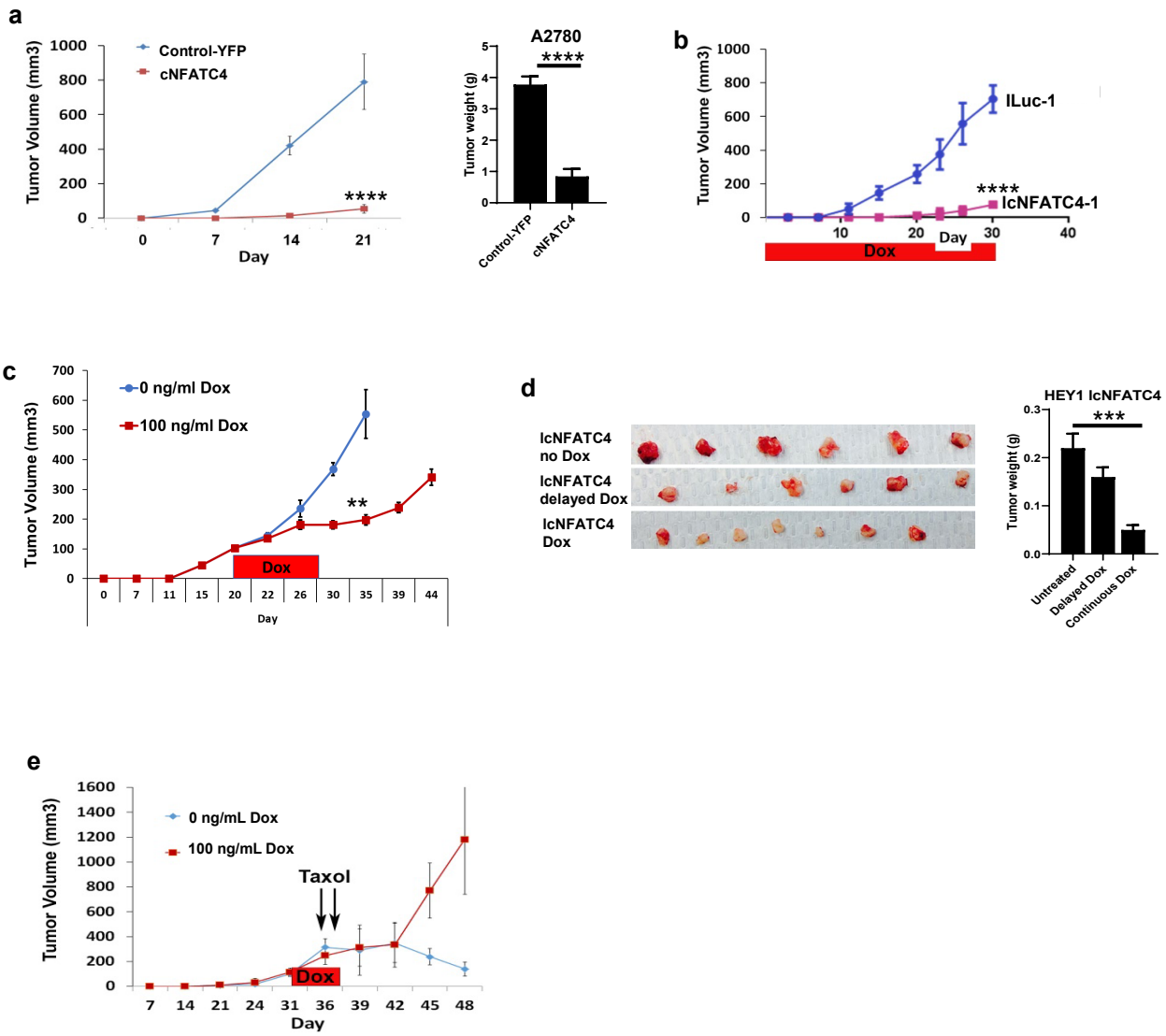

Figure 6

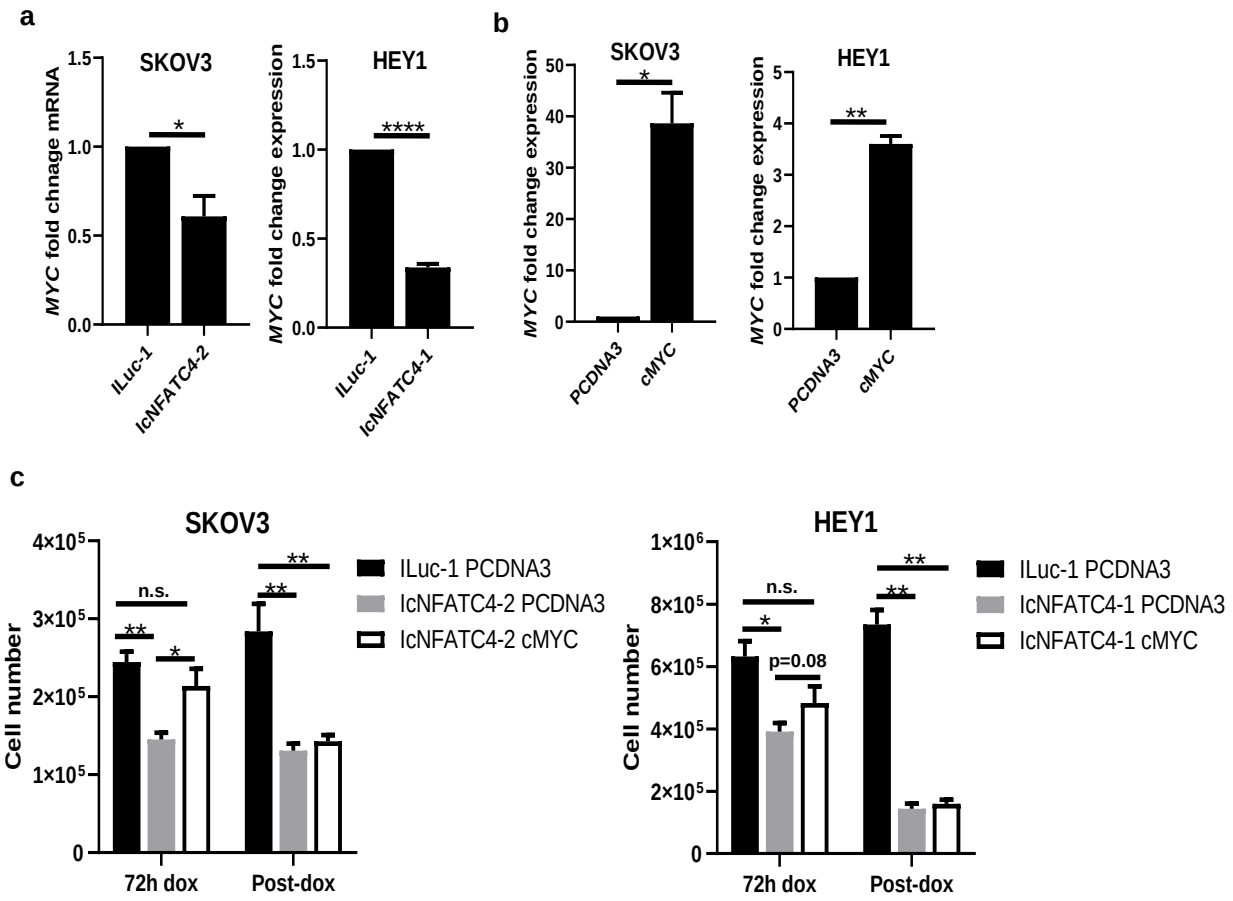

Figure 7